Polycystic Kidney Disease (PKD):

From the clinical/genetic test, through *in vitro* and *in vivo* analysis, and back to humans.

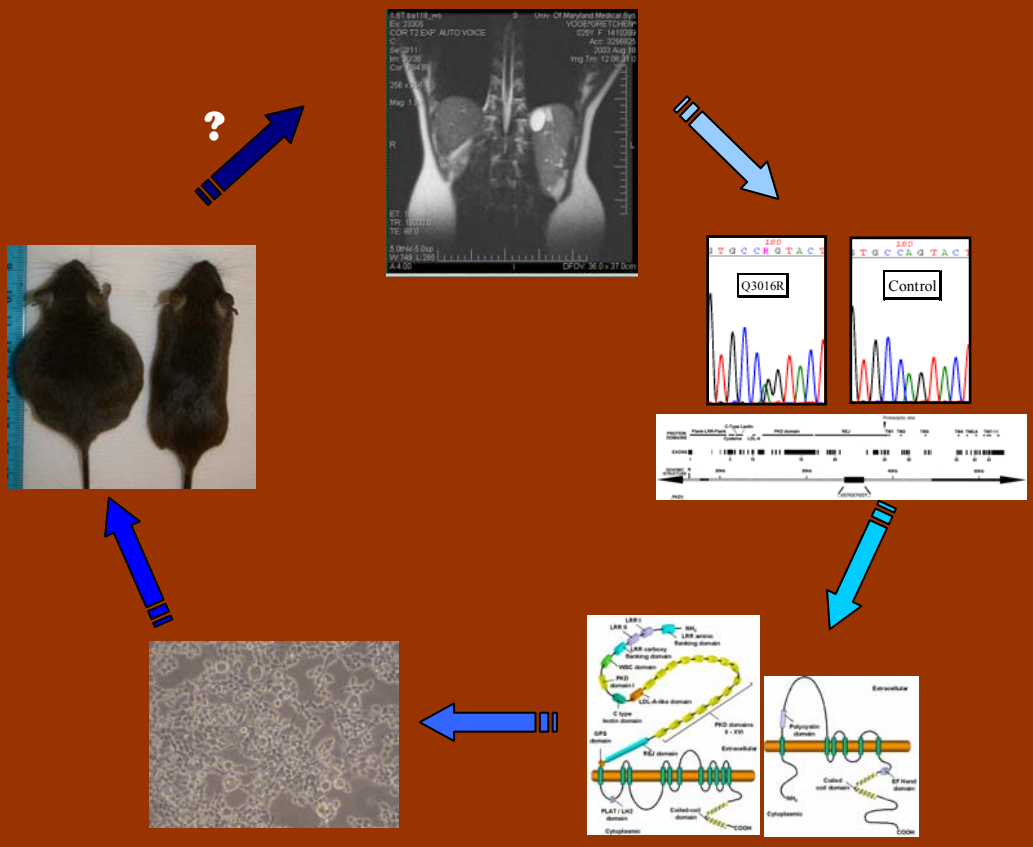

Miguel Angel García González

2006

UNIVERSIDADE DE SANTIAGO DE COMPOSTELA
FACULTAD DE MEDICINA
DEPARTAMENTO DE MEDICINA

Memoria presentada por el Licenciado *Miguel Angel García González* para optar al Grado de Doctor por la *Universidade de Santiago de Compostela*.

Abril, 2006

El Dr. Xosé Manuel Lens Neo, Profesor Asociado del Departamento de Medicina de la Universidade de Santiago de Compostela, y Gregory G. Germino, M.D., Professor del Departamento de Medicina de The Johns Hopkins School of Medicine, Baltimore, USA.

CERTIFICAN

que la presente tesis titulada "*Polycystic Kidney Disease (PKD). From the clinical/genetic test, through in vivo and in vitro analysis and back to humans*" que se presenta para optar al grado de Doctor fue realizada bajo nuestra dirección por el Licenciado D. Miguel Angel García González y está en condiciones de ser leída ante el tribunal correspondiente.

Y, para que así conste, firma la presente en Santiago de Compostela a 27 de Marzo de 2006.

VºBº VºBº

Dr. Xosé Manuel Lens Neo Gregory G. Germino, M.D

VºBº

D. Miguel Angel García González

Al Dr. Lens, la Dra. Watnick y el Dr. Germino

quienes pusieron los cimientos de este trabajo,

A mi familia, en especial a mis Padres,

por su esfuerzo en mi formación y cariño constante

A Raquel,

el amor y apoyo incondicional que me muestra.

<u>Todo te lo debo a ti</u>.

"There are two ways to live your life. One is as though nothing is a miracle. The other is as though everything is a miracle".

Albert Einstein. ***Quoted in Des MacHale,*** **Wisdom** ***(London, 2002).***

INDEX

ÍNDICE EN ESPAÑOL

FIGURES

TABLES

Resumen

El objeto de estudio de esta Tesis son dos enfermedades quísticas renales hereditarias: Poliquistosis Renal Autosómica Dominante, siglas en inglés ADPKD (*Autosomal Dominant Polycystic Kidney Disease*); y Poliquistosis Renal Autosómica Recesiva, corresponde al acrónimo inglés ARPKD (*Autosomal Recessive Polycystic Kidney Disease*). En ambas se ha establecido la existencia de un componente genético, sin embargo, el estudio molecular se encuentra en diferentes fases en cada una de ellas. Mientras en ADPKD se conocen los genes implicados, su ubicación y anatomía molecular, ARPKD todavía se encuentra en la primera fase de estudio ya que sólo recientemente se ha localizado el gen responsable de la enfermedad. En esta tesis se ha establecido una estrategia racional de búsqueda de mutaciones en los genes responsables de la Poliquistosis Renal y su aplicación en el desarrollo de un test clínico/genético de la enfermedad. En colaboración con Athena Diagnostics, Inc.; dicha estrategia ha sido testada en 82 familias con Poliquistosis Renal con un excelente porcentaje de detección del 83%. Meticulosamente, se ha examinado la predicción patogénica de las sustituciones aminoacídicas y alteraciones en el lugar de expansión (*splice site*) para cada probando. Una fracción sustancial de variantes encontradas en el gen PKD1 también se ha encontrado en sus genes homólogos, posiblemente debido a una conversión génica entre ellos. Evidencias experimentales de esta tesis dan soporte a la idea de que PKD1 es un gen altamente mutable. Se ha observado la existencia de individuos con una gran cantidad de sustituciones aminoacídicas, mientras que otros sólo poseen una pequeña cantidad, sugiriendo que ciertos haplotipos podrían ser más mutables que otros. También, dichos resultados remarcan la precaución que se debe tomar, desde un punto de vista clínico, a la hora de distinguir entre una variante con sentido perdido (*missense*) pero dentro de la normalidad y aquellas que son probables de causar la enfermedad. Se ha identificado un número de individuos con múltiples cambios pero sin que ninguno de ellos pueda ser clasificado como definitivamente patogénico

(definidos como codones de parada prematura, deleciones, inserciones,...). Se presenta la hipótesis de que en algunos casos, a pesar de no tener una única mutación patogénica, el efecto combinado de varias substituciones con sentido alterado no-patogénicas pueden producir un alelo hipomórfico. Por ejemplo, varias variaciones con sentido alterado o cambios "silenciosos" pueden resultar en una función reducida e inadecuada debido a la alteración de la eficiencia translacional, ya sea por su efecto aditivo en el mismo alelo o en combinación con una mutación en el otro alelo. Nuestros descubrimientos tienen distintas implicaciones: 1) Las muestras utilizadas como controles deben de ser étnicamente iguales para evaluar las variantes raras, 2) El análisis del DNA no es suficiente para aportar un diagnóstico definitivo en aquellas variantes con sentido alterado "particulares", 3) Se necesitan mejores herramientas para evaluar las consecuencias de dichos cambios.

Así pues, este manuscrito propone que los sistemas *in vitro* pueden ser utilizados para determinar la función de la Poliquistina y además analizar si está alterada por la presencia de las variantes asociadas a la enfermedad. Esta parte de la Tesis no había sido contemplada inicialmente en los objetivos, pero debido al significado incierto de un número elevado número de variantes con sentido alterado, se ha planteado la necesidad de buscar un sistema que determinara la patogenicidad de dichas variantes. Se partía de la hipótesis que algunos de los cambios con sentido alterado serían patogénicos (habían sido encontrados apareciendo *de novo*). En algunos casos, se encontró evidencia directa que muestra su patogenicidad, sin embargo en otros resultó indeterminada la manera en que la función de la proteína podría estar alterada. En éstos, se barajó la posibilidad de utilizar sistemas *in vitro* para evaluar mutaciones putativas y polimorfismos. Estos resultados tienen varias implicaciones importantes: 1) Se ha demostrado que los sistemas *in vitro* pueden ser utilizados para distinguir entre polimorfismos y mutaciones, 2) Estos sistemas pueden ser utilizados para determinar los efectos de las variaciones de la secuencia en los genes candidatos.

Los datos proporcionados por la secuenciación directa de la totalidad de la región codificadora de PKD1 y PKD2 son una valiosa herramienta para el análisis y un mejor conocimiento de la enfermedad. Se han testado las distintas hipótesis propuestas por la comunidad científica como causantes de la alta mutabilidad de PKD1. Así pues, se ha concluido que las causas principales de la alta mutabilidad del gen PKD1 se deben al efecto de la conversión génica con sus genes homólogos, a su alto % en GC y a la presencia de un tracto de polipirimidina en el intrón 21. Por el contrario, no se ha encontrado evidencias que soporten la hipótesis propuesta por el grupo del Dr. Harris, implicando a los dinucleótidos CpG como responsables directos de la alta mutabilidad en PKD1.

Puesto que todavía se conoce relativamente poco sobre las vías de señalización en PKD, se ha invertido mucho esfuerzo en el desarrollo modelos de ratón ADPKD que puedan ser utilizados en el estudio de la biología de las Poliquistinas. Hasta el momento, un número de laboratorios (hasta 10 líneas mutantes diferentes publicadas) han generado ratones portando alelos mutados tanto para *Pkd1* (*Pkd1*$^{-/-}$) como para *Pkd2* (*Pkd2*$^{-/-}$). Puesto que los quistes se desarrollan a través del mecanismo "two hit", no fue una sorpresa que los heterocigotos sean uniformemente viables y con escasas manifestaciones renales y hepáticas. Por el contrario, el estado homocigoto resulta en una elevada mortandad embrionaria mediano/tardía, dependiendo del modelo. Esta temprana mortandad en estado homocigoto limita los tipos de preguntas que pueden ser contestadas con estos modelos de ratón. Wu y col. han generado un alelo instable de *Pkd2* con una duplicación que genera mutaciones somáticas al azar. Este es el único modelo que se acerca al comportamiento de la enfermedad en humanos, pero sin embargo, no permite una perdida génica regulada. El Dr. Piontek, ha generado un alelo *floxeado* (flanqueado por dos secuencias *lox-p*) que puede ser utilizado controlando el momento y el lugar de la mutación en Pkd1. Dicho modelo no existe para Pkd2. Dado que el comportamiento en PKD1 y PKD2 podría diferir, creemos que ambos modelos son necesarios para el mejor conocimiento de la biología de las Poliquistinas y de la enfermedad. En esta Tesis se presenta el primer alelo *floxeado* de *Pkd2*

(*Pkd2*^{cond}) con el fin de estudiar las consecuencias de la perdida de la Poliquistina-2 en un determinado tejido y en un momento puntual, y cuyo objetivo es la caracterización de dicho modelo. En el momento de la muerte, los ratones homocigotos presentan Poliquistosis renal y pancreática, edema severo, anormalidades cardiacas, hemorragias espontáneas y polihidramnios. De modo interesante, el modelo knock-out de ratón *Pkd2* presenta similitudes al de *Pkd1* pero no son totalmente iguales. Los ratones *Pkd2*$^{-/-}$ presentan anormalidades en la determinación axial derecha/izquierda (isomerismo pulmonar derecho, cambio embrionario, colocación del corazón y localización abdominal al azar). Esto sugiere que la función de PKD1 y PKD2 podrían no superponerse en todos los tipos celulares.

Con el mismo fin y puesto que hasta el momento no ha sido descrito ningún modelo de ratón que represente en su totalidad la ARPKD, también se ha desarrollado un modelo *floxeado* de *Pkhd1*. Varios grupos han intentado modelar la enfermedad en ratones alterando el *Pkhd1* murino, pero ninguno ha conseguido representar todas las manifestaciones clínicas. Así pues, se presenta un alelo funcional de Pkhd1 (*Pkhd1*$^{flox3-4}$) el cual, después de una recombinación mediada por Cre, genera un alelo mutante putativo (*Pkhd1*$^{del3-4}$) con los exones 3 y 4 eliminados. Al igual que en humanos, una fracción sustancial de *Pkhd1*$^{del3-4/del3-4}$ murieron en fase perinatal, y los sobrevivientes, todos ellos presentaban una variedad de anormalidades hepatobiliares que incluía la fibrosis hepática congénita, quistes coledocales y colangitis ascendente. Representando el fenotipo humano, muchos de ellos mostraron un crecimiento retardado, enfermedad quística pancreática severa y diferentes grados de afectación renal.

Así pues, en esta Tesis ha sido desarrollada una estrategia para la búsqueda de mutaciones en los genes causantes de ADPKD, y testado la eficacia de la misma en un grupo de 82 pacientes. Con un 85% de detección de las mutaciones causantes de la enfermedad, es la estrategia más eficaz descrita hasta el momento, la cual esta siendo aplicada por Athena Diagnostics como único test de aplicación en la clínica para la Poliquistosis Renal Autosómica Dominante (PKDx). La información

proporcionada por este trabajo ha sido utilizada para el desarrollo de un método novedoso en el análisis del comportamiento génico de PKD1. También han sido generados satisfactoriamente los dos primeros modelos condicionales de ratón de los genes causantes de ADPKD y ARPKD. El entendimiento de los genes y el estudio en los modelos animales experimentales, proporcionará una base sólida para un mejor conocimiento de la biología de las enfermedades y su aplicación para la búsqueda de posibles terapias.

1. Introduction.

1.1. Autosomal Polycystic Kidney Disease (ADPKD).

1.1.1. Clinical Manifestations of ADPKD.

Autosomal dominant polycystic kidney disease (ADPKD) is one of the most common inherited disorders in humans (Gabow, 1985), affecting ~1/600-1/1000 individuals, and which the main clinical manifestation is the formation of bilateral fluid-filled renal cysts, leading to gross enlargement of the kidneys (Figure 1).Cysts are thought to form *in utero* and increase in size and number throughout life. This typically results in end-stage renal failure (ESRD) in 50% of patients by the age of 60, where men manifest ERSD in average 6 years earlier than women. Around 90% of the patients that live into their 70´s develop the disease. Kidney transplantation is required in 30-35% of ADPKD patients by the age of 52, increasing to 60-85% by the age of 70 (Germino et al., 2001).

Figure 1. End-stage ADPKD kidney shown on left, same scale normal kidney on right. *Picture taken form www.nhpress.com*

Until now, genetic testing has not been used as a diagnostic method. Three major reasons explain this: a) the main gene responsible for ADPKD (*PKD1*) is very large; b) mutations have been found throughout its entirety; and c) at least 5 confounding pseudo-genes have been described proximally on the same chromosome. Instead, the major mode of clinical diagnosis is via ultrasound, considering ADPKD when multiple bilateral renal are present in the kidney. Also, as shown in table 1, the number of cyst required for a

Age range	Number of cysts required for a diagnosis
< 18 years	2 cysts total
18–30 years	3 cysts total, bilateral distribution
30–60 years	4 cysts total, bilateral distribution
> 60 years	8 cysts total, bilateral distribution

Table 1. Number of cysts required for the diagnosis of ADPKD, dependent on age. *Reproduced from Germino and Chapman, 2001.*

correct ADPKD diagnosis is age-dependent. Those individuals with mutations in the *PKD1* gene and less that 30 years old that do not present any detectable cyst in their kidneys, were found to have less than 5% chance of developing ADPKD (Germino, 2001).

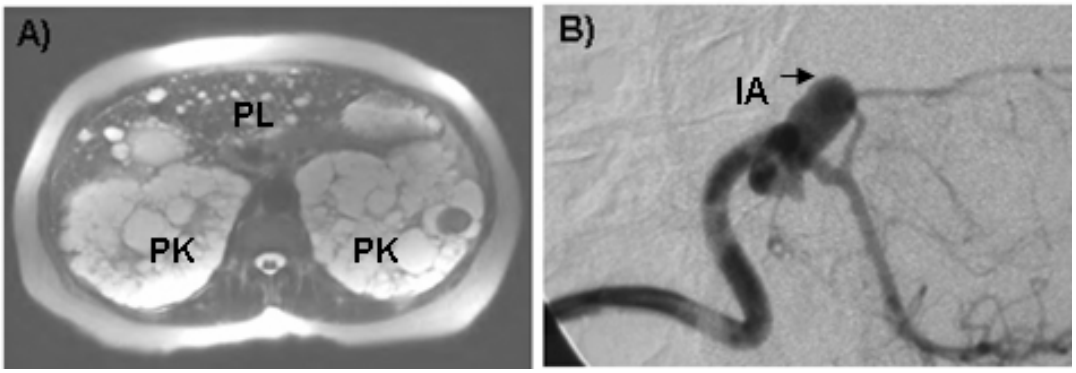

Figure 2. ADPKD phenotypes. ADPKD patient which MRI (A) shows polycystic kidneys (PK) and polycystic liver (PL), and which angiography (B) shows an intracranial aneurysm (IA). *Pictures donated by Dr. Watnick.*

ADPKD is not solely a disease of the kidneys, however, it is a systemic disorder. Patients often develop extrarenal manifestations like polycystic liver and pancreas, intracranial aneurysms, hernias and valve abnormalities, many of which have been responsible for a significant fraction of morbidity. The high frequency of these clinical manifestations has confused ADPKD with other diseases over the time. Gabow et al (1990) have shown that, liver (Figure 2A) and pancreatic cysts are two extrarenal cystic manifestations found in ~10% ADPKD patients. Other than cystic phenotypes, ADPKD patients have also been associated to a number of vascular and cardiac abnormalities, including intracranial aneurysms (~5%), aortic insufficiency (~12%) and mitral valve prolapse (~26%). Intracranial aneurysms (Figure 2B) have also been leading to subarachnoid hemorrhage and are becoming an important factor in morbidity and mortality of ADPKD patients. Even these are not the most common cause of cerebrovascular death in ADPKD patients. One of the early manifestations of the disease is hypertension (10-15% of affected children), which becomes more common in adult ADPKD patients close to the age of 30 with normal renal function (Pirson et al.., 1998).

Also, it has been shown that ADPKD patients from the same family manifest a great variation in the severity and progression of the disease. This interfamilial variability could be due to the different manifestations of *PKD1* and *PKD2*, the mutational spread across these genes, the influence of modifier genes and the second-hit nature of ADPKD. *PKD2* presents a milder form of the disease than *PKD1*, but in general terms, mutations of *PKD1* and *PKD2* show similar clinical phenotypes. Also, alterations in certain regions could result in variation of the protein function, driving to different levels of severity (Torra et al., 1997). The role of genes acting as modifiers, like eNOS and CFTR, has been studied which, (Persu et al., 2002, Osullivan et al., 1998) depending of their splice pattern, act in a beneficial or unhelpful manner in disease progression. The third possibility of a potential influence on intrafamilial variability is the recessive nature of ADPKD at the cellular level. This phenomenon is called second-hit, because even having an autosomal dominant transmission, the cyst formation requires a second somatic mutation at the cellular level and a monoclonal growth for its expansion (Figure 3). Qian et al (1999) review that only 2% of the nephrons acquire a second somatic mutation to form a cyst and suggested that the number of second-hits could be affected either by environmental or genetic factors, giving the phenotypic variability within a family with the same genomic mutation.

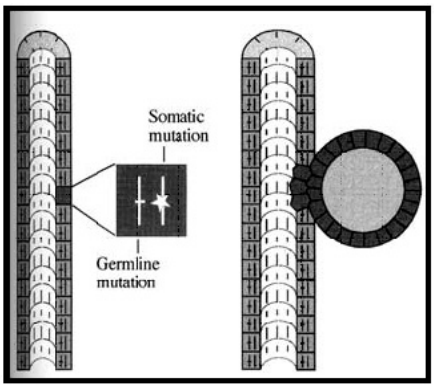

Figure 3. Knudson's "two-hit" model is the likely explanation for the focal cyst formation seen in ADPKD. *Reproduced from Qian and Watnick, 1999.*

Up to this moment, there is no effective therapy for ADPKD other than treatment for hypertension, tract infections, dialysis or kidney transplantation. Several treatment theories have been tested in mouse and rat cystic models for PKD with a different outcome. Restrictive protein diets and vasopressin V2 receptor antagonists have been shown to be beneficial for the disease progression in these models (Gattone et al., 2003, Torres et al., 2004), but there is still not a truly effective therapy that could be applied in humans. Antimutagens or antioxidants (for reducing the number of second-

hits), cAMP (which promotes cell proliferation and secretion into the cyst) antagonists and retinoids and vitamin D (modulators of proliferation, apoptosis and cell growth) are other modulators hypothesized to be possibly effective targets for therapies.

1.1.2. ADPKD Genes: PKD1 and PKD2.

As previously mentioned, *PKD1* and *PKD2* are the genes link to ADPKD. PKD1 is a 53 kb gene mapped into the chromosome 16p13.3 (Reeders et al., 1985) which consists of 46 exons yielding a predicted transcript of 14 kb in length with a 228 nucleotides 5´ untranslated region (UTR) and a 1019 nucleotides in the 3´UTR (European Polycystic Kidney Disease Consortium, 1994; Burn et al., 1995; International Polycystic Kidney Disease Consortium, 1995; Hughes et al., 1995) Its genomic structure has a number of features that complicate its evaluation and likely contribute to its frequent mutation rate (Burn et al., 1995) such as:

- It is highly GC-rich with a large number of CpG dinucleotides –known hot spots for C-T transitions.
- ~70% of the gene's length is replicated multiple times elsewhere on chromosome 16 with high sequence fidelity (95% identity) (European Polycystic Kidney Disease Consortium, 1994; Burn et al., 1995; Bogdanova et al., 2001; Watnick et al., 1998).

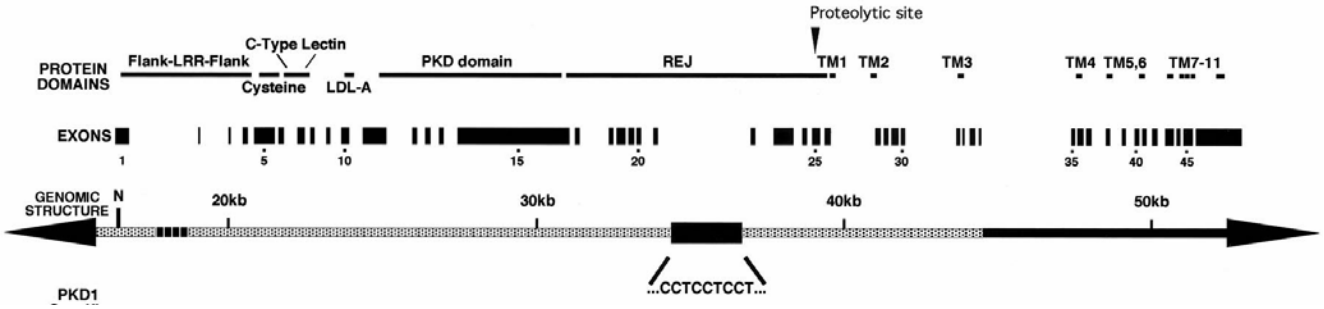

Figure 4. Genomic structure of PKD1. *PKD1* extends approximately 50 kb and contains 46 exons. It is bisected by two large polypyrimidine tracts, of approximately 2.5 and 0.5 kb, in introns 21 and 22, respectively (...CCTCCTCCT...). The replicated portion of the gene begins before the 5' untranslated region and is thought to end in exon 34 (stippled rectangle). LRR, leucine-rich repeats; LDL-A, low-density lipoprotein type A; REJ, receptor for egg jelly motif; TM, transmembrane domain. *J Am Soc Nephrol. 2001 May;12(5):955-63.*

- PKD1 contains a 2.5 kb polypyrimidine tract (largest in the human genome) in intron 21, possibly able to form a triple-helical structure which may play a role in the mutability of neighboring areas (Figure 4, Patel et al., 2004).

These structures may regulate DNA replication, RNA transcription and processing, induce mutations in neighboring sequences and enhance recombination between homologous sequences (Wang et al., 1996; Faruqi et al., 2000).

The search for mutations in PKD1 has been difficult; they have been found spread across the gene, there is no a major recurrence of a particular mutation in the ADPKD population and PKD1 is a big gene with 5 pseudogenes. These pseudogenes make very difficult to differentiate between the sequence of PKD1 and its homologues (European Polycystic Disease Consortium, 1994). In 1997, Watnick et al. published a strategy avoiding this problem, using a long-range PCR based on specific primers for *PKD1*, diluting it $1x10^4$ and performing nested PCRs to analyze the exonic sequences. This new technique has allowed for additional advances in mutational screening; however it has still not become practical for diagnostic purposes.

Mutations in *PKD1* account for approximately 85% of ADPKD cases, and the remaining have been found in *PKD2.* In 1996, Mochizuki et al. mapped *PKD2* in chromosome 4q21-23 showing that three non-related families contained nonsense mutations in a gene with homology to *PKD1* (~25% identity and ~50% similarity). The genomic DNA of *PKD2* spans over 68 kb and contains 15 exons and mRNA is 5.4 kb with an open reading frame of 968 amino acids predicted to have a molecular weight of 110 kDa (Figure 5).

A small number of families have another form that has not yet been mapped (Daoust et al., 1995; Bogdanove et al., 1995; de Almeida et al., 1995; Ariza et al., 1997., McConnell et al., 2001). These unlinked families may be the result of methodological errors or complicated bilineal inherence (Paterson et al., 1998A; Paterson et al., 1998B; Pei et al., 2001).

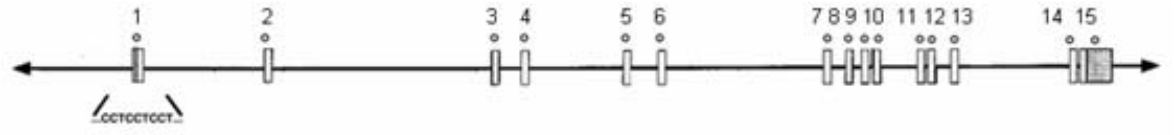

Figure 5. Genomic structure of PKD2. PKD2 extends over 68Kb and contains 15 exons. Exon1 is highly rich in GC%

1.1.3. PKD1 and PKD2 protein products: Polycystin-1 and Polycystin-2.

The protein product of *PKD1*, polycystin-1 (PC1), is 4302 amino acids in length with a predicted molecular weight of 462 kDa (International Polycystic Kidney Disease Consortium, 1995). Hughes et al. (1995) predicted polycystin-1 to be an 11-transmembrane protein with a large extracellular domain of approximately 2550 amino acids, and a short intracellular C-terminal domain of approximately 225 amino acids (Figure 6). In the large N-terminal extracellular domain there are multiple motifs that could suggest a role for polycystin-1 in cell-cell and cell-matrix interactions:

- two leucine-rich repeats (LRR), probably associated in protein-protein interactions, flanked by cysteine-rich repeats (exons 2 and 3),
- a C-type lectin domain, which is thought to be involved in the extracellular binding of carbohydrates, and possibly play a role in cell adhesion,
- a LDL-A domain usually found in tandem arrays on lipoprotein receptors, and are possibly involved in ligand-binding (exon 10),
- 16 PKD domains, similar to the Immunoglobulin domains, a ligand-binding sites in cell-surface proteins (one copy is in exon 5 and the others are in tandem from exons 11 to 15),
- a receptor for egg jelly (REJ) domain initially described in sea urchin, with unknown function (Moy et al., 1996),
- a G protein-coupled receptor proteolytic site (GPS), previously described as a cleavage site in the neuronal G protein-coupled receptor latrophilin, has been confirm to be present in PD1

(Qian et al., 2002). Cleavage of PD1 has recently been shown to be essential for proper biological function, with cleavage-deficient knock-in mice developing massively cystic kidneys (FASEB meeting, 2005).

In addition to the N-terminal extracellular motifs, there are two notable intracellular motifs:

- the lipoxygenase homology 2 (LH2) domain (a noncatalytic domain thought to facilitate binding),
- an intracellular α-helical coiled-coil domain known to form multimeric complexes with proteins with and without similar coiled-coil domains.

Mochizuki et al. also predicted that the protein product of *PKD2*, polycystin-2 (PC2), has (Figure 6):

- 6 transmembrane domains with the C- and N-terminus in the cytoplasm:
- a large extracellular loop between the 1st and 2nd transmembrane domains
- and in its c-terminus, a α-helical coiled-coil domain necessary for PC1/PC2 and PC2/PC2 interaction and a Ca^{2+}-binding EF-hand motif associated to Ca^{2+}-binding activity.

Polycystin-2 has been shown to function as a non-specific cation channel with highest permeability for calcium and identified as the founding member of the TrpP (transient

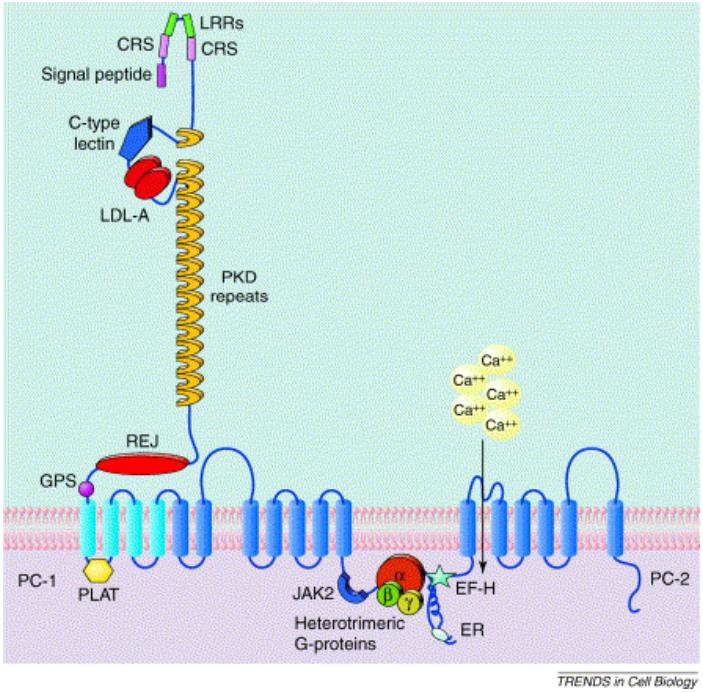

Figure 6. PKD1 and PKD2 protein products: Polycystin-1 and Polycystin-2.

receptor potential) channel family.

1.1.4. Polycystin-1 and –2 localization and expression.

Polycystin-1 and polycystin-2 are integral membrane proteins, but their subcellular localization is still controversial, because they can change their localization dependent of the cell culture model that has been used:

- Using a 3-D model of MDCK cells, Scheffers et al. (2000) found that PC1 was present in the cytoplasm, co-localized in desmosomes in cells and localizes in the membrane only after incorporation of desmoplakin into these desmosomes. On the other hand, Bukanov et al. (2002) showed that PC1 localizes to the basolateral membrane when the MDCK cells form tubules and in cytoplasm when cysts were formed.
- Several studies suggest that the use of overexpression models may lead to different localization patterns than would be seen in the endogenous state. For example, Scheffers et al. found expression of endogenous PC2 in the Golgi apparatus and plasma membrane of MDCK cells, but focally in the ER (Endoplasmic Reticulum) when PC2 was over-expressed (Scheffers et al., 2002). These overexpressed results also were found by Koulen et al. (2002).
- It has also been suggested that, the subcellular localization of these proteins can change in response to the presence or absence of the other protein. Grimm et al. showed that PC1, in the presence of polycystin-2, both localize to the ER, and in the absence of PC2, to the plasma membrane and ER (Grimm et al., 2003). In contrast, mouse and human kidney cells expressing a transgenic human *PKD1* showed that only a small percentage of PC2 colocalized in the plasma membrane with PC-1 (Newby et al., 2002).
- Recently, the community has been interested in the localization to the renal primary cilia of the gene products that are mutated in cystic kidney diseases (Yoder et al., 2002) like PC1 and

PC2 (Nauli et al., 2003), polaris, cystin, nephrocystin, inversin and fibrocystin/polyductin proteins (Morgan, 2002, Wang, 2004) suggesting a potential role of ciliary function and renal flow in the progression of cystic kidney diseases. It has since been suggested that PC1 and PC2 function as flow sensors on renal cilia and control a mechanotransduction pathway.

Recently, a publication by Kottgen et al. suggested that PC2 goes to the membrane, independently of PC1. They showed that PC2 contains a phosphofurin acidic cluster sorting (PACS) protein-interacting binding motif that may play an important role in its trafficking and cellular localization. PACS-1 and PACS-2, through protein casein kinase-2-dependent phosphorylation, obligates PC2 to be retain into the ER. In the absence of phosphorylation or in the absence of the PACS proteins, PC2 would be trafficked to the plasma membrane (Kottgen et al., 2005).

The published data of PC1 and PC2 tissue distribution is less controversial. PC1 appears to have low-level expression in most adult and fetal tissues, with the highest expression level in hepatocytes, fetal kidney, in cystic liver and in cystic kidney (Geng et al., 1997; Peters et al., 1999; Chauvet et al., 2002, Ward et al., 1996). A PC2 expression level seems to be higher than PC1 with similar localization, and is expressed in most adult and fetal tissues (Ong et al., 1999).

1.1.5. Polycystin-1's interacting partners and signaling pathways.

Similarities in the disease progression of patients, coiled-coil domains in both C-termini and similar localization would lead to hypothesized PC1/PC2 physical interaction or its involvement in some common signaling pathways. Qian et al. (1997) showed that PC1 and PC2 interact through their coiled-coil domain in the C-terminus (Figure 6), and naturally occurring mutations in these C-terminal domains disrupted this association. Hanaoka et al. demonstrated that the interaction between PC1 and PC2 create a new calcium-permeable nonselective cation current, and this interaction is necessary for

the regulation of PC2's channel activity and other signaling properties of both proteins (Hanaoka et al., 2000).

PC1's protein structure would suggest that it plays a role in cell-cell interactions and intracellular signaling cascades. Several proteins have been associated PC-1:

- *Cell Matrix proteins*. PC1 co-localizes and co-precipitates with E-cadherin, and α-, β-, and γ-catenin, and is also capable of co-immunoprecipitating them (Huan et al., 1999).
- *Proteins involved in the intermediate filament network.* C-terminal tail of polycystin-1 was able to bind to vimentin, as well as to cytokeratins K8 and K18 (Xu et al., 2001).
- *β-catenin and Wnt signaling.* An integral membrane protein containing the PC1 terminal tail, an extracellular domain of CD16 and a transmembrane domain of CD7 cause elevated levels of β-catenin in Hek293 cells and defects in dorsalization when injected in zebra fish, a phenomenon linked to alterations in Wnt signaling (Kim et al., 1999).
- *G-protein coupled signaling.* Several studies have suggested that polycystin-1 initiates heterotrimeric G-protein coupled signal transduction. A 20 amino acid heterotrimeric G-protein activation sequence in the C-terminus of PC1, a 74-amino acid G-protein binding region that contains the G-protein activation peptide, flanking tyrosine and serine phosphorylation motifs were found by Parnell et al. Polycystin-1 lacks most of the other characteristic of a GPCR, which could suggest to be the founding member of a new GPCRs family (Parnell et al., 1998). Kim et al showed an interaction of PC1 C-terminus with a family member of the G-protein signaling regulators, RGS7, accelerator of the of the Gαi and Gαq subunits intrinsic activity (Kim et al., 1999). More recently, Puri et al. showed that c-terminus PC1 was able to activate NFAT, increased by the inhibition of GSK-3β or by Gαq co-expression (Puri et al., 2004).

- *Activation of JNK kinase and AP-1.* Overexpression of the PC1 C-terminus in mammalian cell lines increase JNK kinase activity leading to the activation of the transcription factor AP-1. This activation was abolished when cells were transfected with dominant negative mutants of GTP-binding proteins Rac-1 and Cdc42, suggesting a role for the Rho family of GTP-binding proteins in polycystin-1 signaling pathways, as well as possible downstream transcriptional alterations in the absence of PC-1 expression (Arnould et al., 1998).
- *Activate JAK/STAT signaling.* Bhunia et al. showed that PC1 up regulates $p21^{waf1}$ and induces cell cycle arrest in G0/G1 phase dependent of the PC-2 co-expression (Figure 6). Also, they showed that *Pkd1*$^{-/-}$ embryos had decreased STAT1 phosphorylation and $p21^{waf1}$ induction (Bhunia et al., 2002).

Most of these models used parts of PC1 because it is very difficult to manipulate the full-length in cell culture systems. However, Boletta et al. developed a stably transfected MDCK cell line expressing the full-length human polycystin-1 protein, slowing the growth rate and protecting them from apoptosis. Additionally these cells were capable of forming spontaneous branching tubules when grown in a collagen matrix, whereas control cells formed cystic structures. They proposed that PC1 play a potential role in cellular differentiation, in the regulation of proliferation and apoptosis, both implicated in cyst formation (Boletta et al., 2000).

The function and signaling pathways of PC1 are still very poorly understood, but we can say that the loss of polycystins results in a detrimental dysregulation of cell proliferation and apoptosis, as well as altered fluid secretion and a disruption of cell-cell and cell-matrix interactions

1.1.6. Murine models of ADPKD.

PKD1 and *PKD2* homologues have been discovered in a variety of organisms, including mouse. Numerous murine models have been created disrupting either *Pkd1* or *Pkd2*, exhibiting similar phenotypes to those found in patients which make them very useful models. The mouse *Pkd1* gene is localized to chromosome 17 with a 79% identity to human *PKD1* at the amino acid level. The cloned cDNA contains 14141 bp and is predicted to have a protein product of 4293 amino acids in length (Olsson et al., 1996). The gene is pretty similar to human *PKD1* and has been shown to contain many of the same protein domains. Several models have been developed for *Pkd1*:

- *Knockout models for Pkd1*. These models try to disrupt PC1 by introducing mutations or cassettes of DNA (LacZ, PgkNeo …) with several Stop codons or deleting critical coding regions. Basically, all of them manifest same phenotypes: Heterozygous mice are basically normal developing few, if any, polycystic kidneys (Figure 7) and liver disease. Homozygous mice die in utero around day e12.5-e18-5, developing kidney cysts at day e15.5, and develop pancreatic cysts as early as day e13.5. A few die shortly after birth with massively cystic kidneys and hypoplastic lungs. This finding suggested that PC1 is not necessary in the early stages of tubule development, but rather plays a role in the establishment and maintenance of normal tubular architecture. (Lu et al., 1997, Guay-Woodford et al., 2003).

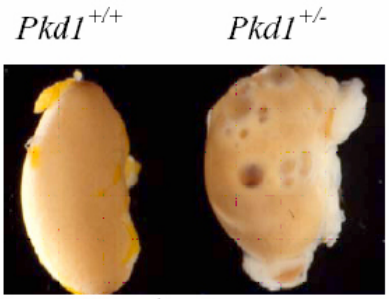

Figure 7. Pkd1$^{-/+}$ mice occasionally develop cystic kidneys when they are more than 1 year of age. *Donated by Dr. Germino's group.*

- *Pkd1$^{-/-}$* embryos also presented other extrarenal manifestations, defects in skeletal development (Lu et al., 2001), cardiac and vascular defects (Boulter et al., 2001), vascular leakiness, polyhydramnios, hydrops fetalis (systemic edema of the entire embryo), and hemorrhages (Kim

et al., 2000) in a variety of different locations (including but not limited to the skin, neck and brain, Figure 8).

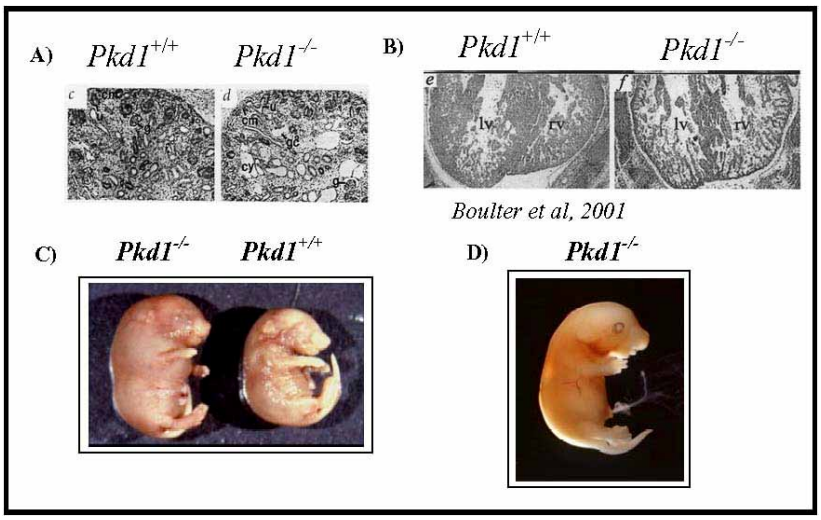

Figure 8: Representative phenotypes seen in Pkd null animals. A) Cyst formation in 15.5dpc embryonic kidneys, B) Disorganized myocardium of embryonic hearts C) Edema D) Hemorrhage. *Figure 8, A, C and D where donated by Dr. Germino's group*

- Piontek et al., (2004) has recently developed a conditional *Pkd1* mouse line that allows inactivating Pkd1 gene in a tissue and time specific manner, using the Cre/lox system. This line contains an FRT-flanked neomycin cassette inserted into intron 1 of *Pkd1* and loxP sites inserted into introns 1 and 4. The loxP sites are specific 34 base pairs sequence originally from bacteriophage that, in presence of Cre (cyclization recombination), catalyze the deletion of the sequence between them by reciprocal recombination. Using cell type specific promoter for Cre, the deletion can be controlled whenever wanted in a specific cell type or tissue (Figure 9). These *Pkd1*$^{del2\text{-}4/Cond}$ mice

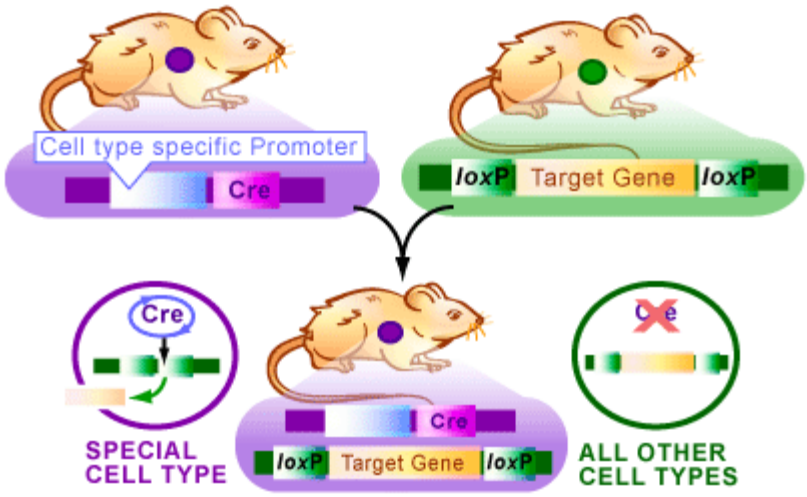

Figure 9. Cre/lox Mouse Breeding. Mice with the Cre protein expressing in a specific cell type are bred with mice that contain a target gene surrounded by *loxP* sites. When the mice are bred, the cells carrying Cre will cause those cells to lose the target gene. *www.bioteach.ubc.ca*

(completed normal before Cre-mediated deletion) crossed to an MMTV-Cre transgenic, where Cre is expressed in a mosaic pattern at low levels in tissues including the kidney and liver, it is the first model that mimics the human disease having a germline and a somatic mutation. Additionally, Piontek et al. conditionally inactivate *Pkd1* in epiblast-derived tissues using Cre recombinase regulated by the *Meox2* promoter (*Meox2-Cre*), thus sparing the placenta. 66% of *Pkd1* mutants survive to birth dying shortly after birth of respiratory failure with massive PKD, edema and hemorrhage. This model showed that placental abnormalities play a significant role in fetal demise and collectively these animal models have demonstrated an essential developmental role for both polycystin genes.

- New insights in renal cystogenesis in $Pkd1^{-/-}$ mice were generated by Nishio et al. (2005). Using $Pkd1^{-/-}$ES cells and $Pkd1^{+/+}$ morulae they generate a chimeric mouse which developed cystic kidneys containing both $Pkd1^{-/-}$ and $Pkd1^{+/+}$ cells, liver and pancreas similar to previously established models. The progression of cyst formation was driven by a shift of the $Pkd1^{-/-}$cells from a cuboidal shape to a flat cell shape, proliferating and replacing the $Pkd1^{+/+}$ cells through JNK-mediated apoptosis to form larger endstage cysts.

The mouse *Pkd2* gene is been mapped on chromosome 5 with a 91% identity and 98% similarity to the human PC2. The cloned cDNA contains 5134 bp and is predicted to have a protein product of 966 amino acids, forming a similar 6 transmembrane-domain protein with both N- and C-termini in the cytoplasm (Wu et al., 1997). Several *Pkd2* animal models have also been created showing similar phenotype to the *Pkd1* animals (Wu et al., 2000), and an interesting left/right axis lateralization defect associated with the dysregulated expression of genes involved in laterality, LeftB, nodal, Ebaf, and Pitx2 (Pennekamp et al., 2002). Wu et al. created another interesting *PKD2* model generating an

unstable *PKD2* allele which generates both a mutant and a wild-type exon 1, which then undergoes a somatic conversion *in vivo*, causing eventually a second-hit similar to human disease. When both alleles in these mice become null, they saw the development of clonally expanded cysts, supporting the idea of a two-hit model of ADPKD cyst formation (Wu et al., 1998).

Up to this moment, no Pkd2 conditional knockout mouse has been described, like in Pkd1, which helps to study ADPKD in a time and tissue specific manner. In this thesis, we describe the first conditional *Pkd2* model that, using a Cre/lox system, will help to find different aspects of the disease pathogenesis. This model has an additional aspect to $Pkd1^{Cond}$ model, which makes it more interesting. The conditional allele, with a Pgk-Neomycin cassette in intro 13, works as a hypomorphic allele associated with a severe vascular phenotype. $Pkd2^{flox11\text{-}13}$ is a powerful tool not only for studying ADPKD, but also to define the biology and the implicated aspects responsible of the vascular phenotype in humans.

1.2. Autosomal Recessive Polycystic kidney Disease (ARPKD).

1.2.1. Clinical Manifestations of ADPKD.

ARPKD is a hereditary cystic disease is a significant cause of pediatric morbidity and mortality affecting the kidneys and the biliary tract (Osathanondh et al., 1963; Osathanondh et al., 1964) with an estimated incidence of 1 in 20,000 live births (Zerres et al., 1998). 50% of the affected neonates die shortly after birth by respiratory insufficiency with a critical degree of pulmonary hypoplasia, enlarged echogenic kidneys and oligohydramnios due to poor renal output. The oligohydramnios cause the Potter sequence with pulmonary hypoplasia, characteristic facies, and deformities of the spine and limbs (Reuss et al., 1990). The other half, survive to adulthood with chronic lung disease (12%), hypertension, progressive renal insufficiency with 50% of them developing ESRD in the first decade, and portal tract fibrosis (Guay-Woodford et al., 1996; Roy et al., 1997, Fonck et al, 2001, Guay-

Woodford et al., 2003)

The kidney phenotype of affected neonates consists in a symmetric enlargement of both kidneys with dilated collecting ducts extended radially from the renal pelvis to the cortex (Holthofer et al., 1990). In less severely affected children, the collecting duct dilation is less prominent and the course is more chronic with loss of glomeruli, tubular atrophy and interstitial fibrosis (Fonck et al., 2001). The number and distribution of collecting ducts and nephrons are appropriate (Osathanondh et al., 1964) and there is no evidence of either tubular obstruction or dysplastic elements (Kissane et al., 1990). Hypertension occurs in 75-100% of patients which is typically quite severe and develops in the context of a normal GFR (Guay-Woodford et al., 2003; Zerres et al., 1996).

ARPKD livers showed congenital hepatic fibrosis. This consisted of abnormal development of biliary tree, increasing the number of tortuous interlobular bile ducts located in the periphery of the portal tract. Only a few, if any, normal bile ducts are evident. There are varying degrees of portal fibrosis, hypoplasia of the small portal vein branches, and hepatic arteriolar prominence (Bernstein et al., 1992; Desmet et al., 1992). The degree of portal tract fibrosis defines the clinical manifestations which it is quite variable (D'Agati et al., 1994).

1.2.2.. ARPKD gene: PKHD1.

Initial molecular genetic studies had shown that all typical ARPKD manifestations, including perinatal and late onset, result from mutations at a single locus (Zerres et al., 1994; Guay-Woodford et al., 1995). At the time that this disease started to be seriously considered, Lens et al. (1997) suggested that the *PKHD1* gene was localized in a critical region of < 3.1 Mb (Figure 10). As a continuation of Lens results, Dr. Onuchic used recombination-mapping studies to reduced candidate region into a large region (~500kb) of chromosome 6p12 (Figure 11). *PKHD1* is predicted to have a minimum of 86 exons assembled in a complicated pattern of alternative splice variants which transcribes a large full-

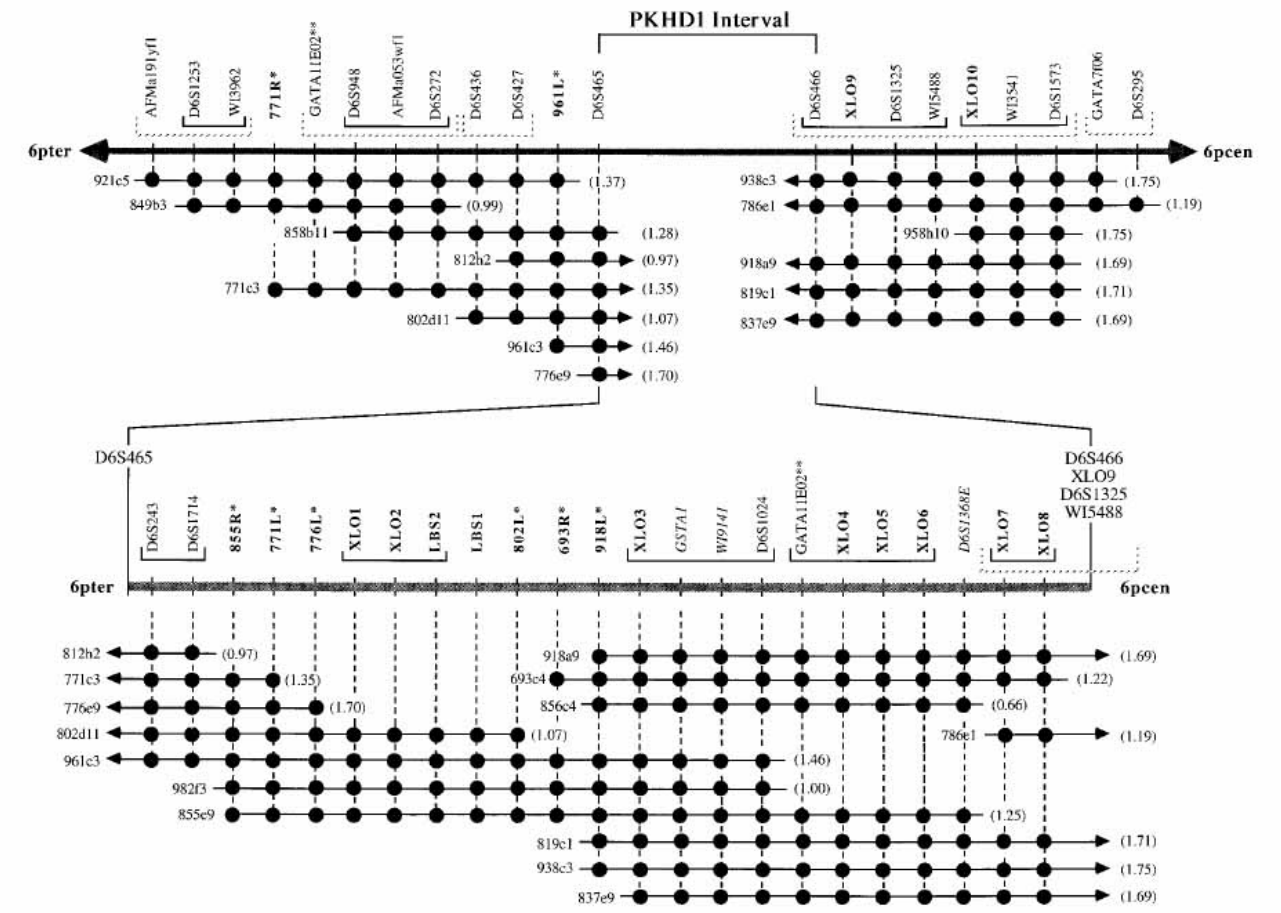

Figure 10. STS contig map of the PKHD1 interval and flanking region. At the top, the 5-cM segment defined by the markers D6S1253 and D6S295, which includes the PKHD1 interval, is indicated by a horizontal arrow. The markers are listed in physical order across the top and the corresponding YACs are shown below. The markers presented in boldface were isolated in the current study. A more detailed map of the minimal PKHD1 interval is presented at the bottom. The CEPH identification number of each YAC is listed on the left, and its size as listed in the database is shown in parentheses on the right. Solid dots indicate confirmed marker content. YAC ends are identified by a single asterisk. GATA11E02 maps to two unique positions within the contig (double asterisk). The three ESTs in the interval are italicized. Solid brackets define sets of markers within which individual STSs cannot be physically ordered. Dotted brackets identify sets of markers whose relative order has been determined based upon evidence from a single YAC. YAC 961c3 is prone to acquiring an internal deletion that removes markers LBS1, 802L, and 693R. The deletion allows ordering of the markers LBS1 and LBS2. The position of markers has been evenly spaced in the region and does not reflect true physical distances. Genomics 1;41(3):463-6(1997).

length mRNA of ~13kb and encodes a full-length protein of 4074aa.

The protein, polyductin-1 (PD-1) is predicted to be a type I membrane protein that with multiple IPT and PbH1 repeats in the extracellular N-terminus and a short cytoplasmic C-terminus of ~200aa. PD1 function is still unknown, but based on its structure is predicted to function as either a receptor or

ligand.

Ward et al, 2002, using a comparative genomic approach, identified the gene at the same time as Onuchic using a mutation detection strategy in both the PCK rat and human ARPKD. They named the protein product of *PKHD1* as fibrocystin,

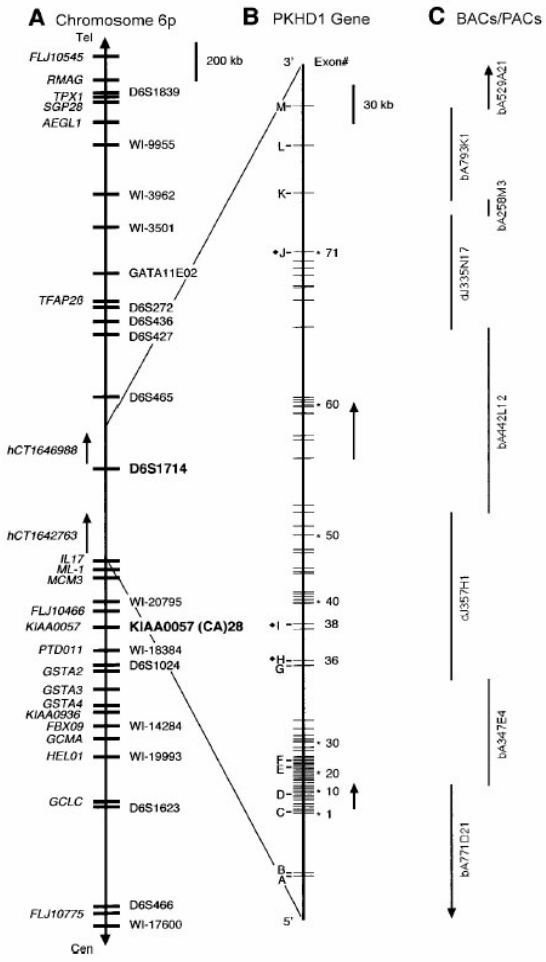

Figure 11. Chromosomal localization and genomic organization of PKHD1.
A, Schematic representation of chromosome 6p12. Currently known genes are identified on the far left (italics), and STSs/polymorphic markers are on the right. The closest flanking genetic markers that define the minimal PKHD1 interval are indicated (boldface). Not all of the 35 overlapping sets of expressed sequences described in the text are shown. B, Genomic organization of PKHD1. Exons identified by numbers have been shown to be part of PKHD1 transcripts. Letters indicate exons that belong to either hCT1642763 or hCT1646988 and that have not been confirmed by our analyses. The black diamond identifies, in hCT1642763 and hCT1646988, overlapping exons whose boundaries differ from those used in the present study. Arrows indicate the positions of the Gene Unit 6 and Gene Unit 442L12 transcripts described in the text. C, BACs and PACs sequenced by the Sanger Centre that cover the interval.

generating a controversy about the right way to call this protein. To avoid any conflict, many groups in the community decided to name it as Polyductin/Fibrocystin-1. Because the ARPKD work of this thesis is been develop based on Lens and Onuchic previous results and interaction with them, we will use Polyductin-1 as the term to define the PKHD1 product. The two groups independently identified essentially identical sequences for the transcript that encodes the longest open reading frame. Both groups equally concluded that Northern blots of kidney tissue for *PKHD1* showed a high molecular weight smear, but their interpretation of the significance and cause of the smear was different. Ward et al. suggested that this smear was likely the result of specific properties of the *PKHD1* transcript that made it unstable and prone to rapid degradation. On the other hand, Onuchic et al. postulated that the

smear might be the result of the gene's complicated pattern of splicing.

Since PKHD1 undergoes a very complicated splice pattern it was very difficult to predict the exonic/intronic structure of the gene. Onuchic et al. (2002) discovered that the amplification of two long RT-PCR products containing the longest open reading frame (ORF) predicted that PKHD1 contained 67 exons transcribing a 12.6 kb full-length cDNA (Figure 12B). But this is not the total exon number of PKHD1; they found a substantial number of additional exons that were variably present in *PKHD1* transcripts, predicting a conservative estimation of at least 86 exons (Figure 12A). A large number of distinct transcripts were found as the result of

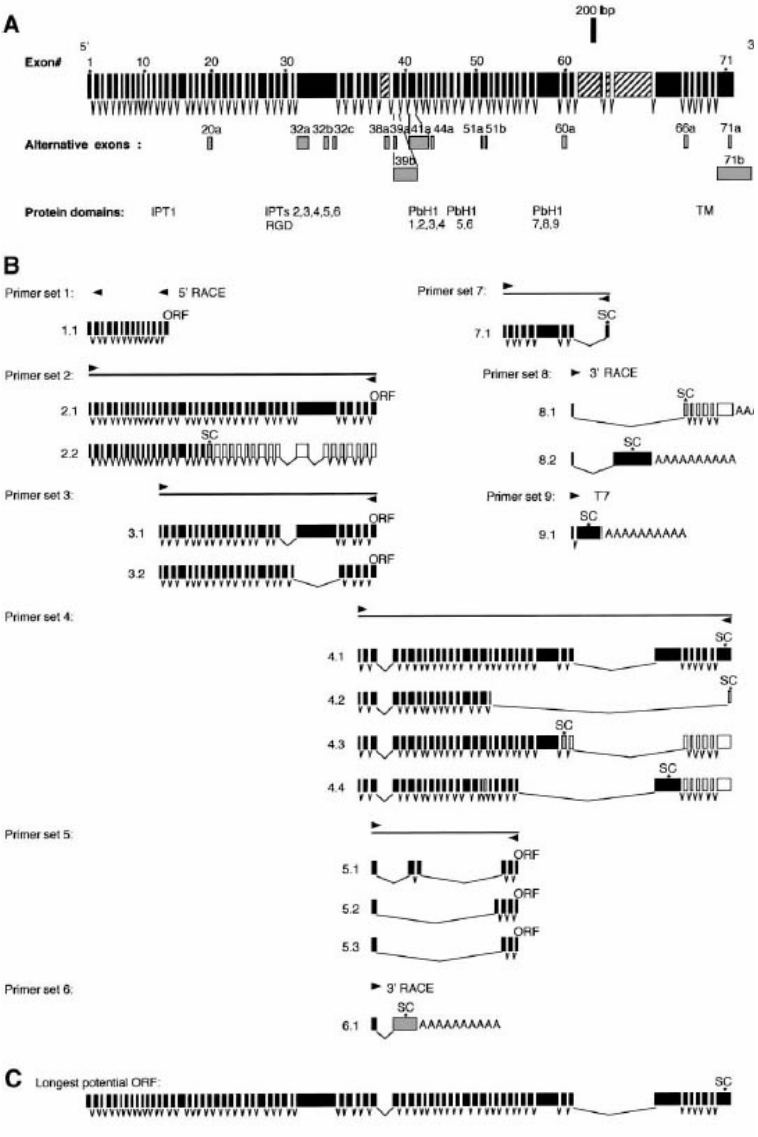

Figure 12. Structure of full-length PKHD1 and its splicing variants. A, Set of 71 nonoverlapping exons that spans the entire length of PKHD1 (upper row) and 15 additional overlapping exons that use different splice sites (gray boxes, lower row). Exons, which are not present in the cDNA that encodes the longest ORF, are indicated by hatched boxes. The position of important protein domains is indicated. B, Approximate location of each primer set used to amplify various cDNAs, with representative set of amplified products (below each schema). White boxes indicate noncoding exons in the corresponding transcripts while gray boxes identify exons with alternative boundaries (A). The templates used for each amplification are as follows: human adult kidney double-stranded cDNA for primer sets 1–4, 6, and 8; human kidney mRNA and total RNA for primer sets 5 and 7; human adult kidney cDNA library for primer set 9. "SC" indicates approximate location of stop codons, and "ORF" indicates that an open reading frame extends throughout the length of the fragment. C, Longest ORF identified by RT-PCR/cDNA amplification. This ORF is the composite sequence of products 2.1 and 4.1 of panel B and includes a total of 67 exons. Am. J Hum Genet. 2002 May;70(5): 1305-17.

the alternative exons combination, but also having the unique combination of the 67 ORF-related *PKHD1* exons (Figure 12C). It has been not described how many of the transcripts are translated into protein, but it can be easily imagined that this single gene might encode numerous distinct polypeptides.

Recently, PKHD1 has been describe to have a homologue named *PKHDL1*, with an identity of 25.0% and similarity of 41.5%, predicted to function as a receptor with inducible T lymphocyte expression (Hogan et al., 2003).

1.2.3. Polyductin/Fibrocystin-1, expression and location.

This novel protein of 4,074 amino acids, which Onuchic et al. (2002) have named "polyductin" (PD1) and Ward et al. (2002) has called "fibrocystin", is predicted by SMART to be a Type I membrane protein with a 3,858 amino acid extracellular amino terminus, a single transmembrane-spanning domain, and a short carboxyl terminus (Figure 13). PD1 contains multiple IPT domains, mostly related with a number of receptor molecules such as HGFR and plexin A3, and PbH1 repeats most commonly associated with polysaccharidases. Multiple potential N-glycosylation sites and three putative cAMP/cGMP phosphorylation sites were predicted within the cytoplasmic C-terminus. The overall structure suggests that PD-1 acts as either a ligand or a receptor (or both) involved in either cell-cell recognition or cell-

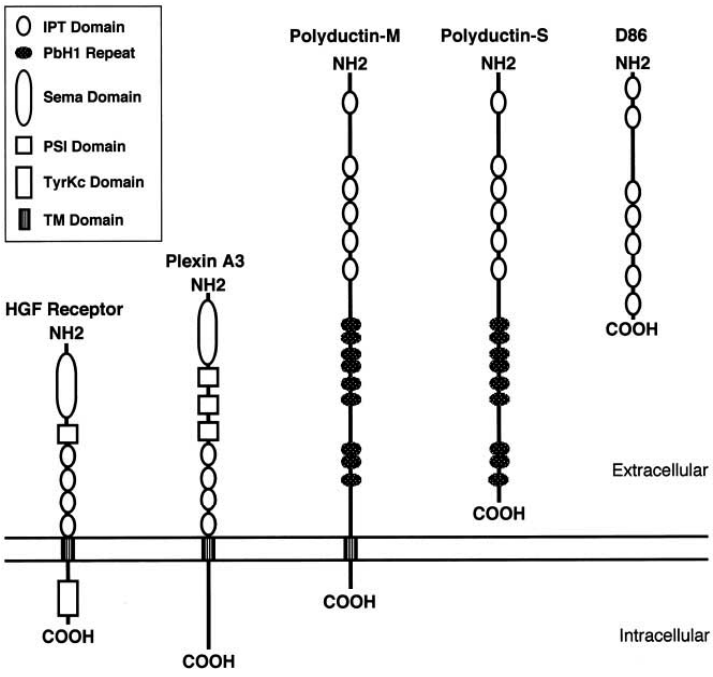

Figure 13. Structure of polyductin and related proteins. Multiple tandemly repeated IPT domains are common features of the group. Polyductin-M shares the general structure of the HGFR and plexin A3, in having a long extracellular domain, a single TM domain, and a short cytoplasmic carboxyl terminus. Am. J Hum Genet. 2002 May;70(5): 1305-17.

matrix interactions. The prediction for the translated alternative splice products classifies the PD-1 isoforms into two groups:

- The first group includes the longest continuous ORF which may also contain molecules lacking some middle domains, a single TM element, and may be associated with the plasma membrane (PD1-M, Figure 13).
- A second group of isoforms lacking the TM domain, that probably may be secreted (PD1-S, Figure 13).

A possible third group would behave similar to neurexin family of genes (Missler et al., 1998), coding shorter fragments with variable number of IPT and PbH1 domains, and different specificities or binding affinities for targeting factors.

Several studies have localized PD-1 in the cilia/basal body and possibly other sub-cellular locations like apical membrane and in cytoplasm (Ward et al., 2003; Wang et al., 2004; Zhang et al., 2004, Menezes et al., 2004). Renal cystic disease has been associated with defects in the function of primary cilia, being suggested by many investigators that cilia may hold the key to understanding renal tubular structure and function (see review by Watnick T et al., 2003). Interestingly, a recent comparative genomic strategy comparing genomes of species with and without flagella/basal bodies identified a *PKHD1*-related gene as a probable component of the Flagellar Apparatus Basal Body Proteome (Li et al., 2004).

Human PD-1 has been shown to be primarily expressed in blood-derived cell-lines and upregulated in T cells following activation, biliary and pancreatic duct epithelia, and in cortical and medullary collecting ducts and thick ascending limbs of Henle of the kidney. Analyses of mouse developing tissues showed specific staining in the ureteric bud branches, intra- and extrahepatic biliary ducts, pancreatic ducts, and salivary glands (Menezes et al., 2004).

1.2.4. Polyductin-1's interacting partners and signaling pathways.

This area is a new land to discover but, recently, Kaimori et al. (oral communication at the ASN, 2005) suggested that PD-1 has opposing effects on canonical Wnt signaling and marked effects on cellular morphology that depend on cell density.

1.2.5. PKHD1 animal models.

Up until now, there are not many animal models described for PKHD1. The *PCK* rat, used by Ward et al to identify human *PKHD1*, was the first animal model for ARPKD (Lager et al., 2001). These rats develop progressive cystic enlargement after one week of age with the cysts arising from the thick ascending limb of Henle's loop (TAL), distal tube (DT) and collecting duct (CD) in the corticomedullary region and outer medulla. The rats also develop severe polycystic liver disease, with bile duct abnormalities present at birth. The biliary tree is markedly distorted, showing multiple dilatations of the bile ducts and focal budding. Cholangiocyte cilia in the PCK rat were abnormal with bulbous extensions and diminished length. Recently, the kidneys of *PCK* rats have been shown to have dysregulated renal cAMP activity that responded well to treatment with V2 receptor antagonists (Gattone et al., 2003) improving the kidney function.

Unfortunately, many investigators consider the rat as an expensive and limited model for the analysis of diseases. Several groups have failed to develop a mouse model that mimics the human disease (Moser et al., 2005). This could be related to the complicated splice phenomenons of *Pkhd1*, limiting the possible strategies applicable for the generation of the model. In this thesis, we describe the first mouse model for ARPKD mimicking the human disease, by using a floxed system that allows tissue and timed the conditional inactivation of the gene.

2. Aims

2.1. General Aims

One major obstacle to develop a therapy for polycystic kidney disease is the limited understanding of the disease into the genetic, molecular and pathogenic level. This thesis introduces the first genetic test for clinical diagnosis of ADPKD (PKDX, Athena Diagnostics). The importance of the PKDX test is enormous, because it could be used for diagnostic uncertainties, pre-symptomatic evaluations, donor testing for living-related transplants, etc. The basis of this test was basically developed by scientific investigators from the Germino laboratory, applying their knowledge and methods for complete sequencing of the PKD genes. The major goals of this thesis was to help in the development of these methods and, together with Athena Diagnostics, test the efficiency and establish a classification for the genetic changes found in ADPKD patients. Using the information provided by the analysis of the PKD genes (structure, composition, organization, etc) and the genetic changes found on the ADPKD patients; it will be establish a statistical method to help in a better knowledge of the these genes and the mutagenesis mechanisms involved on them. A parallel aim is to understand how mutations result in the disease phenotype and try to get a mechanistic understanding of the disease process, which can then be used to guide the rational development of therapies.

To develop therapies for ADPKD and ARPKD, it is necessary to generate first the tools (molecular genetic studies, *in vitro* culture systems, and genetically faithful mouse models in an integrated fashion). As mentioned in the introduction, it has been describe a very useful *Pkd1* mouse model able to control its inactivation in a temporal and spatial specific manner. A very big goal for this thesis is, to generate novel ADPKD ($Pkd2^{flox11\text{-}13}$) and ARPKD ($Pkhd1^{flox3\text{-}4}$) conditional mouse models to be applied for a better understanding of the biological consequences caused by their mutations and

their application for development of a therapy.

2.2. Specific Aims.

2.2.1 SUBPROJECT I: Mutational screening and analysis of the entire PKD1 and PKD2 genes in 82 unrelated ADPKD families through the clinical /genetic PKDX test.

- *Aim #1:* Design of a mutation analysis strategy to help in the develop of a clinical/genetic test for the ADPKD genes (*PKDX*® test).
- *Aim #2:* Check the efficiency of *PKDX*® test in a group of 82 unrelated ADPKD families.
- *Aim #3:* Analysis and classification of the changes found in *PKD1* and *PKD2* genes
- *Aim #4:* Develop of a statistical method for the analysis of gene behavior.
- *Aim #5:* Test of this statistical method in the PKD genes.

2.2.2 SUBPROJECT II: Conditional Inactivation of Murine PKD2 using a tri-allelic system.

- *Aim #1:* Create a murine *Pkd2* model using gene targeting techniques.
- *Aim #2:* Test whether the neomycin cassette results in a hypomorphic allele.
- *Aim #3:* Confirm that the floxed allele is functional.
- *Aim #4:* Test whether inactivation of *Pkd2* leads to PKD phenotypes.

2.2.3. SUBPROJECT III: Generation of a conditional murine model of PKHD1 gene.

- *Aim #1: Create a murine Pkhd1 model using gene targeting techniques.*
- *Aim #2: Test the hypothesis that inactivation of mouse Pkhd1 can mimic human ARPKD.*
- *Aim #3: Determine whether PKHD1^{del3-4} is a null allele.*
- *Aim #4: Characterize the complex transcriptional profile in PKHD1.*

3. Mutational screening and analysis of the entire PKD1 and PKD2 genes in 82 unrelated ADPKD Families through the PKDX test (SUBPROJECT I).

3.1. Abstract.

Autosomal dominant polycystic kidney disease (ADPKD) occurs as a result of mutations in either of two genes, *PKD1* or *PKD2*. The disease is characterized by age dependent growth of renal cysts such as ESRD with typically ensues during mid adulthood. Given the age dependent expression of ADPKD, there has been intense interest in developing reliable techniques for presymptomatic DNA diagnosis. These tests have potential value in the pre-transplant evaluation of donors and in early treatment protocols should they become available.

The development of PKD gene testing has been hampered by the complicated structure of the *PKD1* gene. *PKD1* is replicated in several highly homologous copies that make it difficult to assay the bona fide *PKD1* gene. We have overcome these obstacles by developing a long-range PCR technique, which now forms the basis for the only available clinical DNA test (PKDx). In order to assay the sensitivity of this test we collected DNA samples from 82 individuals who were judged to have PKD using standard clinical criteria. Definite disease causing mutations (frameshift, stop codon or splice site) were identified in 34 patients (41.46%, *PKD1*=24, *PKD2*=10). Eight additional patients (9.9%) had in frame deletions or insertions. We observed an extraordinarily high level of variability in the *PKD1* gene with a mean of 13.2 genetic variants per patient (range 0-60). Many of these variants were novel, non-conservative missense changes (36.4% patients). However, the suspected pathogenicity of these amino acid substitutions was difficult to confirm based on our current understanding of PKD1 structure and function. We conclude that clinical interpretation of PKD gene testing will be challenging because of the high frequency of amino acid substitutions in PKD1. These limitations need

to be understood to develop appropriate algorithms for the use of gene testing in ADPKD. Future efforts will focus on developing in vitro systems to evaluate the functional consequences of these mutations.

3.2 Material and Methods.

3.2.1. Patient recruitment.

Eighty-two unrelated ADPKD patients were recruited from an outpatient clinic, after obtaining informed consent and approval from the Ethic Committee and IRB. Some of the probands in this study were subjected to ultrasound criteria for ADPKD diagnosis, linkage equilibrium, and classified according to sex, ethnicity, birth date, family history, renal and extrarenal phenotype criteria (liver aneurysms, other vascular phenotypes, infertility, ESRD, GFR, and others). A blood sample from each proband was then coded and sent to Athena Diagnostics, Inc. for sequence analysis.

3.2.2. Mutation detection and DNA Sequence Analysis.

Sequence analysis of patient samples was performed using methods described in detail previously (Watnick et al., 1997; Watnick et al.,1999; Phakdeekitcharoen et al., 2001) and optimized in collaboration with Athena Diagnostics, Inc. Briefly, genomic DNA was derived from whole blood using a Puregene® DNA extraction kit (Gentra Systems, Inc. Minneapolis, MN). The amplified product served as template for highly specific long-range PCR amplification of eight segments encompassing the entire *PKD1* duplicated region. This crucial step prevents the spurious amplification of *PKD1* homologues that would otherwise confound the analysis. The eight long-range PCR products served as template for 43 nested PCR reactions while the unique region of the *PKD1* gene (Table 2) and the entire *PKD2* gene (Table 3) were amplified from genomic DNA as 28 additional gene segments.

All 71 PCR products were then bi-directionally sequenced using ABI Big Dye terminator chemistry (versions 3.1 and 1.1 depending upon primer position and/or fragment length) followed by

Exonic fragment	Size *bp*	PCR annealing temp. °C	Primers		DHPLC Temp. °C
			Forward (5'-3')	Reverse (5'-3')	
35	219	60	GGGCTTGGCTGCAACTGC	GGAGGGGCTAGGGGCATC	64
36	280	63	CCTCCCTGTGAGCTGCCTCTC	GGCCTGTAGCCTACCCCTGG	65, 66
37	325	61	TCCATCACGGGGGACCCCTCT	AAAGGGGGACAGGAGTGTCCT	65
38	268	60	AAAGCCCTGCTGTCACTGTGG	TAGGGTCTGGCTGGACTAAAG	65
39	265	61	GGGTCTCTGGTGGCCGCTCA	ATGCCAGAGCTCCGCTAAAGG	66
40	265	61	CACTCCTGTTGGGTTTTGATG	CGGCACTCCTGGAGAACTACT	65
41	330	64	CGGCCTCCTGACCAGCCTGGCTC	TAGGCCAGCGGGGGCCGGAGGAGTG	66
42	319	60	TGCCACCCGCTCCTACTGA	TGGAGGCGCGGGGTCT	70
43	378	64	CGTCCCTCCCGCCCTCCTGA	TCTGTCTGCTTGCAGCCCTGGGGTGTG	68
44	285	62	GCCTCGCTGCTCTTCCTG	GCTGAGCTGAGCTAAGACGCCCTCC	64, 66
45	379	61	AGCTCAGCTGTACGCCCTCA	TGTCCCTCTCCCCCCCACTG	65
46a	450	72	GAGAGGGACACGCCCTGGGCTCTGC	GGCAAGGCGGCTGGGCAGTGCTGG	66
46b	240	68	CCCGTGGCCCATCCCCGGGCCTGCGG	TACGTGCAGCCATTCTGCCTGGCCC	66

Table 2. Oligonucleotide primers for templates from exons 34 to 46 of the of PKD1 gene (non-replicated region).

electrophoresis on an ABI 3730 capillary sequencer (Applera Corporation, Norwalk, CT). The entire coding region of the *PKD1* and *PKD2* genes including the highly conserved exon/intron splice junctions between all 61 exons of both genes were analyzed.

Exon	Primers	Sequence (5′ → 3′)	Size (bp)	T_m (°C)
1a	F41	CGC GCC GGA CGC CAG TGA CC	279	72
	R48	CCT GCC GGG AGC ACG ACG AGA GC		
1b	F42	CCG CGG CCT CCC CTT CTC CTC C	291	72
	R49	CTG GGC TGG GGC ACG GCG GG		
1c	F43	GGG GCT ACC ACG GCG CGG GC	220	72
	IR19d	CAG ATG CAC GAA CCA GAA CGG CCG G		
2	IF5	AAA TGA TAT CTT TTC TTT TCT TCA	188	55
	IR20	AAC TTT CCC ATT AGT GCA AG		
3	IF6	CCA AAA TGT TTA TCC ACA GG	268	55
	IR5	AGG TAC TTT CAA AGT TAT TTC CA		
4	IF7	TGG TTA TGC AAC GAT GCA GG	355	63
	IR7b	CCG AGT GCC AAT GAG TCA CA		
5	IF1c	CGG TCA AGT GTT CCA CTG AT	362	58
	IR1	AGG TTT TTC TGG GTA ACC CTA G		
6	IF2	TTT AAT TGT TCT TAT TTA CAT GCA	298	55
	IR8	TTG TAG AAT AGA ATA GGA AAT TTG G		
7	IF8	TTG GTG AAG AAA AAT ATA CTA GTC A	318	55
	IR9	TGG AAC TCA TTT TTT TTA AAG A		
8	IF9b	TTT TAT TAT ACA CAG TCA CAC CA	282	55
	IR10	CTA CTC TGA CTA AAT TTT TCT TCT T		
9	IF15	TTT GGT TTT GTA TTG TGG TG	194	55
	IR21	AAG GAT TTA CGA AGT TTA AAT TG		
10	IF18	TAA TTC CAA ATT ATG TTT CTT CC	216	55
	IR15b	TGA AAC AAT GCT CAT TTT ATG		
11	IF10	AAA CCA AGT CTT TTA TTT TTT CTC	235	55
	IR11	GGG CTA GAA ATA CTC TTA TCA CC		
12	IF11	GAT GAA TGT TAT CTG TAT CCT CTC	221	55
	IR3	TAG GTA CCA AAT CAA ATC CG		
13	IF3	GTC TCA GTG TTC TGC TCC TC	235	55
	IR4	AAA TTC TGC CAA TTC CTT TA		
14	IF17	TGT ACT GTG TTT TCC TTG CA	226	55
	IR17	AAA TAC AAC TGT CAG CAA CAT A		
15	IF12b	ACA CCA GTT TCT TTT TCC CT	382	55
	R14	ATC GGT CAC AAA GAC TAG CA		

Table 3. Oligonucleotide primers for amplifying the exons of the PKD2 gene from genomic DNA.

3.2.3. LR PCR.

Specific details of the primer sequences, annealing temperatures, and extension times used for each LR template of the *PKD1* duplicated region are provided in Table 4. 300 to 400 ng of genomic DNA was used as template for each LR product, except that for exon 1. The LR PCR amplification was performed in a Perkin Elmer 9600 thermal cycler, with denaturation at 95°C for 3 minutes and 35

cycles of a two-step protocol that included denaturation at 95°C for 20 s followed by annealing and extension at a temperature and for a time specific for each primer pair (Table 4). A final extension at 72°C for 10 min was included in each program. The total PCR volume was 50 µl, with 4 U of r*Tth* DNA polymerase XL (Perkin Elmer Cetus, Norwalk, CT) and a final magnesium acetate concentration of 0.9 mM. A hot-start protocol, as recommended by the manufacturer, was used for the first amplification cycle.

Template	Primers	Sequence (5' →3')	Position (5')	Size (kb)	Tm (°C)	ET (min)
T1	BPF14[b]	CCATCCACCTGCTGTGTGACCTGGTAAAT	2043	2.2	69	7
	BPR9	CCACCTCATCGCCCCTTCCTAAGCAT	4290			
T2 to T7	BPF9[b]	ATTTTTTGAGATGGAGCTTCACTCTTGCAGG	17907	4.6	68	7
	BPR4	CGCTCGGCAGGCCCCTAACC	22489			
T8 to T12	BPF12	CCGCCCCCAGGAGCCTAGACG	22218	4.2	68	7
	BPR5[b]	CATCCTGTTCATCCGCTCCACGGTTAC	26363			
T13 to T15	F13	TGGAGGGAGGGACGCCAATC	26246	4.4	68	7
	R27[b]	GTCAACGTGGGCCTCCAAGT	30612			
T15 to T21	F26[b]	AGCGCAACTACTTGGAGGCCC	30603	3.4	70	4.5
	R2	GCAGGGTGAGCAGGTGGGGCCATCCTAC	33953			
T22	BPF15	GAGGCTGTGGGGGTCCAGTCAAGTGG	36815	0.3	72	1
	BPR12[b],[c]	AGGGAGGCAGAGGAAAGGGCCGAAC	37136			
T23 to T28	BPF6	CCCCGTCCTCCCCGTCCTTTTGTC	37325	4.2	69	7
	BPR6[b]	AAGCGCAAAAGGGCTGCGTCG	41524			
T29 to T34	BPF13[b]	GGCCCTCCCTGCCTTCTAGGCG	41504	5.8	68	8
	KG8R25[b]	GTTGCAGCCAAGCCCATGTTA	47316			

Table 4. Oligonucleotide primers for long-range specific templates from exons 1 to 34 of the PKD1 gene . [a]Tm, annealing temperature; ET, extension time. [b]PKD1-specific. [c]Bold type in the BPR12 primer sequence identifies intentional replacement of C by A, to enhance discrimination of PKD1 from the homologues primer. *J Am Soc Nephrol. 2001 May;12(5):955-63.*

For the exon 1 LR product (T1), the LR template was generated using 500 ng of genomic DNA. The LR PCR amplification protocol was modified to include denaturation at 95°C for 1 min and 35 two-step cycles of denaturation at 95°C for 30 s followed by annealing and extension at 69°C for 7 min. The total PCR volume was 50 µl, with 1 µl of Advantage-GC genomic polymerase (Clontech, Palo Alto, CA), GC melt of 1.5 M, and a final magnesium acetate concentration of 1.1 mM.

3.2.4. Mutation Detection.

The LR templates were serially diluted to $1:10^4$ or $1:10^5$, to remove genomic contamination, and were then used as templates for nested PCR of 200- to 400-bp exonic fragments (Watnick et al., 1997; Watnick et al., 1999). The sequences and PCR conditions for each new pair are summarized in Table 5. Intron-based primers were positioned approximately 30 to 50 bp away from consensus splice sites. Exons larger than approximately 400 bp were split into overlapping fragments of ≤350 bp. Two microliters of diluted LR product was used as template for the amplification of each exon.

Exon	Primer Sequence (5'-3')	Fragment Size (bp)	Tm (°C)
1	1F1: 5'-GGTCGCGCTGTGGCGAAGG-3'	328	67
	1R1: 5'-CGGCGGGCGGCATCGT-3'		
	1F2: 5'-ACGGCGGGGCCATGCG-3'	348	67
	1R2: 5'-GCGTCCTGGCCCGCGTCC-3'		
2	2F: 5'-TTGGGGATGCTGGCAATGTG-3'	272	62
	2R: 5'-GGGATTCGGCAAAGCTGATG-3'		
3	3F: 5'-CCATCAGCTTTGCCGAATCC-3'	171	62
	3R: 5'-AGGGCAGAAGGGATATTGGG-3'		
4	4F: 5'-AGACCCTTCCCACCAGACCT-3'	299	62
	4R: 5'-TGAGCCCTGCCCAGTGTCT-3'		
5	5F1: 5'-GAGCCAGGAGGAGCAGAACCC-3'	259	65
	5R1: 5'-AGAGGGACAGGCAGGCAAAGG-3'		
	5F2: 5'-CCCAGCCCTCCAGTGCCT-3'	284	65
	5R2: 5'-CCCAGGCAGCACATAGCGAT-3'		
	5F3: 5'-CCGAGGTGGATGCCGCTG-3'	294	65
	5R3: 5'-GAAGGGGAGTGGGCAGCAGAC-3'		
6	6F: 5'-CACTGACCGTTGACACCCTCG-3'	281	65
	6R: 5'-TGCCCCAGTGCTTCAGAGATC-3'		
7	7F: 5'-GGAGTGCCCTGAGCCCCCT-3'	311	65
	7R: 5'-CCCCTAACCACAGCCAGCG-3'		
8	8F: 5'-TCTGTTCGTCCTGGTGTCCTG-3'	215	65
	8R: 5'-GCAGGAGGGCAGGTTGTAGAA-3'		
9	9F: 5'-GGTAGGGGGAGTCTGGGCTT-3'	253	65
	9R: 5'-GAGGCCACCCCGAGTCC-3'		
10	10F: 5'-GTTGGGCATCTCTGACGGTG-3'	364	65
	10R: 5'-GGAAGGTGGCCTGAGGAGAT-3'		
11	11F2: 5'-GGGGTCCACGGGCCATG-3'	311	67

	11R2: 5'-AAGCCCAGCAGCACGGTGAG-3'		
	11midF: 5'-GCTTGCAGCCACGGAAC-3'	386	65
	11midR: 5'-GCAGTGCTACCACTGAGAAC-3'		
	11F1: 5'-TGCCCCTGGGAGACCAACGATAC-3'	303	67
	11R1: 5'-GGCTGCTGCCCTCACTGGGAAG-3'		
12	12F: 5'-GAGGCGACAGGCTAAGGG-3'	311	64
	12R: 5'-AAGCCCAGCAGCACGGTGAG-3'		
13	13F: 5-TGGAGGGAGGGACGCCAATC-3	308	67
	13R: 5-GAGGCTGGGGCTGGGACAAG-3		
14	14F: 5-CCCGGTTCACTCACTGCG-3	220	64
	14R: 5-CCGTGCTCAGAGCCTGAAAG-3		
15	15F16: 5-CGGGTGGGGAGCAGGTGG-3	280	67
	15R16: 5-GCTCTGGGTCAGGACAGGGGA-3		
	15F15: 5-CGCCTGGGGGTGTTCTTT-3	270	64
	15R15: 5-ACGTGATGTTGTCGCCCG-3		
	15F14: 5-GCCCCCGTGGTGGTCAGC-3	250	67
	15R14: 5-CAGGCTGCGTGGGGATGC-3		
	15F13: 5-CTGGAGGTGCTGCGCGTT-3	256	67
	15R13: 5-CTGGCTCCACGCAGATGC-3		
	15F12: 5-CGTGAACAGGGCGCATTA-3	270	65
	15R12: 5-GCAGCAGAGATGTTGTTGGAC-3		
	15F11: 5-CCAGGCTCCTATCTTGTGACA-3	259	60
	15R11: 5-TGAAGTCACCTGTGCTGTTGT-3		
	15F10: 5'-CTACCTGTGGGATCTGGGG-3'	217	67
	15R10: 5-TGCTGAAGCTCACGCTCC-3		
	15F9: 5-GGGCTCGTCGTCAATGCAAG-3	267	67
	15R9: 5-CACCACCTGCAGCCCCTCTA-3		
	15F8: 5-CCGCCCAGGACAGCATCTTC-3	261	64
	15R8: 5-CGCTGCCCAGCATGTTGG-3		
	15F7: 5-CGGCAAAGGCTTCTCGCTC-3	288	64
	15R7: 5-CCGGGTGTGGGGAAGCTATG-3		
	15F6: 5-CGAGCCATTTACCACCCATAG-3	231	65
	15R6: 5-GCCCAGCACCAGCTCACAT-3		
	15F5: 5-CCACGGGCACCAATGTGAG-3	251	64
	15R5: 5-GGCAGCCAGCAGGATCTGAA-3		
	15F4: 5-CAGCAGCAAGGTGGTGGC-3	333	67
	15R4: 5-GCGTAGGCGACCCGAGAG-3		
	15F3: 5-ACGGGCACTGAGAGGAACTTC-3	206	64
	15R3: 5-ACCAGCGTGCGGTTCTCACT-3		
	15F2: 5-GCCGCGACGTCACCTACAC-3	265	67
	15R2: 5-TCGGCCCTGGGCTCATCT-3		

	15F1: 5-GTCGCCAGGGCAGGACACAG-3	228	68
	R27: 5-AGGTCAACGTGGGCCTCCAA-3		
	15F1-1: 5-ACTTGGAGGCCCACGTTGACC-3	276	69
	15R1-1: 5-TGATGGGCACCAGGCGCTC-3		
	15F1-2: 5-CATCCAGGCCAATGTGACGGT-3	266	64
	15R1-2: 5-CCTGGTGGCAAGCTGGGTGTT-3		
16	16F: 5-TAAAACTGGATGGGGCTCTC-3	294	56
	16R: 5-GGCCTCCACCAGCACTAA-3		
17	17F: 5-GGGTCCCCCAGTCCTTCCAG-3	244	67
	17R: 5-TCCCCAGCCCGCCCACA-3		
18	18F: 5-GCCCCCTCACCACCCCTTCT-3	342	67
	18R: 5-TCCCGCTGCTCCCCCCAC-3		
19	19F: 5-GATGCCGTGGGGACCGTC-3	285	67
	19R: 5-GTGAGCAGGTGGCAGTCTCG-3		
20	20F: 5-CCACCCCCTCTGCTCGTAGGT-3	232	64
	20R: 5-GGTCCCAAGCACGCATGCA-3		
21	21F: 5-TGCCGGCCTCCTGCGCTGCTGA-3	232	67
	TWR2: 5-GTAGGATGGCCCCACCTGCTCACCCTGC-3		
23a	TWF1 5'CTGCACTGACCTCACGCATGT3'	377	62
	23R1 5'GCCAAAGGGAAAGGGATTGGA3'		
23b	23F2 5'CCGCGGAGCCTGCTGTGCTAT3'	631	56
	23R2 5'TGCCACGGGCCTGAAAGCATA3'		
24	24F 5'TATGCTTTCAGGCCCGTGGCA3'	382	62
	24R 5'AGAGCCCATACCCGGTCCAGTCC3'		
25	25F 5'GGACTGGACCGGGTATGGGCTCT3'	392	62
	25R 5'CACCCAGGCCCTCCTCGACTC3'		
26	26F 5'CTGGGTGGGCTCGGCTCTATC3'	553	65
	26R 5'TGGTAGCGATGCTCACGTCACTT3'		
27	27F 5'CAGGCCAAAGCTGAGATGACTTG3'	339	62
	27R 5'AGAGGCGCAGGAGGGAGGTC3'		
28	28F 5'CCCTCTGCCCCCGCATTG3'	380	62
	28R 5'GGAGAGCCAGATGTGCTTGTCAA3'		
29	29F 5'GGTGCTGGCCGCGAGTAAGG3'	414	62
	29R 5'CCGTGCTGTGTGGAGGAGAG3'		
30	30F 5'CCTCTTCCTGCCCAGCCCTTC3'	318	62
	30R 5'CTTCCCGAGCAGCCTTTGGTG3'		
31	31F 5'GTCCCATATATCCAGCATTCT3'	330	56
	31R 5'ACAGTGTCTTGAGTCCAAGC3'		
32	32F 5'GCCTTGGCGCAGCTTGGACT3'	185	65
	32R 5'ACACCCAGCAAGGACACGCA3'		
33	33F 5'GGTGTGCGGGCTGCGTGT3'	459	62

	33R 5'CTCGGCAAGGACCTGCTGGAT3'		
34	34F 5'GAGAGGAGGGGGCTCTGAAG3'	475	62
	34R 5'AAAAACCCGCCCATAATTTC3'		

Table 5. Nested primers used for mutation detection.

3.2.5. Analysis of the Electronic Database Information.

The following GenBank sequences (accessed at http://www.ncbi.nlm.nih.gov/Web/Genbank) were used as reference files for this report: L39891 for *PKD1* genomic nucleotide positions, L33234 for *PKD1* cDNA positions, and AC002039 for the sequences of the homologous loci.

3.2.6. Generation of Polycystin-1 Cleavage Mutant Constructs.

The wild type construct (AF20, great donation of Dr. Germino) was the base plasmid for the generation of the cleavage mutants. AF20 was derived from pCI-*PKD1*-Flag (Hanaoka et al., 2000) by eliminating the BglII site of the vector. The cleavage mutants were generated in a two-step PCR procedure by using pfu DNA polymerase and AF20 as template. 5′ and 3′ PCR products with compatible ends were generated with the desired mutant nucleotide included in one of the primers, digested with the appropriate enzymes, and then cloned into the same sites of the AF20 in a tri-molecular ligation reaction.

3.2.7. Cleavage Assay.

The construct was transfected into various mammalian cells by using Lipofectamine Plus (Life Technologies, Rockville, MD). The cells were lysed in buffer [20 mM sodium phosphate, pH 7.2/150 mM NaCl/1 mM EDTA/10% (vol/vol) glycerol 0.5% Triton X-100] containing complete protease inhibitor cocktails (Roche Molecular Biochemicals) for 1 h on ice. The cleared supernatant was subjected to immunoprecipitation (IP) by using either agarose-conjugated α-Flag (Sigma) or affinity-purified α -CT or α -GFP (Roche Molecular Biochemicals). The IP product was resolved on a 4% or 3–8% SDS gel, electro-blotted to a poly (vinylidene difluoride) membrane, and probed with various antibodies.

3.3. Results:

3.3.1 PKDX family test.

A systematic direct sequencing-based analysis of *PKD1* and *PKD2* mutations and variants has been performed in a group of 82 ADPKD patients. Samples were screened for all 46 exons of *PKD1* and for 15 exons of *PKD2* and its respective exon-intron junctions comprising the transcript with the longest continuous ORF of both genes. It has been detected 34 (41.5%) patients associated with definitive mutation (Stop Codon, Frameshift, or Splicing defect): 24 (29.3%) of them to *PKD1* (eight Stop Codons, 15 Frameshift, and 1 Splicing variant) and 10 (12.2%) to *PKD2* (six Stop Codons, 3 Frameshift, and 1 Splicing variant). In addition, It has been identify eight (9.7%) patients associated to an in-frame deletion or insertion alteration (6 *PKD1* and 2 *PKD2*) and 25 (30.5%) to one or more missense change (24 *PKD1* and 1 *PKD2*). A novel, recurrent, highly pathogenic mutation was found in three families without other possible association to any pathogenic variant. The inclusion of these three families would go up the detection rate from 81.7% to 85.2%. No disease causing variants were detected in 12 patients (14.6%) (Table 6).

A)

	Truncation and Splicing			**Inframe Mutations**		**Amino acid changes**	**No mutation**
	Stop Codon	**Frameshift**	**Splicing**	**Insertions**	**Deletions**		
PKD1	8 (9.7%)	15 (18.3%)	1 (1.21%)	0 (0%)	6 (7.3%)	25 (30.5%)	14 (17%)
	Total 24 (29.26%)			Total 6 (7.4%)			
PKD2	6 (7.3%)	3 (3.7%)	1 (1.21%)	0 (0%)	2 (2.4%)	1 (1.2%)	
	Total 10 (12.3%)			Total 2 (2.5%)			
Total	14 (17%)	18 (22%)	2 (2.42%)	0 (0%)	8 (9.75%)	26 (31.7%)	
	Total 34 (41.46%)			Total 8 (9.9%)			
	68 (82.9%)						

B)

	Truncation and Splicing	**Inframe insertions and deletions**	**Amino acid changes**	**Silent changes**
PKD1	21 (19 Novel)	6 (6 Novel)	73 (52 Novel)	111 (75 Novel)
PKD2	6 (3 Novel)	2 (2 Novel)	6 (4 Novel)	6 (5 Novel)

Table 6. Results of PKDX family test. A) Classification of the different changes associated to the disease for ADPKD patients linked to PKD1 or PKD2. B) Total number of individual changes found in each gene.

The following criteria has been used to predict whether a sequence variant was pathogenic: 1) the potential chain-terminating effect on the longest predicted polypeptide; 2) disruption of a canonical splice site or creation of a novel site; 3) alteration in the polarity or change of an amino acid, 4) structural disruption of the protein domain and; 5) assessment of the variant frequency in the total number of patients.

The difficulty of classifying the missense changes as pathogenic becomes more complicated in families that have one or more missense change associated to a definitive mutation. 47 patients (57.3%) were associated to a unique mutation (38 *PKD1*, 46.3%; 9 *PKD2*, 11%) and 20 (24.3%) to one or more pathogenic changes (16 *PKD1*, 19.5%; 4 *PKD2*, 4.9%). The total number of changes per patient for both genes is variable from one (JHUJHU605-1; 0 changes in *PKD1* and 1 change in *PKD2*), to sixty-one (JHU411; 60 changes in PKD1 and 1 change in *PKD2*). The minimum total number of changes found in a patient associated to a mutation is three (JHU576 and JHUYP109, both with 3 changes in *PKD1*and none in *PKD2*) (Table 7).

Pedigree	Mutations Disease Associated		Other unclassified amino acid changes	# of Changes per patient	
	PKD1	***PKD2***		***PKD1***	***PKD2***
JHU605	S91X			4	0
JHU 567	R1436X			24	0
JHU YP108	Y2265X			5	1
JHU563	R2430X		R807Q	19	1
JHU593	Q2556X			3	2
1539998	Q2686X			5	0
JHU574	E2810X			4	0
JHU620	W4011X			22	0
JHU578		R306X	L247F	3	3
JHU583		R306X	P36H	5	1
JHU607		R742X		21	1
JHU594		R872X		22	3
JHU566		R872X		1	3
JHU608		R872X		4	2
JHU568	W305 fsX		W305C	4	1
JHU582	P694 fsX			1	0
JHU585	A696 fsX			6	2
JHU508	V1718 fsX			5	2
JHU613-1	D2152 fsX		E624K	21	0

JHU611	P2224 fsX			29	1
JHU600	P2975 fsX			25	2
JHU609	I3109 fsX			41	1
JHU579	I3109 fsX			23	2
JHUYP116		720ins1	D3494E	3	2
JHU586		720ins1		22	1
JHU577	F2834fsX			4	1
JHUYP111	N116 fsX		S1619F(*PKD1*) and M583I(*PKD2*)	7	1
JHUMP15	R1672 fsX			5	1
JHU599	L3343 fsX		R1312Q	20	1
JHUYP104	G3792 fsX			4	2
JHUYP115	N101del			20	0
JHUYP107	V546del		R1142W	25	1
JHU560	A2894del			21	1
JHU592	K3232del		A1516T	3	1
JHU571	L3287del		V2267M and F4007L	10	0
JHUYP112	V4129del		S4053F	19	2
JHU596		103del	H201Q and Q2182R	35	1
JHU416		605del		2	3
JHU591-2		786del2		4	2
JHU580	IVS19+?GxT			5	1
JHU562		IVS7-1GxA		3	2
JHU559	C47S		M800L in *PKD2*	24	3
JHU612-1	A271D			4	0
JHU602	Y420C		R1351W , W2882R and E2966D	25	1
JHUYP103	Y528C		R1942H	28	1
JHU570	P579Q			5	1
CP001	R611W			6	0
JHUYP105	T1773I			3	2
JHUYP100	T1861I and R2166C			8	1
JHU411	S1047L		Q2182R	60	1
JHU587	C210F and R2329Q			6	2
JHU565	T2422K			24	0
JHU603	R2516C			4	0
JHU597	R2643C			3	1
JHUYP101	R2767C			4	2
JHU589	F2853S			22	2
JHU601B	Q3016R			43	1
JHU 576	N3295K			3	0
JHU564	A2302G and G3326R		I3367V	4	1
JHU617	L3730Q		L1394V	5	1
JHUYP114	R4149C			22	1
JHU572		S349P		17	1
JHU569	L2619P			22	2
JHUYP109	E2771K			3	0
JHU575	N1034S			17	1
JHU614-1			A1516T and E586D	10	0
JHU588	L2448P			39	0

JHU606			-	5	2
JHU584			R2200C (JHU 573)	20	1
JHU595			R2121R, V3408L and IVS24+ G-C	16	2
JHU 573			IVS24+ G-C, R2200C (JHU584)	5	0
JHUYP102			V3408L (JHU 595, JHU596)	21	0
JHU590			G109G IVS24+G-T IVS41- C-T	3	1
JHU178			P1168S (JHU565)	2	1
JHU610			S196S	40	2
JHU604			3'UTR G-A	2	0
JHU616-1				17	0
JHU615-2				0	1
JHUYP110				3	0
JHUYP113				2	1
JHU598				19	0
JHUYP106				4	1

Table 7. Summary of Mutation Changes Identified in the 82 families.

It is been found patients having with more than one changes classified as missense changes presumably responsible of the disease (for example JHUYP100, JHU587 and JHU564), but only one can be really responsible of it. The patient JHU587 has one fully conserved amino acid changed in the extracellular region of the PC-1 (C201F) and the other in a highly conserved amino acid of REJ domain (R2329). The missense change A1516T is a novel change of a highly conserved amino acid in *PKD1*-R9 of PD1 found in two families, associated to an inframe deletion (K3232del, JHU592) and to a highly conserved novel amino acid change (E586D, JHU614-1). Two novel missense mutations and unclassified novel amino acid substitutions has been found in JHU602: a fully conserved amino acid substitution on the consensus structure of the C-Type-Lectin domain changing the structure of the domain (Y420C), a CpG change in a fully conserved amino acid change on PKD-R7 domain (R1351W), and a non conserved amino acid change (W2882R), all of which are likely to be highly pathogenic. Two novel amino acid substitutions of highly conserved amino acids of *PKD1* (A2302G and I3367V) were found in JHU564 (Table 7).

Some patients were associated to a mutation disease associated, but also presented another possible change that, following the criteria previously establish by other investigators, could be

classified as responsible of the disease. 18 *PKD1*-patients and 4 *PKD2*-patients have more than one change that could be classified as responsible of the disease (Table 7).

3.3.2. PKD1 and PKD2 Mutations.

Among the putative mutant alleles, 22 were predicted to cause chain-termination. 13 frameshift variants (deletions, insertions and duplications), eight nonsense mutations and one splice variant where found in *PKD1,* and two frameshift, three nonsense mutations and one splicing in *PKD2*. N116fsX (JHU111 and JHU 577) and I3109fsX (JHU579 and JHU609) were found to be recurrent (Table 8).

Variant	Exon	Mutation		Mutation Effect		Domain	Pedigree	Rate	Reference
		cDNA	Protein	Stop Codon	Splice Site				
***PKD1* gene**									
Frameshift:									
	3	559delTTTAA	N116fsX	117		LRR2	JHUYP111	1/164	NOVEL
	5	1124insCT	W305 fsX	334		PKD R1	JHU568	1/164	NOVEL
	10	2291ins1	P694 fsX	713			JHU582	1/164	NOVEL
	10	2297ins1	A696 fsX	713			JHU585	1/164	NOVEL
	15	5225delAG	R1672 fsX	1721		PKD R11	JHUMP15	1/164	1
	15	5365insT	V1718 fsX	1770		PKD R12	JHU508	1/164	NOVEL
	15	6666insG	D2152 fsX	2174		REJ	JHU613-1	1/164	NOVEL
	15	6881insA	P2224 fsX	2261		REJ	JHU611	1/164	NOVEL
	23	8713delT	F2834 fsX	2874			JHU577	1/164	NOVEL
	24	9134ins1	P2975 fsX	3068			JHU600	1/164	NOVEL
	26	9536ins5	I3109 fsX	3317			JHU579, JHU609	2/164	NOVEL
	30	10239delT	L3343 fsX	3395		TM3	JHU599	1/164	NOVEL
	40	11587delG	G3792 fsX	3824			JHUYP104	1/164	NOVEL
Nonsense:									
	2	483 C>A	S91X	91		LRR1	JHU605	1/164	NOVEL
	15	4517 C>T	R1436X	1436		PKD R8	JHU 567	1/164	NOVEL
	15	7006 C>A	Y2265X	2265		REJ	JHU YP108	1/164	NOVEL
	18	7499 C>T	R2430X	2430		REJ	JHU563	1/164	2
	19	7877 C>T	Q2556X	2556		REJ	JHU593	1/164	NOVEL
	22	8267 C>T	Q2686X	2686		REJ	1539998	1/164	NOVEL
	23	8639 G>T	E2810X	2810		REJ	JHU574	1/164	NOVEL
	44	12243 G>A	W4011X			TM9	JHU620	1/164	NOVEL
Splicing:									
	19	VS19+1 G>T.	VS19+1 G>T.		Loss of acceptor site	REJ	JHU580	1/164	NOVEL
***PKD2* gene**									
Frameshift:									
	11	2226ins1	720 fsX				JHU586, JHUYP116	2/164	NOVEL
	12	2422delAG	786dfsX			COILED COIL	JHU591-2	1/164	NOVEL

Nonsense:									
	4	982 C>T	R306X			TM1	JHU578 , JHU583	2/164	5
	11	2224 C>T	R742X				JHU607	1/164	6
	14	2680CxT	R872X				JHU594 , JHU566, JHU608	3/164	
Splicing:									
	7		IVS7-1GxA		Loss of donor site		JHU562	1/164	NOVEL

Table 8. Truncating and Splice variants. *Ref: N. Novel.; 1 Watnick et al., 1999; 2 Phakdeekitcharoen et al., 2000; 3 Rossetti et al., 2001; 4 Peral et al., 1997; 5 Veldhuisen et al., 1997; 6 Peral et al., 1998; 7, Peral et al., 1996; 8 Rossetti et al., 2002; 9 Thomas et al., 1999; 10 Rossetti et al., 1996; 11 Reiterová y col., 2002; 12 ; 13 Inove et al., 2002; 14 Perrichot et al., 1999; 15 Bogdanova et al., 2001; 16 Watnick et al., 1998; 17 Perrichot te al., 2000; 19 Aguiarri et al., 2000; 20 Bateman et al., 1999.*

N116fsX was associated in both families to another possible pathogenic change (F2834fsX in JHU577 and S1619F in JHU577). D2152fsX (JHU613-1) and L3343fsX (JHU599) were associated to another variant (Table 7).

All frameshift deletions were caused by sequence motifs that possess an axis of internal symmetry and vary in length between 5 and 18 bp. Symmetric elements spanning 5 bp or more appear to be overrepresented in the vicinity of short human gene deletions. For example, N116fsX is on an ATTTAATTTA motif, where a deletion of 5 amino acids was found (559delTTTAA) in *PKD1*. These types of motifs can be found along *PKD1* and *PKD2*. This mechanism of mutagenesis is the responsible for all of the *PKD1* and *PKD2* deletions in our pool of families and 76% of previous published deletions. Other mechanisms of deletion such as direct repeats, palindromes and quasipalindromes sequences have been shown to be responsible of frameshift and small deletions at least in *E. coli* (de Boer JG et al., 1984), but we could not observe any of these type.

All inframe deletions (6, *PKD1* and 2, *PKD2*) were novel and fully or highly conserved in our group of families, the total published population likely being pathogenic (Table 9). For this type of study, where the clinicians want to determine if their patients are or are not ADPKD, it is risky to classify inframe and missense as pathogenic. More definite information or other approaches are needed to determine the potential implications of these changes.

All single nucleotide changes were analyzed for potential splice effects using Splice Site Prediction by Neural Network (SSPNN; http:/fuitfly.org/seqtools/splice.html). Splice site scores predicted the theoretical impact upon donor and acceptor site strength and the probability that sequence variants created novel splice sites. This was very useful to predict the effect of certain nucleotide changes on splicing. 3 variants were predicted to alter splicing with alterations, SS scores >50%. One variant in *PKD1* and another in *PKD2* disrupted the canonical GT splice donor or AG acceptor and presumably caused exon-skipping. One missense change was predicted to alter splicing in a fully conserved residue Q3016R.

	Exon	Mutation		Domain	Conservation			Pedigree	Variant Detection	Reference
		cDNA	Protein		Fugu	Mouse	Level			
***PKD1* gene**										
	3	514-551delCAA	N101del	LRR2	N	N	Fully	JHUYP115	1/164	NOVEL
	8	1848-1851delTGG	V546del		V	V	Fully	JHUYP107	1/164	NOVEL
	23	8892-8898delCCAACTCCG	A2894del		AGA	VGS	Fully	JHU560	1/164	NOVEL
	28	9905-9909delAAG	K3232del	PLAT	I	K	Highly	JHU592	1/164	NOVEL
	29	10070-10074delCTC	L3287del	TM2	L	L	Fully	JHU571	1/164	NOVEL
	45	12597-12600delTGG	V4129del		V	V	Fully	JHUYP112	1/164	NOVEL
***PKD2* gene**										
	1	374-378delTGG	103del	Poly-Glu		V	Highly	JHU 596	1/164	NOVEL
	8	1879-1882delTTC	605del	TM5		F	Highly	JHU416	1/164	NOVEL

Table 9. Deletions inframe

Of the 81 amino acid substitutions, 75 were *PKD1* and 6 *PKD2*. Of the 75 PKD-1 amino acids substitutions, 35 residues were fully conserved from *Fugu rubripes* to *Homo sapiens*, 30 residues were highly conserved in mammalians from *Mus musculus* to *Homo sapiens,* and 10 had no conservation. To assess the statistical probability of pathogenicity for each amino acid substitution, we applied the matrix criteria described by Miller and Kumar. This matrix, developed using disease-associated human genetic variations and interspecific comparisons as well as Graham's chemical difference matrix,

defines the relative likelihood that a missense change represents a polymorphism versus a pathogenic alteration (Figure 14).

In this study, of 29 missense changes, 20 were predicted to have a higher pathogenic potential than polymorphic probability, six were predicted to be potentially pathogenic substitutions with an equal provability of being pathogenic and polymorphism, and three of these missense changes were predicted to be polymorphism. All these missenses are novel and unique in this study and only one (E2771K) was described previously by Rossetti et al. (2001), indicating the high probability to be disease associated. In these patients, we define as unclassified the variant changes that appear only once, not common in the population, and are associated to another change in the same patient.

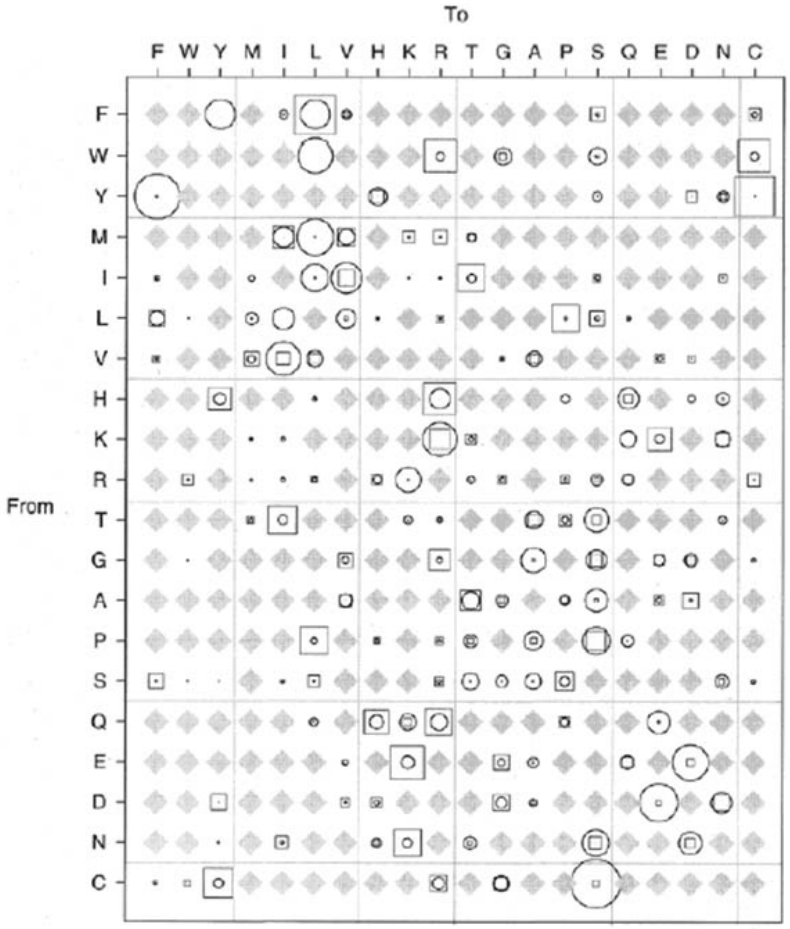

Figure 14. Plots showing the relative frequencies of amino acid changes observed in interspecific comparisons (circles) and detected in disease patients (squares). The width of the symbols is proportional to the relative frequency of a given amino acid change. Diamonds indicate amino acids changes that cannot be observed as a result of a single base mutation. Horizontal and vertical lines across the graph denote groups of amino acids with relatively similar properties, thus, residue changes to an amino acid with similar properties are found along diagonal elements of the grid. Human Molecular Genetics, 2001, Vol. 10 No. 21.

Of the 25 unclassified variants, 11 were predicted to have the probability to be highly pathogenic, 9 equally pathogenic and 5 polymorphisms. 21 amino acid substitutions were predicted to be polymorphism with a high prevalence on the population since it appears in homozygosity or is a

conserved amino acid group change. 5 of 21 were predicted to be polymorphism, 10 having the equal probability to be pathogenic or polymorphism, and 6 were predicted to be highly pathogenic (Table 10).

Exon	Mutation		Domain	Path./ P. Provability	Conservation			Pedigree	Variant Detection	Reference
	cDNA	Protein			Fugu	Mouse	Level			
***PKD1* gene:**										
Pathogenic Variants. Missense.										
1	351GxC	C47S	LRR N-Flank	P.H.	W	C	Highly	JHU559	1/164	NOVEL
5	840GxT	C210F		Equal	C	C	Fully	JHU587	1/164	NOVEL
5	1023CxA	A271D	WSC	Path.H.	A	A	Fully	JHU612-1	1/164	NOVEL
6	1470AxG	Y420C	C-TYPE-LECTIN	Path.H.	F	Y	Fully	JHU602	1/164	NOVEL
7	1794AxG	Y528C	C-TYPE-LECTIN	Path.H.	Y	Y	Fully	JHUYP103	1/164	NOVEL
9	1947CxA	P579Q		Equal	P	P	Fully	JHU570	1/164	NOVEL
9	2042CxT	R611W		Path.H.	R	R	Fully	CP001	1/164	NOVEL
13	3312AxG	N1034S	PKD R4	P.H.	G	S	Highly	JHU575	1/164	NOVEL
13	3351CxT	S1047L	PKD R4	Path.H.	M	S	Highly	JHU411	1/164	NOVEL
15	4262CxT	R1351W	PKD R7	Path.H.	R	R	Fully	JHU602	1/164	NOVEL
15	5529CxT	T1773I	PKD R12	Path.H.	S	T	Fully	JHUYP105	1/164	NOVEL
15	5793CxT	T1861I	PKD R13	Path.H.	T	S	Fully	JHUYP100	1/164	NOVEL
15	7116CxG	A2302G	REJ	Equal	S	A	Highly	JHU564	1/164	NOVEL
16	7197GxA	R2329Q	REJ	Equal	E	R	Highly	JHU587	1/164	NOVEL
18	7476CxA	T2422K	REJ	Equal	T	T	Fully	JHU565	1/164	NOVEL
18	7554T>C	L2448P	REJ	Path.H.	L	L	Fully	JHU588	1/164	NOVEL
19	7757CxT	R2516C	REJ	Path.H.	R	R	Fully	JHU603	1/164	NOVEL
20	8067TxC	L2619P	REJ	Path.H.	L	L	Fully	JHU569	1/164	NOVEL
21	8138CxT	R2643C	REJ	Path.H.	R	R	Fully	JHU597	1/164	NOVEL
23	8509CxT	R2767C	REJ	Path.H.	R	R	Fully	JHUYP101	1/164	NOVEL
23	8522GxA	E2771K	REJ	Path.H.	E	E	Fully	JHUYP109	1/164	3
23	TxC	F2853S		Path.H.	F	F	Fully	JHU589	1/164	NOVEL
29	10096CxA	N3295K	TM2	Path.H.	N	N	Fully	JHU 576	1/164	NOVEL
30	10187GxC	G3326R	TM3	Path.H.	G	G	Fully	JHU564	1/164	NOVEL
39	11040TxA	L3730Q		Equal	F	L	Highly	JHU617	1/164	NOVEL
46	12658CxT	R4149C		Path.H.	R	R	Fully	JHUYP114	1/164	NOVEL
Pathogenic Variants. Splicing										
25	9258AxG	Q3016R		Path.H.	Q	Q	Fully	JHU601B	1/164	4
Unclassified Variants.										
1	318CxA	P36H	LRR-NF	Equal	T	P	Highly	JHU583	1/164	NOVEL
2	485GxA	A92Y	LRR1	Equal	F	A	Highly		1/164	7
5	814CxT	H201Q		P.H.	C	C	Fully	JHU 596	1/164	NOVEL
10	2081GxA	E624K		Path.H.	V	E	Highly	JHU613-1	1/164	NOVEL
15	3637CxT	R1142W	PKD R5	Path.H.	K	Q	Highly	JHUYP107	1/164	NOVEL
15	4146GxA	R1312Q	PKD R7	Equal	N	Q	NO	JHU599	1/164	NOVEL

15	4757GxA	A1516T	PKD R9	Equal	T	I	Highly	JHU592 JHU614-1	2/164	NOVEL
15	5067CxT	S1619F		Path.H.	A	S	Highly	JHUYP111	1/164	NOVEL
15	6707CxT	R2166C	REJ	Path.H.	P	R	Highly	JHUYP100	1/164	NOVEL
15	6756AxG	Q2182R	REJ	Path.H.	G	Q	Highly	JHU596 JHU411	2/164	NOVEL
15	6809CxT	R2200C	REJ	Path.H.	R	R	Fully	-	5/164	NOVEL
16	7138CxT	G2309R	REJ	Path.H.	G	H	Highly	-	4/164	NOVEL
23	8855TxA	W2882R		Path.H.	G	Q	NO	JHU602	1/164	NOVEL
Polymorphisms										
5	950CxT	L247F		Equal	Q	W	NO	JHU578	1/164	NOVEL
5	1004CxT	T263S(H)		P.H.	Q	T	Highly		2/164	NOVEL
8	1925CxT	P572S(H)		Equal	G	P	Highly		4/164	NOVEL
9	1973AxC	E586D		P.H.	A	E	Highly	JHU614-1	1/164	NOVEL
11	2427AxG	Q739R		Path.H.	R	Q	Highly	-	11/164	NOVEL
15	3527CxG	L1106V	PKD R4	P.H.	S	V	Highly	JHU565	1/164	NOVEL
14	3486TxC	M1092T(H)	PKD R4	Equal	T	T	NO	-	30/164	8
15	3678GxC	G1156A	PKD R5	P.H.	Y	D	NO	JHUYP107	1/164	NOVEL
15	3713CxT	P1168S	PKD R5	Equal	-	P	Highly	JHU565 JHU178	2/164	NOVEL
15	4229CxT	R1340W	PKD R7	Path.H.	H	H	NO	JHUYP114 JHUYP100 , JHU588	3/164	NOVEL
15	4391CxG	L1394V	PKD R8	P.H.	V	L	Fully	JHU617	1/164	NOVEL
15	4406TxG	W1399R(H)	PKD R8	Path.H.	Q	R	NO	-	22/164	NOVEL
15	6036GxA	R1942H	PKD R14	Equal	R	R	Fully	JHUYP103	1/164	NOVEL
15	6038GxA	V1943I(H)	PKD R14	P.H.	V	V	Fully	-	5/164	NOVEL
15	7010GxA	V2267M	REJ	Path.H.	V	V	Fully	JHU571	1/164	NOVEL
19	7853GxC	E2548Q(H)	REJ	Equal	R	V	NO	-	4/164	NOVEL
21	8124AxG	H2638R(H)	REJ	Path.H.	Y	L	NO		32/164	NOVEL
21	8231CxT	P2674S	REJ	Equal	V	S	NO	JHU 567	2/164	NOVEL
22	8334CxT	T2708M	REJ	Equal	T	T	Fully	JHU594	1/164	NOVEL
23	8411CxA	P2734T	REJ	Equal	P	P	Fully	JHU569	1/164	NOVEL
23	8415AxT	Q2735L	REJ	Equal	S	Q	Highly	JHU569	1/164	NOVEL
23	8651GxA	G2814R	REJ	Path.H.	A	G	Fully	-	6/164	NOVEL
23	8924GxA	V2905I		P.H.	V	V	Fully	-	1/164	3
24	9109GxC	E2966D		P.H.	G	E	Highly	JHU602	1/164	10
31	10311AxG	I3367V		P.H.	I	V	Fully	JHU564	1/164	NOVEL
33	10433GxC	V3408L(H)		Equal	E	V	Highly	-	5/164	NOVEL
34	10693CxA	D3494E		P.H.	-	D	Highly	JHUYP116	1/164	NOVEL
35	10743CxT	A3511V(H)		Equal	L	I	Fully	-	13/164	NOVEL
42	11835CxT	A3875V		Equal	S	A	Highly	-	1/164	NOVEL
44	12230TxC	F4007L		Path.H.	F	F	Fully	JHU571	1/164	NOVEL
44	12341AxG	I4044V(H)	TM10	Equal	H	I	Highly	-	42/164	10
45	12371CxT	S4053F		Path.H.	G	T	Highly	JHUYP112	1/164	NOVEL
45	12386CxT	A4058V(H)		Equal	T	A	Highly	-	12/164	10
***PKD2* gene:**										
Pathogenic Variants. Missense.										
4	1111TxC	S349P		Path.H.	-	S	Fully	JHU572	1/164	NOVEL
Unclassified Variants.										

8	1815GxA	M583I		Equal	-	M	Fully	JHUYP111	1/164	NOVEL
13	2486GxA	R807Q		Equal	-	R	Highly	JHU563	1/164	NOVEL
Polymorphisms										
1	149CxT	R28P		Path.H.	-	R	Highly	-	50/164	10
1	634GxA	A190T		Equal	-	A	Highly	-	3/164	NOVEL
13	2464AxC	M800L		P.H.	-	M	NO	JHU559	1/164	11

Table 10. Amino Acid Substitutions. *Ref: N. Novel.; 1 Watnick et al., 1999; 2 Phakdeekitcharoen et al., 2000; 3 Rossetti et al., 2001; 4 Peral et al., 1997; 5 Veldhuisen et al., 1997; 6 Peral et al., 1998; 7, Peral et al., 1996; 8 Rossetti et al., 2002; 9 Thomas et al., 1999; 10 Rossetti et al., 1996; 11 Reiterová y col., 2002; 12 ; 13 Inove et al., 2002; 14 Perrichot et al., 1999; 15 Bogdanova et al., 2001; 16 Watnick et al., 1998; 17 Perrichot te al., 2000; 19 Aguiarri et al., 2000; 20 Bateman et al., 1999*

R1340W (PKD repeat 7) was previously characterized to be a non-conservative missense change demonstrating segregation with the disease (Rosseti et al., 2002). It is very unlikely to be responsible of the disease for many reasons, because it is present in 3 patients, all of them were associated with another novel missense change fully conserved and predicted to be highly pathogenic. On the other hand, it is possible that changes like this could work as modifiers, been responsible of the intrafamilial variability.

3.3.3. PKD1 and PKD2 polymorphisms.

There was an impressive degree of sequence variability, particularly in the PKD1 gene, among patients in the study sample. In addition to the sequence alterations described in previously, we also detected a large number of polymorphisms (Table 11). Polymorphisms were defined as 1) sequence variants not predicted to alter an amino acid 2) Missense changes found in homozygosity in at least one patient and 3) intronic sequences of unknown significance and 4) Changes in the 3' UTR of unknown significance.

On average, the 82 study participants had 13.1 PKD1 sequence variants per patient with a range of 0 to 60. In contrast there was an average of only 1.1 PKD2 variants per patient with a range of 0-3. A total of 112 Silent and intronic variants were found in *PKD1*, 4 in the 5´UTR, 33 intronic changes, 74 in the coding sequence and 1 in the 3´UTR. In *PKD2*, 4 were found in the coding sequence and 2 in the non-coding region (Table 11). These changes are not only important for a

clinical perspective (intragenic modifiers), also they have an enormous value in the understanding of the structure, behavior and evolution of these genes

#	Designation	cDNA Change (s)	Location	Domain	Frequency (%)	Reference
***PKD1* Polymorphisms.**						
1	T263S(H)	1004C>T	Exon 5		2/164	NOVEL
2	P572S(H)	1925C>T	Exon 8		4/164	NOVEL
3	M1092T(H)	3486T>C	Exon 14	PKD R4	30/164	8
4	W1399R(H)	4406T>G	Exon 15	PKD R8	22/164	16
5	V1943I(H)	6038G>A	Exon 15	PKD R14	5/164	NOVEL
6	E2548Q(H)	7853G>C	Exon 19	REJ	4/164	NOVEL
7	H2638R(H)	8124A>G	Exon 21	REJ	32/164	NOVEL
8	P2674S(H)	8231C>T	Exon 21	REJ	2/164	3
9	F3066L (H)	9407T>C	Exon 25		38/164	NOVEL
10	V3408L(H)	10433G>C	Exon 33		5/164	NOVEL
11	A3511V(H)	10743C>T	Exon 35		13/164	NOVEL
12	I4044V(H)	12341A>G	Exon 44	TM10	42/164	3, 17, 18, 14,10
13	A4058V(H)	12386C>T	Exon 45		12/164	10
14		104C>T	Exon 1	5´UTR	1/164	Novel
15		145C>T	Exon 1	5´UTR	2/164	Novel
16		160C>T	Exon 1	5´UTR	1/164	Novel
17		210C>T	Exon 1	5´UTR	1/164	Novel
18	L72L	425C>T	Exon 1	LRR1	2/164	Novel
19	G109G	538A>T	Exon 3	LRR2	1/164	Novel
20	IVS4+1G>A(H)		Intron 4		1/164	Novel
21	S196S	799C>T	Exon 5		2/164	Novel
22	A341A	1234C>T	Exon 5	PKD R1	5/164	3
23	L373L(H)	1330T>C	Exon 5		36/164	3, 15
24	G441G	1534G>A	Exon 6	C-LECTIN	1/164	Novel
25	H570H	1921C>T	Exon 8		1/164	3
26	IVS9+2del7		Intron 9		12/164	Novel
27	IVS9+2 T>A		Intron 9		1/164	Novel
28	IVS9+28del7 (H)		Intron 9		4/164	8
29	ISV9-44G>C		Intron 9		1/164	8
30	IVS9-4A>G		Intron 9		42/164	8
31	IVS10-4 G>A		Intron 10		1/164	Novel
32	P738P(H)	2425C>G	Exon 11		4/164	Novel

33	A745A	2448C>G	Exon 11		1/164	Novel
34	A898A	2905A>C	Exon 11	PKD R2	4/164	9
35	P900P	2911G>A	Exon 11	PKD R2	10/164	16, 9
36	D910D	2941C>T	Exon 11	PKD R2	10/164	16, 9
37	IVS11-5C>T		Intron 11		2/164	8
38	IVS11+23C>T(H)		Intron 11		4/164	Novel
39	IVS12-15C>T		Intron 12		5/164	Novel
40	G1021G(H)	3274T>C	Exon 13	PKD R4	30/164	16, 9
41	L1037L	3392A>G	Exon 13	PKD R4	15/164	9
42	E1061E	3394G>A	Exon 14	PKD R4	1/164	Novel
43	P1076P	3439G>A	Exon 14	PKD R4	1/164	Novel
44	A1124A	3583C>T	Exon 15	PKD R4	25/164	9
45	S1125S	3586C>T	Exon 15	PKD R5	25/164	9
46	F1163F	3700C>T	Exon 15	PKD R5	1/164	Novel
47	T1171T	3724C>G	Exon 15	PKD R5	1/164	Novel
48	D1310D	4141C>T	Exon 15	PKD R7	1/164	Novel
49	L1357L	4282G>T	Exon 15	PKD R7	1/164	Novel
50	S1373S	4330C>T	Exon 15	PKD R7	1/164	Novel
51	S1452S	4567T>C	Exon 15	PKD R8	1/164	Novel
52	P1511P	4744G>A	Exon 15	PKD R9	1/164	Novel
53	A1555A(H)	4876A>C	Exon 15	Extracellular	42/164	16, 1, 9
54	T1558T	4885G>A	Exon 15	Extracellular	9/164	2
55	S1603S	5020C>T	Exon 15	Extracellular	1/164	Novel
56	T1724T(H)	5383C>T	Exon 15	PKD R12	40/164	9
57	A1818A(H)	5665G>A	Exon 15	PKD R13	5/164	8
58	G1860G	5791C>A	Exon 15	PKD R13	1/164	Novel
59	A1894A	5893C>T	Exon 15	PKD R14	1/164	8
60	L1921L	5974G>A	Exon 15	PKD R14	2/164	9
61	V2026V	6289C>T	Exon 15	PKD R15	1/164	Novel
62	R2121R	6574C>T	Exon 15	PKD R16	1/164	Novel
63	T2180T	6751C>T	Exon 15	REJ	1/164	Novel
64	A2202A	6817G>A	Exon 15	REJ	1/164	Novel
65	V2257V	6982G>A	Exon 15	REJ	1/164	Novel
66	IVS16+10 G>A		Intron 16	REJ	1/164	Novel
67	R2359R	7289G>C	Exon 17	REJ	3/164	Novel
68	L2389L(H)	7376T>C	Exon 17	REJ	46/164	1, 2, 9.
69	G2425G	7486C>T	Exon 18	REJ	1/164	Novel
70	L2481L(H)	7652C>T	Exon 18	REJ	39/164	1
71	IVS19+24 C>A		Intron 19	REJ	2/164	Novel

72	L2570L(H)	7919T>C	Exon 20	REJ	31/164	1, 9
73	IVS20+ C>A		Intron20	REJ	1/164	Novel
74	ISV20-16C>G		Intron20	REJ	2/164	Novel
75	IVS22+8G>A (H)		Intron 22	REJ	1/164	1
76	S2729S	8398G>A	Exon 23	REJ	2/164	Novel
77	A2749A	8458G>A	Exon 23	REJ	1/164	Novel
78	S2766S	8509C>T	Exon 23	REJ	1/164	13
79	D2789D	8578C>T	Exon 23	REJ	2/164	Novel
80	S2813S	8650C>T	Exon 23	REJ	2/164	3
81	S2893S	8890C>G	Exon 23		2/164	3
82	A2971A(H)	9124T>C	Exon 24		2/164	Novel
83	IVS24-20G>A (H)		Intron 24		3/164	Novel
84	IVS24-17A>G(H)		Intron 24		6/164	Novel
85	IVS24+17A>G		Intron 24		32/164	Novel
86	S3007S	9232C>T	Exon 25		1/164	Novel
87	V3065V(H)	9406G>C	Exon 25		38/164	Novel
88	V3090V	9481C>T	Exon 26	TM1	3/164	Novel
89	P3110P(H)	9543T>C	Exon 26		37/164	6
90	IVS26+76C>A		Intron26		1/164	Novel
91	IVS27-13T>C(H)		Intron27		15/164	8
92	T3223T	9880G>A	Exon 28	PLAT	2/164	6
93	S3265S	10006C>T	Exon 29		1/164	Novel
94	IVS29-4 C>T		Intron29		1/164	Novel
95	A3455A	10576C>T	Exon 34		1/164	Novel
96	L3589L	10976C>T	Exon 36	TM5	5/164	Novel
97	IVS37-4 C>T		Intron 37		1/164	Novel
98	IVS37-10 C>A		Intron 37		1/164	Novel
99	IVS38+11G>A		Intron 38		4/164	Novel
100	R3752R	11385C>A	Exon 39	Polycystin motif	1/164	Novel
101	L3753L	11465G>C	Exon 39	Polycystin motif	1/164	Novel
102	IVS39- 72		Intron 39		1/164	Novel
103	IVS41+ C>T		Intron 41		1/164	Novel
104	IVS41+5insGGG		Intron 41		2/164	Novel
105	IVS41-11C>T	C>T	Intron 41		2/164	Novel
106	S3893S(H)	11890C>T	Exon 42		3/164	8
107	IVS43+42C>A		Intron 43		6/164	Novel
108	R3971R	12124C>T	Exon 43		3/164	Novel
109	L4025L	12286C>T	Exon 44		1/164	Novel
110	L4035L	12316C>T	Exon 44	TM10	1/164	Novel

111	IVS44+22delG		Intron44		4/164	Novel
***PKD2* Polymorphisms.**						
1	R28P	149CxT	Exon 1		50/176 (28.40)	10
2	R60R	246GxA	Exon 1		1/176 (0.56)	Novel
3	G140G	486GxA	Exon 1		22/176 (12.5)	Novel
4	IVS6-4 C-T		Intron 6		1/176 (0.56)	Novel
5	L539L	1683GxC	Exon 7		1/176 (0.56)	Novel
6	IVS8+5 G-A		Intron 8		1/176 (0.56)	Novel

Table 11. Amino Acid Substitutions. *Ref: N. Novel.; 1 Watnick et al., 1999; 2 Phakdeekitcharoen et al., 2000; 3 Rossetti et al., 2001; 4 Peral et al., 1997; 5 Veldhuisen et al., 1997; 6 Peral et al., 1998; 7, Peral et al., 1996; 8 Rossetti et al., 2002; 9 Thomas et al., 1999; 10 Rossetti et al., 1996; 11 Reiterová y col., 2002; 12 ; 13 Inove et al., 2002; 14 Perrichot et al., 1999; 15 Bogdanova et al., 2001; 16 Watnick et al., 1998; 17 Perrichot te al., 2000; 19 Aguiarri et al., 2000; 20 Bateman et al., 1999*

3.3.4. Mutational analysis using in vitro systems.

This aim was not initially proposed in this thesis. For a clinical point of view, it was imperative that missense changes and deletions *inframe* with uncertainty significance were subjected to further screening. Based on our analysis of pathogenicity, we knew which of the missense changes almost certainly had to be pathogenic. Nonetheless, in many cases it was unclear how the substitutions might alter function. *In vitro* systems not only can be used as a complementary study to test protein function, also can determine how this is altered by mutations (Qian et al., 2002).

We propose this tool as a complement to distinguish between polymorphism and mutations, as well as to assess the effects of various sequence variants like missense and deletion *inframe*. One example it is, if cleavage of polycystin-1 is important for its function, then one might predict that pathologic mutations affecting the sequence at or near the GPS would disrupt this process and (Figure 19A). A few mutations have been localized within the REJ domain (Figure 19B). Included in this set are nine germline missense mutations (Q3016R, L2993P, and E2771K), a de novo missense mutation (H2921P), an acquired somatic missense mutation (F2853S), an inframe deletion (6868-5aaDel), a nonsense stop codon (E3020X), and two generated mutations predicted to affect the cleavage (L3048F

and LT3048-9FS). Each of the residues was conserved, relative to its position amongst various species and they were characterized as highly pathogenic changes.

Therefore, we generated a series of expression constructs bearing the mutations and tested for the effect of each substitution on cleavage. We found that Q3016R, L2993P, H2921P, F2853S, and E2771K mutations almost completely inhibited cleavage (Qian et al., 2002). 6868-5aaDel, L3048F and LT3048-9FS partially inhibited cleavage, and E3020X did not generate a stable protein (Fig. 19C). As expected, four polymorphisms (F3064L, E2996D, R2791Q and R2985) in the same region were did not affect the cleavage pattern.

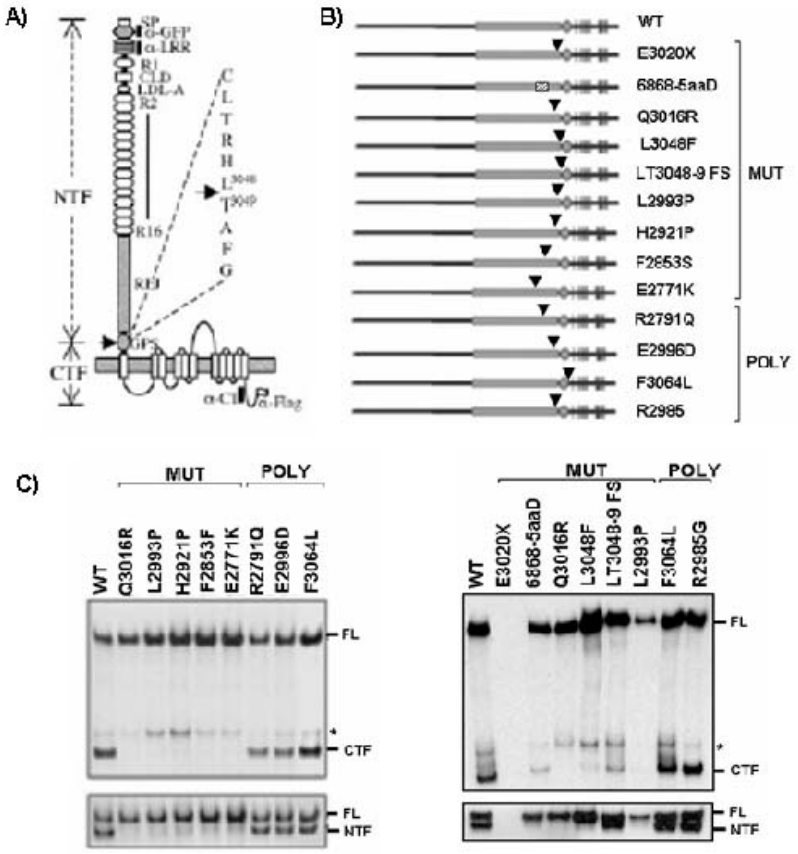

Figure 15. In vitro system for characterization of human mutations. A) A schematic diagram of the domain organization of polycystin-1. SP, signal peptide; R1 and R2–16, PKD repeats; CLD, C-type lectin domain. The cleavage site with the adjacent sequence is represented at right. A black bar indicates epitopes recognized by the antibodies used in this study. The positions of Flag-epitope and the GFP-tag are indicated. WT encodes FL polycystin-1 with a Flag-epitope, whereas GFP-WT has both a GFP-tag and a Flag-tag (Qian et al., 2002). B) Schematic structures of nine disease-associated mutant forms of polycystin-1 and four normal variants. An arrowhead marks the relative position of the substitution in each protein. ‘‘MUT’’ identifies disease-associated mutations and ‘‘POLY’’ identifies polymorphic variants. C) Immunoblots probed with antisera that recognize C-terminus (top) and N-terminus (bottom). FL=full length product, CTF=160KDa cleavage product, NTF= 400KDa cleavage product. The asterisk indicates an additional band of uncertain nature.

3.3.5. Intra- and intergenic analysis.

A total number of 224 different changes in PKD1 and 21 in PKD2 have been found along both genes by the PKDX test (Figure 15). We observed an extraordinarily high level of variability in the

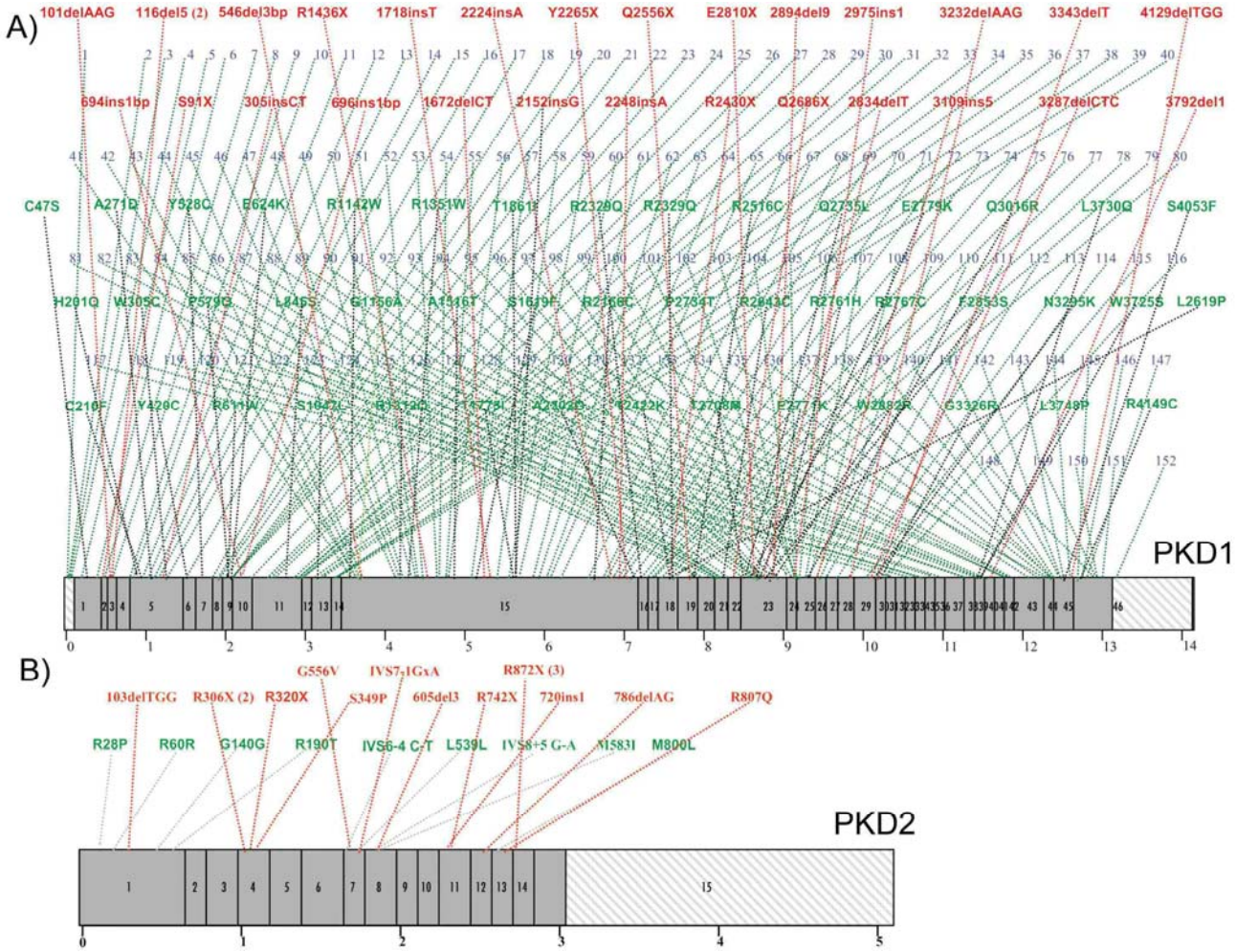

Figure 16. Diagram showing the mutations detected in the screening of the PKD1 (A) and PKD1 genes (B). Red color shows the definitive mutations, green the missense changes and the numbers represent the polymorphisms shown in table 11.

PKD1 gene, with a mean of 13.04 genetic variants per patient for PKD1 (range 0-60) and 0.92 genetic variants per patient for PKD2 (range 0-3) (Table 7).

One of our aims was to understand the mechanisms involved in PKD1 and PKD2 mutagenesis. In order to study the mutagenesis rate in both genes, it has been generated a table assigning specific codes to the different categories according to the type of change, pathogenicity, and conservation. Using this code classification (Table 12), each 4302 amino acids of *PKD1* and 969 of *PKD2* for every single patient of all 82 included in this study was categorized with a code number, generating a table of

432,333 independent amino acid codes We performed several analyses using this table arranging the study into three main parts: We performed several analyses arranging the study into three main parts:

- Intragenic analysis of *PKD1*.
- Intragenic analysis of *PKD2*
- Mutagenesis rate of *PKD1* and *PKD2*.

Change	Type	Pathogenicity	Conservation	Heterozygous	Homomozigous
None				0	0
Definitive Mutation	Stop Codon			11	110
Definitive Mutation	Insertion			12	120
Definitive Mutation	Deletion			13	130
Deletion inframe			Fully	21	210
Deletion inframe			Highly	22	220
Deletion inframe			No	23	230
Amino acid change	Missense	Patogenic higher	Fully	311	3110
Amino acid change	Missense	Patogenic higher	Highly	312	3120
Amino acid change	Missense	Patogenic higher	No	313	3130
Amino acid change	Missense	Equal	Fully	321	3210
Amino acid change	Missense	Equal	Highly	322	3220
Amino acid change	Missense	Equal	No	323	3230
Amino acid change	Missense	Polymorphism Higher	Fully	331	3310
Amino acid change	Missense	Polymorphism Higher	Highly	332	3320
Amino acid change	Missense	Polymorphism Higher	No	333	3330
Amino acid change	Unclassified	Patogenic higher	Fully	341	3410
Amino acid change	Unclassified	Patogenic higher	Highly	342	3420
Amino acid change	Unclassified	Patogenic higher	No	343	3430
Amino acid change	Unclassified	Equal	Fully	351	3510
Amino acid change	Unclassified	Equal	Highly	352	3520
Amino acid change	Unclassified	Equal	No	353	3530
Amino acid change	Unclassified	Polymorphism Higher	Fully	361	3610
Amino acid change	Unclassified	Polymorphism Higher	Highly	362	3620
Amino acid change	Unclassified	Polymorphism Higher	No	363	3630
Amino acid change	Polymorphism	Patogenic higher	Fully	371	3710
Amino acid change	Polymorphism	Patogenic higher	Highly	372	3720
Amino acid change	Polymorphism	Patogenic higher	No	373	3730
Amino acid change	Polymorphism	Equal	Fully	381	3810
Amino acid change	Polymorphism	Equal	Highly	382	3820
Amino acid change	Polymorphism	Equal	No	383	3830
Amino acid change	Polymorphism	Polymorphism Higher	Fully	391	3910
Amino acid change	Polymorphism	Polymorphism Higher	Highly	392	3920
Amino acid change	Polymorphism	Polymorphism Higher	No	393	3930
Polymorphism				4	40

Table 12. Codes assigned to the different type of mutations.

3.3.5.A. Intragenic analysis of *PKD1*

For this purpose, the rate of mutagenesis in each exon of PKD1 was calculated for changes grouped in two categories:

- A first group that includes definitive mutations, deletions in frame and missense and highly pathogenic changes (Figure 16A).
- And a second group which includes all changes (Figure 16B).

Exons were arranged along the x-axis and the rate of mutagenesis per 100 amino acids on the y-axis. For each exon, the rate is estimated with a 95% confidence interval. There is a "reference" line showing the 'median' rate. That is, if there were no association between exon and mutagenesis, based on the overall rate of the mutagenesis, the reference rate is what we would expect to see. Therefore, exons that have high rates with 95%

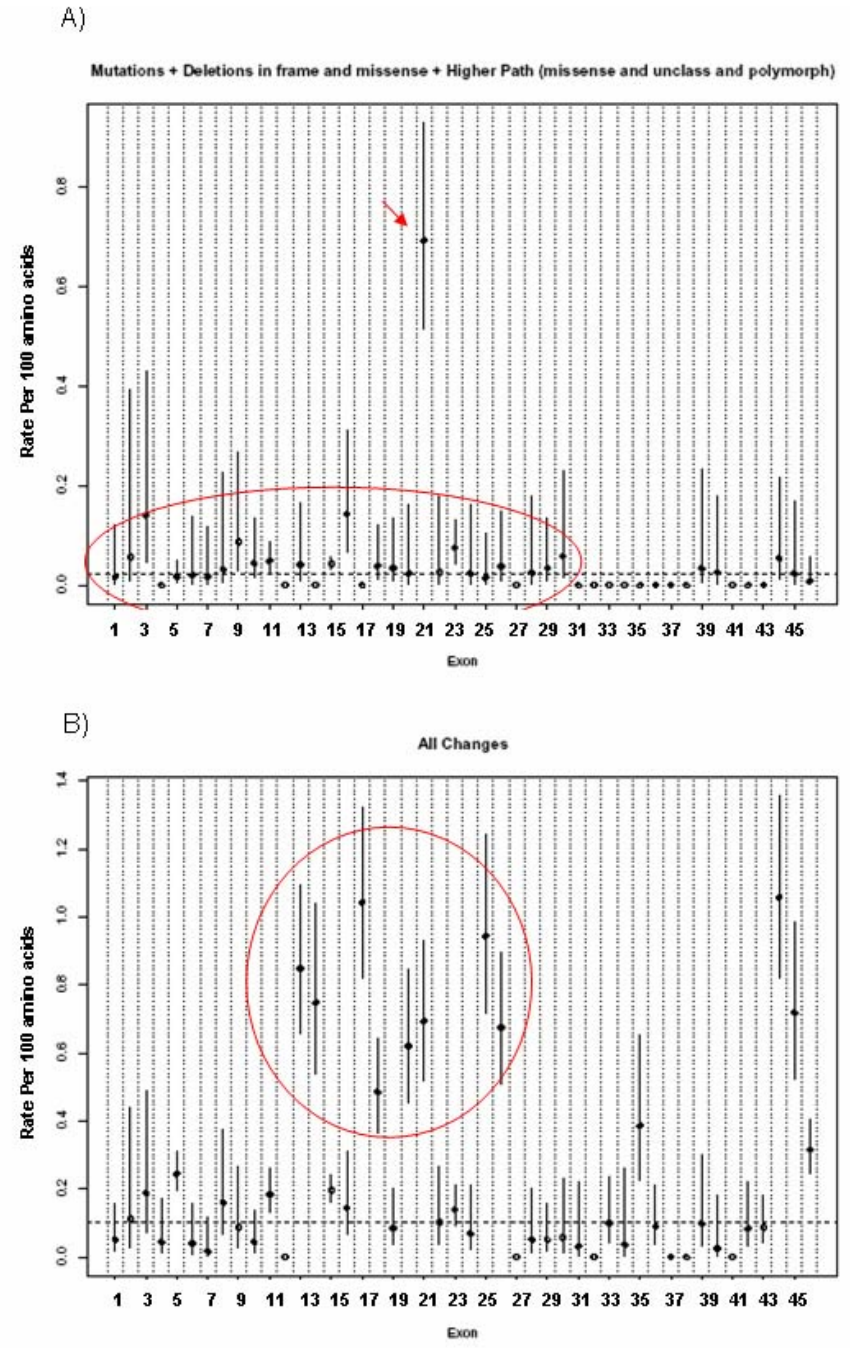

Figure 17. Mutability behavior of PKD1. A) Mutational rate for mutations (stop codons, frameshift and splicing, deletions inframe and highly pathogenic missense) and for all type of changes (B).

confidence intervals that do not overlap the reference line are associated with statistically significantly increased rates of mutagenesis. Using this information, we could determine the rate of mutagenesis per exon in each gene and find possible mutagenic patterns.

Figure 16A shows a cluster of amino acid changes: definitive mutations (frameshift mutation, stop codons and splicing variants), mutations probably associated to the disease (deletions inframe and missense changes) and any changes consider highly pathogenic in the replicated region of *PKD1* (exons 1-32). It also indicates an extremely high rate of mutagenesis for disease associated changes in exon 21, suggesting a mutagenic effect of the polypirimidine tract located in intron 21 into the surrounded areas. When we consider every single type of change in this analysis, high rate mutability appears to be also in an area surrounding exon 21, approximately between exon 13 to exon 26, supporting the previous hypothesis (Figure 16B).

A substantial fraction of the variants present in *PKD1* were also found in the homologues, suggesting the possibility of gene conversion between the homologues and the replicated region of *PKD*1 (Watnick et al., 1998). To verify that this mechanism of mutagenesis is involved, we compared the rates of mutagenesis of the replicated region (exons 1 to 32) versus the non-replicated region (exons 33 to 46). The IRRs represent the incidence rate in exons 1 to 32 divided by the incidence rate in exons 33 to 46. Therefore, IRRs greater than one suggest that exons 1 to 32 have increased mutagenesis as compared to exons 33 to 46, and IRRs less than one suggest that exons 33 to 46 have increased mutagenesis as compared to exons 1 to 32. There does not appear to be a difference in the rate of mutagenesis comparing exons 1-32 and 33-46 for all changes. The interesting thing is the comparison of a) definitive mutations only; b) definitive mutations, deletions in frame, and missense; c) and definitive mutations, deletions in frame, missense and highly pathogenic changes show clear evidence that the replicated region (exons 1-32) has a higher rate of mutagenesis than the non-replicated region (Table 13).

When only definitive mutations were analyzed, the IRR is somewhat higher than when we compare definitive mutations, deletions in frame, missense; definitive mutations, deletions in frame, missense and highly pathogenic (missense and unclassified), but it does not achieve statistical significance probably because the mutagenesis thought gene conversion is not the only phenomenon implicated in the highly mutagenic rate of *PKD1*.

Type of amino acid change	**IRR**	**95% confidence interval**	**p-value**
Definitive mutations only	**2.76**	0.64, 12.0	0.17
Definitive mutations, deletions in frame, and missense	**2.50**	1.09, 5.74	**0.03**
Definitive mutations, deletions in frame and missense and higher pathogenic (missense and unclassified)	**2.52**	1.06, 5.99	**0.04**
Definitive mutations, deletions in frame and missense and higher pathogenic (missense, unclassified, and polymorphisms)	**5.07**	2.15, 12.0	**<0.001**
All changes	0.97	0.80, 1.19	0.79

Table 13. Mutagenesis of the non-replicated vs. replicated region of PKD1.

As we mention in the introduction of this Thesis, there are three possible hypothetic mechanisms involved in the high mutagenic rate of the *PKD1* gene:

- Gene conversion between homologues and the replicated region of *PKD1*.
- Its highly GC-rich content with a large number of CpG dinucleotides, known as hot spots for C-T transitions.
- Influence of the Polypyrimidine tract present in intron 21.

This data shows the first strong statistical evidence that *PKD1* homologues (Figure 16A) and the polypyrimidine tract (Figure 16A-B) are the major phenomenons responsible of the high mutagenic rate in the *PKD1* gene. To test whether GC-rich regions and CpG dinucleotides are involved in *PKD1* mutagenesis, a depth analysis of the gene structure also has been developed.

Table 14 compares the nucleotide content of the human and mouse *PKD1* gene and cDNA, showing that the human *PKD1* gene and cDNA have 10% more of the GC content (GC%) and a higher

CpG dinucleotides content than the mouse genomic and cDNA. On the other hand, *PKD2* does not show this difference between human and mouse (Table 14). It has been shown that only 8-10% of the *Pkd1* knockout mice develop renal cyst. The difference in the mice *Pkd1* gene structure (with only one small polypyrimidine tract and the absence of homologues), in the CG% and in the CpG dinucleotides content could explain why humans have higher mutation rate and greater "second hits" in comparison to mice.

	PKD1				***PKD2***	
	gDNA		**cDNA**		**cDNA**	
	Human	**Mouse**	**Human**	**Mouse**	**Human**	**Mouse**
C	17664	11942	4828	4078	1075	1132
G	15766	11721	4643	3947	1193	1350
A	8486	12675	2148	2830	1398	1306
T	11606	10302	2520	3286	1407	1346
%GC	**62.5**	50.7	**66.9**	56-7	**44.7**	**48.3**
CpG	**2114**	594	**908**	300	155	167

Table 14. GC% and CpG content of Human and mouse PKD1 gene and cDNA.

However, a deep analysis of the gene structure has been develop to investigate whether the GC% or the large number of CpG dinucleotides are directly associated to the high mutation rate of *PKD1*. In the mutation database of the 82 families, CxT changes (*PKD1*, 40.2% and *PKD2*, 46.1%) and GxA changes (*PKD1*, 16.7 % and *PKD2*, 38.4%) were the most abundant (Table 15A). 52 of the 211 individual changes were located in CpG dinucleotides, but only three of these were mutations associated to the disease (Table 15B).

The analysis of GC% and CpG content in the full length *PKD1* coding sequence was also done (Figure 17), to determine if there is a mutational pattern associated to any of these mutagenic mechanisms. It was observed an increase of the GC% in the coding sequence of *PKD1*. Surprisingly, exon 3 has the lowest GC% but it has one of the highest mutagenic rates (Figure 15A).

On the other hand, exons 1 and 42 have the highest GC% and CpG content in addition to the lowest mutational rate. To determine if CpG dinucleotides are surrounded by rich CG% areas and if

A)

		Amino acid change			Polymorphism	Total	%
		Patogenic	Unclassified	Polymorphism			
	GxC	2	1	3	4	10	5,5
	GxT	1	1	0	2	4	2,2
	GxA	2	6	3	19	30	**16,7**
	CxG	1	2	0	6	9	5,0
	CxT	10	8	8	46	72	**40,2**
PKD1	CxA	4	3	0	9	16	8,9
	AxC	1	0	0	3	4	2,2
	AxT	0	1	0	1	2	1,1
	AxG	4	1	4	5	14	7,8
	TxC	3	1	2	8	14	7,8
	TxA	1	1	0	1	3	1,6
	TxG	0	0	1	0	1	0,5
	GxC	0	0	0	1	1	7,6
	GxT	0	0	0	0	0	0
	GxA	0	1	1	3	5	**38,4**
	CxG	0	0	0	0	0	0
	CxT	1	1	1	2	6	**46,1**
PKD2	CxA	0	0	0	0	0	0
	AxC	0	0	1	0	1	7,6
	AxT	0	0	0	0	0	0
	AxG	0	0	0	0	0	0
	TxC	0	0	0	0	0	0
	TxA	0	0	0	0	0	0
	TxG	0	0	0	0	0	0

B)

	CpG			
	Non sense	Amino acid substitution	Silent	Total
CxT	2	14	13	28
CxA	1	2	1	4
CxG	0	1	0	1
GxT	0	2	0	2
GxA	0	9	8	17
GxC	0	0	0	0
Total	3	28	22	52

Table 15. Nature of the PKD1 and PKD2 changes. A) CxT and GxA are the most common type of change found in ADPKD genes. B) 52 changes where linked to CpG dinucleotides.

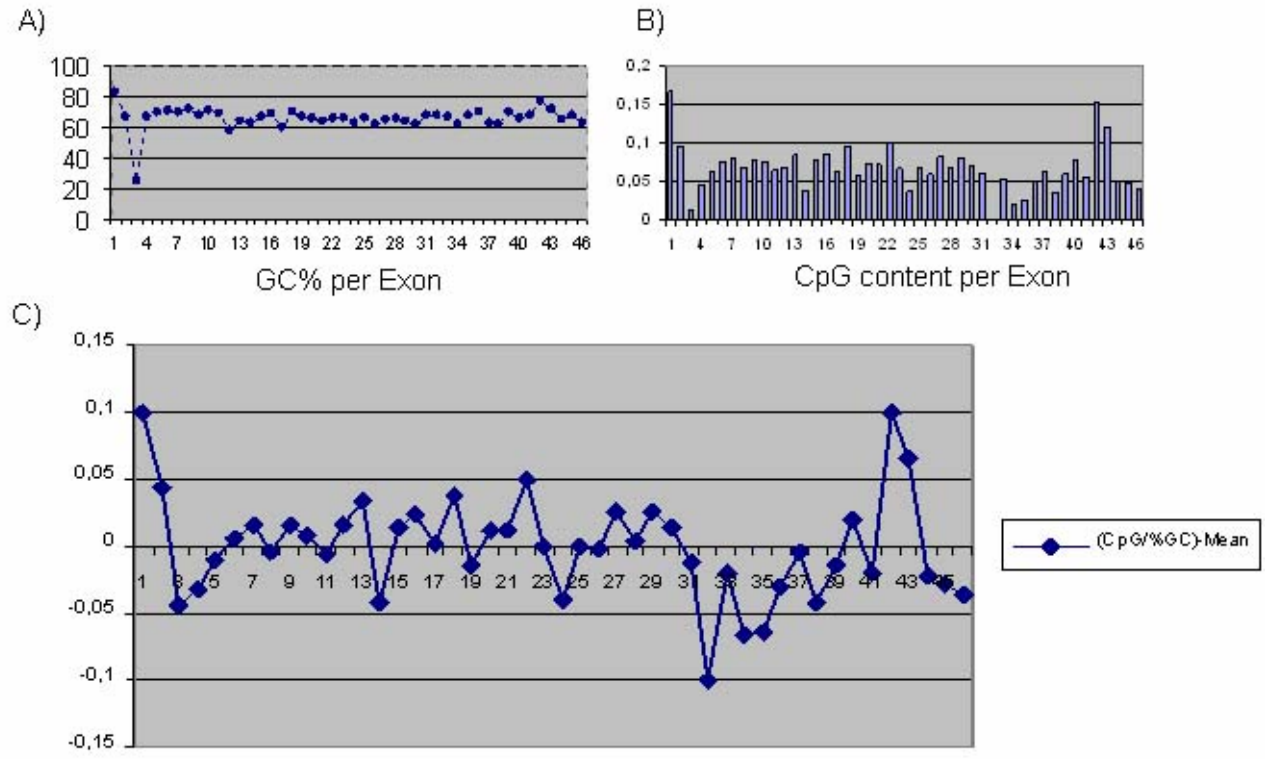

Figure 18. GC% and CpG content of human PKD1 gene. A) GC% rate per exon B) CpG dinucleotides content per exon. C) CpG dinucleotides in GC, normalized by exon.

they are associated with highly mutagenic rate exons, the ratio of CpG to GC% was taken. Unfortunately, we did not find any significant evidence that these two mechanisms are directly implicated into the highly mutagenic rate of *PKD1* gene. We cannot exclude that probably are responsible of some mutations.

3.3.5.B. Intragenic analysis of PKD2

The *PKD2* gene has a lower mutagenic rate per exon. This is especially evident in exon 21 of *PKD1* which has the highest mutagenic rate of 0.7, while the highest mutagenic rate of *PKD2* is only 0.23 in exon 1. The majority of the exons for *PKD2* also have rate of 0. This results in the improvement of the overall mutagenic rate of exons that have a rate grater than 0 based on the standard normalization (Figure 18). In addition, unlike *PKD1*, *PKD2* presents recurrent definitive mutations in exons 4, 11, and 14 with recurrent polymorphisms in exon 1. This recurrence evolutionally conserved could explain the higher mutagenic rate of these exons compare to the ones with rates equal to zero. However when the founder effect is taken into account and the recurrent

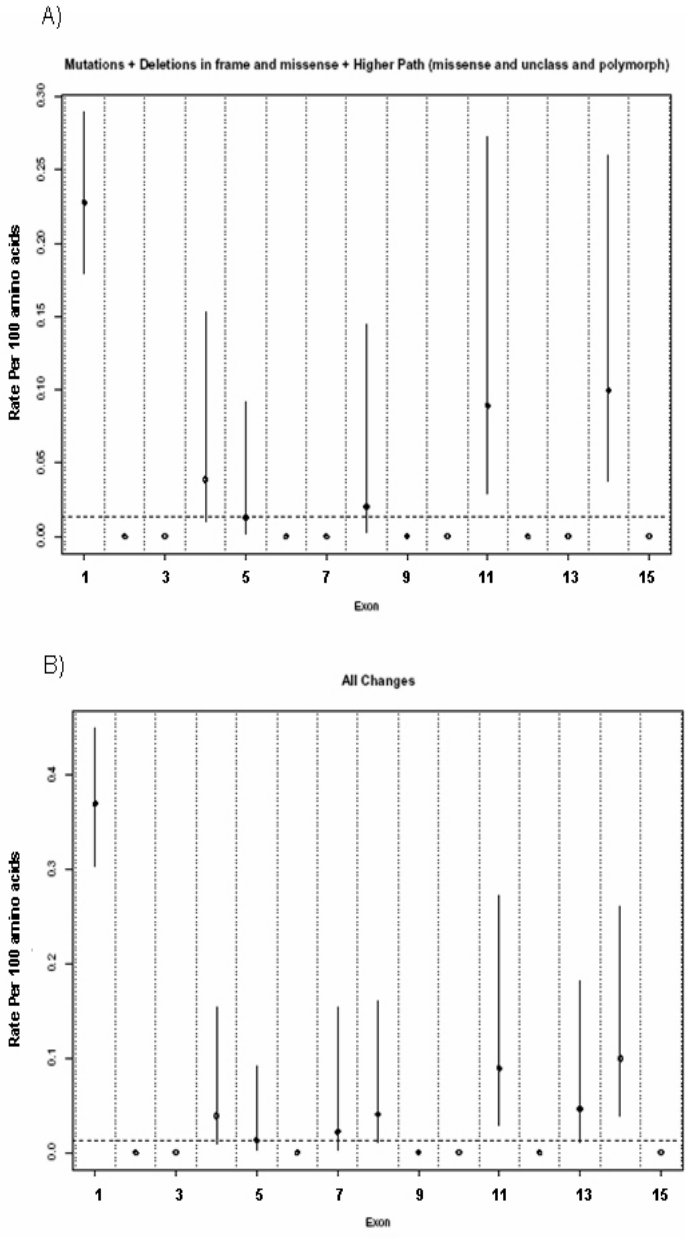

Figure 19. Mutability behavior of PKD2. A) Mutational rate per exon (stop codons, frameshift and splicing, deletions inframe and highly pathogenic missense) and for all type of changes (B).

mutation is actually considered to be unique, then the mutagenic rate would more accurately be closer to the base line.

3.3.4.C. Mutagenesis rate of PKD1 and PKD2.

The quantity that is used to evaluate the rate of mutagenesis is the "incidence rate ratio" (IRR), which is a ratio of the mutagenic rate in *PKD1* to *PKD2* (Table 16). An IRR greater than one indicates that the rate of mutagenesis in *PKD1* is higher than in *PKD2*, an IRR less than one indicates that the rate of mutagenesis in *PKD2* is higher than in *PKD1*, and an IRR of exactly 1 indicates that the rate of mutagenesis in *PKD1* and *PKD2* are equal. The table 16 provides the IRR for each group of changes and their 95% confidence intervals (i.e. a range of values, which we are 95% certain, contains the "true" IRR). The p-value tests the hypothesis that the true IRR is equal to 1. Observation of "all the changes" result in a p-value of <0.001. This means that if the IRR comparing mutagenesis in *PKD1* to *PKD2* truly is equal to 1, then the chance of observing a result as extreme as we observed (i.e. an IRR of 5.89) is less than 1 in 1000. Therefore, it is highly unlikely that the true IRR is equal to 1.

Group of changes	**IRR**	**95% confidence interval**	**p-value**
Definitive mutations only	1.36	0.62, 2.97	0.45
Definitive mutations, deletions in frame, and missense	2.79	1.47, 5.27	**0.002**
Definitive mutations, deletions in frame and missense and higher pathogenic (missense and unclassified)	3.27	1.74, 6.15	**<0.001**
Definitive mutations, deletions in frame and missense and higher pathogenic (missense, unclassified, and polymorphisms)	1.57	1.16, 2.13	**0.004**
All changes	**5.89**	4.60, 7.53	**<0.001**

Table 16. Mutagenic rate of PKD1 vs. PKD2

The IRR was, for all types of variant groups, greater that 1, indicating that *PKD1* is suitable to more mutation phenomenons than *PKD2*. One interesting phenomenon is that PKD2 shows similar provability to get a definitive mutation than PKD1, but significant less probability to get other type of mutation. That suggest than PKD2 has less plasticity than PKD1, and for this reason PKD1 needs more

hits to affect its function. As table 16 shows, *PKD1* is approximately six times (IRR= 5.89) more mutable than *PKD2*.

3.4. Discussion.

Given the age dependent manifestation, the potential for genotype/phenotype correlations and pre-symptomatic testing, there has been much interest in developing reliable techniques for DNA diagnosis in ADPKD (Hannig VL et al, 1991, Phakdeekitcharoen B et al., 2001). Pre-symptomatic testing, for example, may be relevant in a variety of clinical circumstances including the evaluation of living donors from ADPKD families, younger individuals or for those from *PKD2* families who have a milder disease. Moreover, unilateral nephrectomy in an individual at 50% risk of inheriting ADPKD may demand a higher level of certainty with respect to diagnosis since the consequence of uninephrectomy in an individual with ADPKD could lead to more rapid disease progression.

Genetic testing for ADPKD has posed a unique set of challenges in terms of DNA diagnostics. *PKD1* analysis in particular has been complicated because the 5' portion of the gene (exons 1-34) is replicated in at least five highly homologous copies (<2% divergence) on chromosome 16. Several groups were finally able to analyze the PKD1 sequence by using gene-specific primers to amplify large products that can then be screened via nested PCR (Watnick et al., 1997, Peral et al., 1996, Roelfsema et al., 1997 Badenas et al., 1999, Thomas et al., 1999, Watnick et al., 1999 Rossetti et al., 2001 Rossetti et al., 2002) Although some investigators have reported the use of denaturing high-performance liquid chromatography (DHPLC) to screen nested PCR products for mutations, unfortunately this strategy was not cost effective for clinical sample analysis (Rossetti., 2002). The main reason for this is that *PKD1* has a high rate of DNA variants, genetic and allelic heterogeneity, large gene size, and an absence of mutational hot spots at both genes, which has complicated the use of this method as a definitive test for mutational identification and potential genotype/phenotype correlations.

The establishment of a rational strategy to screen the entire coding region for both genes based on directed sequencing will reduce the efforts and costs in the study of ADPKD families. Watnick et al. have developed methods that could be broadly applied to the community for both research and clinical diagnostic purposes exploiting our knowledge about the sequence of *PKD1*, its homologues, and our experience in the use of long-range (LR) PCR. We applied the LR technology to the *PKD1* study and then progressively refined the primer pair combinations/anchor points so that "less-optimal" sources of DNA could also be use for testing. Our approach has since been widely embraced and has now formed the basis for the only PKD DNA test used in clinical practice (PKDX). We have worked closely with Athena Diagnostics to help translate our research-based methods into a useful clinical tool. This is the first transfer of gene discovery results to clinical practice for this disorder. There are a number of circumstances where it can be potentially very helpful (diagnostic uncertainties, pre-symptomatic evaluations in at-risk young adults, donor testing for living-related transplants, etc). The currently available DNA test offered by Athena Diagnostics (*PKD*X) involves direct-DNA sequencing of the entire coding regions of both *PKD1* and *PKD2*.

In order to test the sensitivity of PKDX, we submitted blood samples from 82 patients with clinical ADPKD to Athena Diagnostics for DNA testing. It has been found mutations distributed along the *PKD1* and *PKD2* genes with a detection rate around 83%, the highest until now. Using strict criteria, we were able to identify pathogenic mutations, defined as truncating mutations, splice site mutations, inframe insertions and deletions, in 51.3% of the patients tested. A substantial fraction of PKD mutations (31.7%) were missense changes that may be difficult to interpret in isolated samples or in the absence of a more refined understanding of the domain architecture of PKD proteins. In addition, we found a remarkably high rate of sequence variability in the *PKD1* gene with an average of 13 genetic variants per patient (range 0-60), suggesting that PKDX is indeed highly sensitive, as predicted. Direct sequencing is the most sensitive method showed up to now of detecting DNA

variability in *PKD1* and *PKD2,* but the need for strict interpretation of the results is essential if they are to be used for clinical decision-making. Complete analysis of both genes is especially important because there have been no mutational hot spots identified in either *PKD1* or *PKD2*. For this purpose, a criteria have been established to predict the pathogenicity of amino acid substitutions and potential splice site alterations for each proband.

The PKDX test has revealed a number of important observations:

- Of all the mutations found in *PKD1*, many of them were consider truncating (54.6%) but a significant fraction appears to result in missense changes (45.4%).
- On the other hand, almost all *PKD2* mutations resulted in truncation of the protein (92.5%) many localized in 5´segments and thus unlikely to yield a stable PC2.
- The majority of the *PKD1* mutations are unique to the family in which they were found. In contrast, 2 novel mutations were recurrent in more than one *PKD2* family (R306X in two families and R872X in three).
- 75% of the changes implicating the alteration of an amino acid (truncating, splicing, in frame mutations and amino acid changes) found in both genes were novel. Interestingly, only a small fraction of silent changes (31.6%) were not described previously. The entire in frame mutations were novel.
- While interfamilial variability may be explained in part by the position or nature of the germline mutation, intrafamilial variability is likely to be due to other genetic, environmental and stochastic factors. Several missense that were classified as “normal” or “undetermined” could play a important role in the variability found within the families linked to a unique mutation.

- We have identified a number of individuals with multiple missense changes but no definitive pathogenic mutation associated to the disease. It may be the case that, accumulation of this type of changes can compromise the plasticity shown by *PKD1*, resulting in a hypomorphic allele.
- These data highlight the challenges of distinguishing between "normal" missense variants and those that are likely to be disease-associated. Many of the missense changes found were unique to the family in which they were discovered. In some of the cases, they could be excluded as mutations because they did not segregate with the disease. Frequently, however, we found that the variant either segregated with disease or could not be further tested because of insufficient family material. As an example, it has been found ADPKD families with one novel missense change that was not detected in more than 164 chromosomes, but did not follow our criteria of classification of missense disease associated. This has several important implications: 1) DNA testing alone may not be able to provide definitive diagnosis in the setting of "private missense changes"; 2) further investigation and better tools are needed to evaluate the functional consequences of such missense changed.
- To solve this inconvenience, *in vitro* systems have been proposed to both study PC1 function and to determine how it is altered by disease-associated variants. While this part of the thesis was not originally proposed in the initial set of aims, the large number of missense changes with uncertain significance that have been identified, made it imperative that we tackle this problem. We knew that some of the missense changes almost certainly had to be pathogenic since they were discovered as either *de novo* or acquired mutations. *In vitro* system was used to evaluate putative mutations and

polymorphisms of the REJ domain. These results have several important implications: 1) we have shown that *in vitro* tools can be used to distinguish between polymorphisms and mutations; 2) We can use these systems to asses the effects of various *PKD1* sequence variants.

The data given by the direct sequencing of the entire *PKD1* and *PKD2* coding region has been proved to be a very powerful for a better understanding of both genes. After a comprehensive analysis of all changes through strict criteria, it has been established different approaches to analyze the different phenomenons implicated in the mutagenesis of both genes. It has been develop a statistical method based on a specific code classification for each amino acid of both genes per each individual. This code classification differentiates the unchanged amino acids from the ones that have suffer a change, taking in consideration the type of change (truncation, inframe, missense, polymorphism,…) and its zygote status (homozygous or heterozygous). Using this method, it has been tested different hypothesis proposed previously by other authors:

- Watnick et al. (1998) proposed the gene conversion between duplicated region of PKD1 (exons 1 to 34) and its homologues as a mechanism in the mutagenesis of this gene. They found that a substantial fraction of the variants were present in *PKD1* are also found in the homologues. It has been found changes all along of *PKD1*. The application of his statistical method proved that the duplicated region of *PKD1* is 5.07 times more suitable to changes disease associated than the non-duplicated region, suggesting the influence of a none random mechanism of mutagenesis in this region. Combining the application of this method and Watnick et al. findings, it can be concluded that the high rate of disease associated changes located in the duplicated region of *PKD1* is due to the gene conversion with its homologues.

- The American PKD1 consortium (1995) and Qian et al., (1996) reported an extremely unusual 2.5 kb polypyrimidine tract within intron 21 that may be responsible for the PKD1 increased rate of mutation. It has been suggested that this 2.5 Kb polypyrimidine tract, the longest found in humans, can form intramolecular triplex structures, predisposing to mutation and loss of function (Blaszak et al., 1999). These hypotheses have been tested through a systematic analysis of all type of variants along both genes, founding a highly mutagenic area in the surrounded region of intron 21, near the polypyrimidine tract. Interestingly, we also observed the highest mutagenic rate of PKD1 in exon 21.
- Two other mutation mechanisms hypothetically related to the high mutation rated of PKD1 are the influence of the GC% and CpG sites. It has not been found robust date that supports these hypotheses with the statistical method, but, it suggested the possible association of the CG% to areas of high mutational rate. The implication of mutational mechanism associated to the CpG site was less obvious, with 3 disease associated mutations found in a CpG site. No definitive data was found for definitively confirm these hypotheses.
- A new mutation mechanism has been associated with the high mutation rate of PKD1. It has been proved that symmetric elements along the genomic sequence of PKD1 were hot spots for <u>all</u> frameshift mutations (deletions and insertions) found in the 82 individuals, and in 76% of the frameshift mutations previously reported. This phenomenon has been related with mutagenesis in other genes, but it is the first time that has been related to the mutagenesis of a PKD gene. Deletion breakpoint junction regions were found to be non-

random both at the nucleotide sequence levels, an observation consistent with an endogenous sequence-directed mechanism of mutagenesis (Krawczak et al., 1991).

Also, it has been provided experimental evidence that *PKD1* is highly mutable. Comparing *PKD1* and *PKD2* genes through statistical method, it has been shown that *PKD1* is ~6 times more mutable than *PKD2*. In one striking example, we found one individual who had 60 *PKD1* variants and only 1 *PKD2* polymorphism. Another observation is that while *PKD1* did not show major recurrent mutations, *PKD2* showed recurrence in some individuals. We also have observed that there are individuals who tend to have many changes while there are others who have very few. One potential explanation is that certain haplotypes might be more mutable. Given the high mutability of *PKD1*, we suggest that the prevalence of individual mutations in evolution will increase, resulting in a greater frequency of more than one mutational event directly associated with disease severity per patient. When *PKD2* suffer a mutational event, in most of the cases, result in a change disease associated. On other hand, *PKD1* need more hits to really cause a disease associated mutation, showing the high plasticity of this gene

In this part of the thesis, it has been introduce the only clinical test (PKDX, Athena Diagnostics) offered for diagnosis of ADPKD patients. It has been proved to be the most effective test describe up to now, with 83 % of detection rate. It has been established a critic criteria for classification of the changes found in the ADPKD genes. Also, it has been presented a novel approach for analysis of mutagenesis for the ADPKD genes based on statistical analysis, which can be applied for the analysis of other genes. Based on this method, it has been proved the implication of different mutagenic mechanisms involved in the PKD genes.

4 Conditional Inactivation of Murine PKD2 using a tri-allelic system (SUBPROJECT II).

4.1. Abstract

Homozygous inactivation of either murine *Pkd1* or *Pkd2* results in embryonic lethality, limiting the use of these models to study adult phenotypes. Several groups have made floxed alleles of *Pkd1* but since the function of *Pkd1* and *Pkd2* may not be entirely overlapping, a floxed allele of *Pkd2* would be a valuable tool. We generated mice with a loxP site in *Pkd2* intron 10 and a loxP-FRT-PGKneo-FRT cassette in intron 13 ($Pkd2^{flox11\text{-}13}$). Cre-mediated recombination between the loxP sites was predicted to result in loss of the C-terminal tail of the protein, which mimics many disease-associated mutations. We found that $Pkd2^{cond}$ behaved as a hypomorphic allele. Matings of $Pkd2^{flox11\text{-}13/+}$ heterozygotes yielded only 3/57 live homozygotes. However, when the neomycin cassette was deleted mice that were homozygous for the resulting $Pkd2^{delneo}$ allele were fully viable and fertile. Next, we bred $Pkd2^{delneo}$ mice with a Cre deleter strain to produce mice that carried a germ line deletion of exons 11-13 and we found that this allele ($Pkd2^{Ko11\text{-}13}$) functioned as a true null. In order to determine whether $Pkd2^{delNeo}$ could be inactivated *in vivo*, we generated mice that were heterozygous for $Pkd2^{Kol11\text{-}13}$ and $Pkd2^{DelNeo}$ in combination with a Meox-2 directed Cre recombinase. Since Meox-2 Cre results in greater than 95% (somatic) deletion of floxed DNA segments, these mice die shortly after birth and have all the features of the classic *Pkd2* null phenotype, including severe edema, renal cysts, pancreatic cysts, and randomization of left/right axis. This system has provided three new *Pkd2* alleles: a hypomorphic allele, a new knock-out allele that is predicted to lack the *Pkd2* C-terminus, and a conditional allele that can be used to selectively inactivate *Pkd2 in vivo*. These models will provide a rich source of cells for *in vitro* inactivation of *Pkd2*.

4.2. Matherial and Methods.

4.2.1 Generation of Pkd2^{cond} targeting construct.

The goal in this project was to develop a line of animals in which we could regulate the timing and location of a Pkd2 mutation. It has been engineered a targeting construct with two lox P sites flanking exons 11-13 along with an FRT-flanked neomycin cassette (gift of Dr. Gail Martin) inserted into intron 13 (Fig. 20A-C). Cre-mediated recombination between the lox P sites should result in the loss of exons 11-13 generating a frameshift with a premature termination codon early in exon 14. This change is similar to several truncating mutations that have been associated with the human disease. The targeting construct was entirely sequenced and then electroporated into 129SV/J stem cells.

~230 clones were screened by Southern blot analysis and 21 legitimate targeting events were identified. Since the two lox P sites were separated by ~1.5 kb, it has been predicted that the proximal site would be lost in a subset of the clones after the homologous recombination. This was assayed by PCR and as expected, all but three clones had lost the lox P site located in exon 11. Of these clones, one was injected into C57BL/6 blastocysts and obtained six highly chimeric (>95%, assayed by coat color) animals (four females and two males). The two male chimeras were bred to C57BL/6 females and the agouti animals were tested for germ line transmission of the floxed allele by Southern blot as demonstrated in Fig 20D. The blot demonstrates that four of the pups in this particular litter have germ line transmission of the floxed allele. PCR analysis confirmed the presence of both lox P sites

4.2.2. Functional inactivation of the Pkd2^{cond} allele.

To test whether the deletion of exons 11-13 would result in a functional null allele (*Pkd2$^{Ko11-13}$*), heterozygous *Pkd2*^{cond} (also called *Pkd2$^{flox11-13}$*) F1 mice were bred with *Meox-Cre* transgenic mice to produce *Pkd2$^{flox11-13/+}$* male offspring that were also positive for the *Meox-Cre* transgene. Expression of the latter results in deletion of floxed DNA segments in >95% of the carrier's germline (Tallquist et al., 2000). Thus, the majority of its offspring should have either the *Pkd2^{+}* or *Pkd2$^{del11-13}$* allele. Given

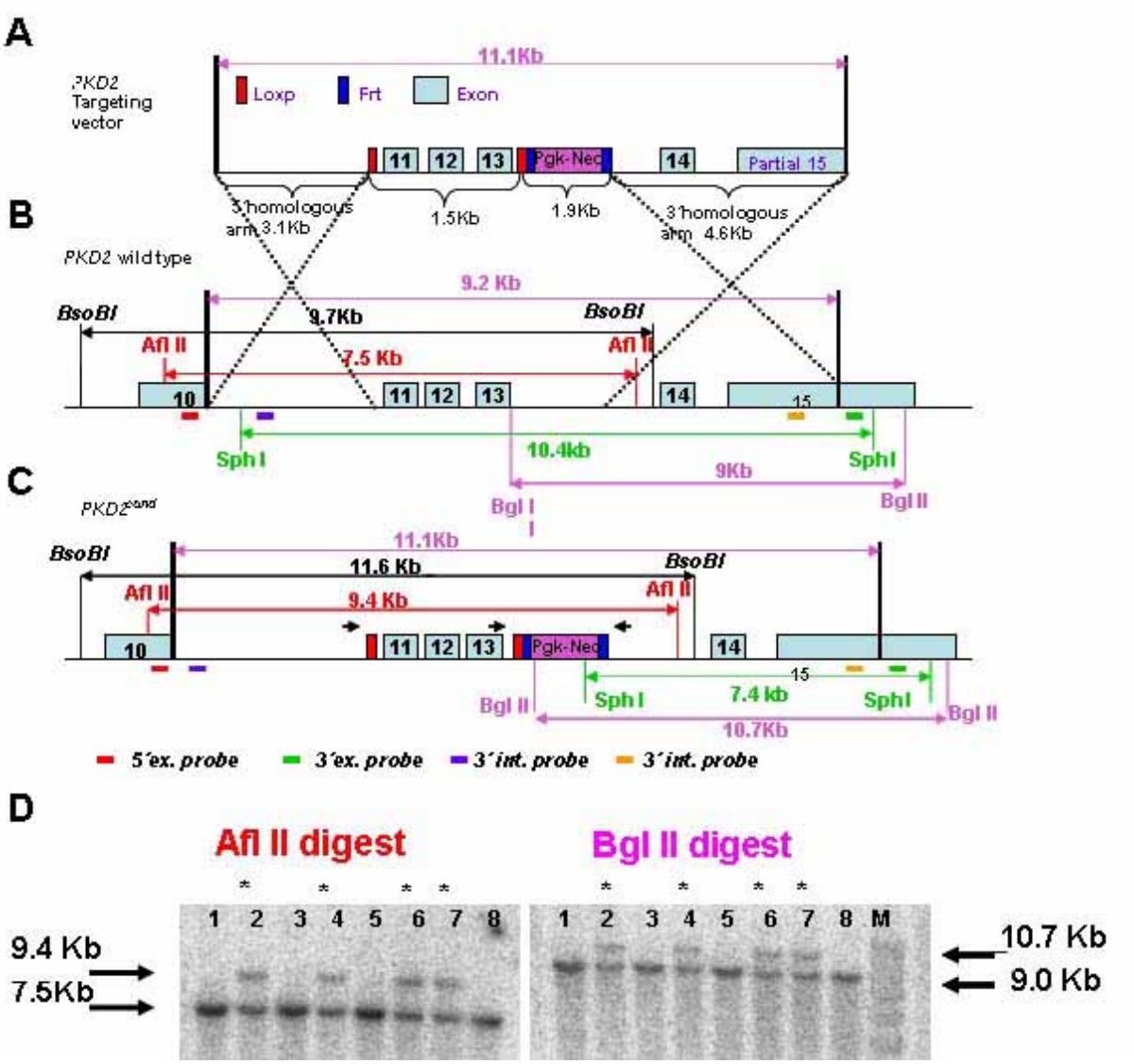

Figure 20. Pkd2 Genomic map and Targeting contruct. A) Targeting construct is 11Kb in length and contains Lox P sites and a FRT-flanked neomycin cassette. B) Wild-type allele. C) Predicted restriction map after homologous recombination. Probes used to analyze stem cells and mice are shown. Arrows denote primers designed to assay Flp mediated detection of Pgk.Neo cassette and Cre mediated deletion of exons 11-13. D) Southern blots from offspring o chimeric animals. Tail DNA was digested with two restriction enzymes and probed with a 5´external probe (AfkII) or a 3´internal probe (BglII). Four pups (asterisks) have germ line transmission of the targeting construct.

that the homozygous state for null mutations of *Pkd1* results in embryonic lethality, we reasoned that $Pkd2^{Ko11\text{-}13/\ Ko11\text{-}13}$ heterozygotes also were unlikely to be viable. We tested this hypothesis by setting up a series of 10 crosses between $Pkd2^{flox11\text{-}13/+}$; $Meox2^{Cre/+}$ males and females to evaluate the pregnancies.

4.2.3. Genotyping.

Genomic DNA from mouse-tails was obtained as follows. In short, ~5mm long piece of the tails were digested in Proteinase K buffer (50 mM Tris pH 8.5, 1 mM EDTA, .5% Tween 20) at 60°C for about 2h with shaking. After inactivation of the enzyme at 99°C for 15min, 1µl of the solution was used for PCR genotyping with primer locations shown in Figure 21, and whose sequences are as follows:

Primer a (MG-Pkd2loxp-F): CCT TTC CTC TGT GTT CTG GGG AG.

Primer b (MG-Pkd2loxp-R): GTT TGA TGC TTA GCA GAT GAT GGC.

Primer c (MG-Pkd2Pgk-F): GGG GTT TCC TAT GAA GAG TTC CAA G.

Primer d (MG-Pkd2Pgk-R): CTG ACA GGC ACC TAC AGA ACA GTG.

Primer e (MG-Pkd2PGKR2): GCC AGA GGC CAC TTG TGT AG.

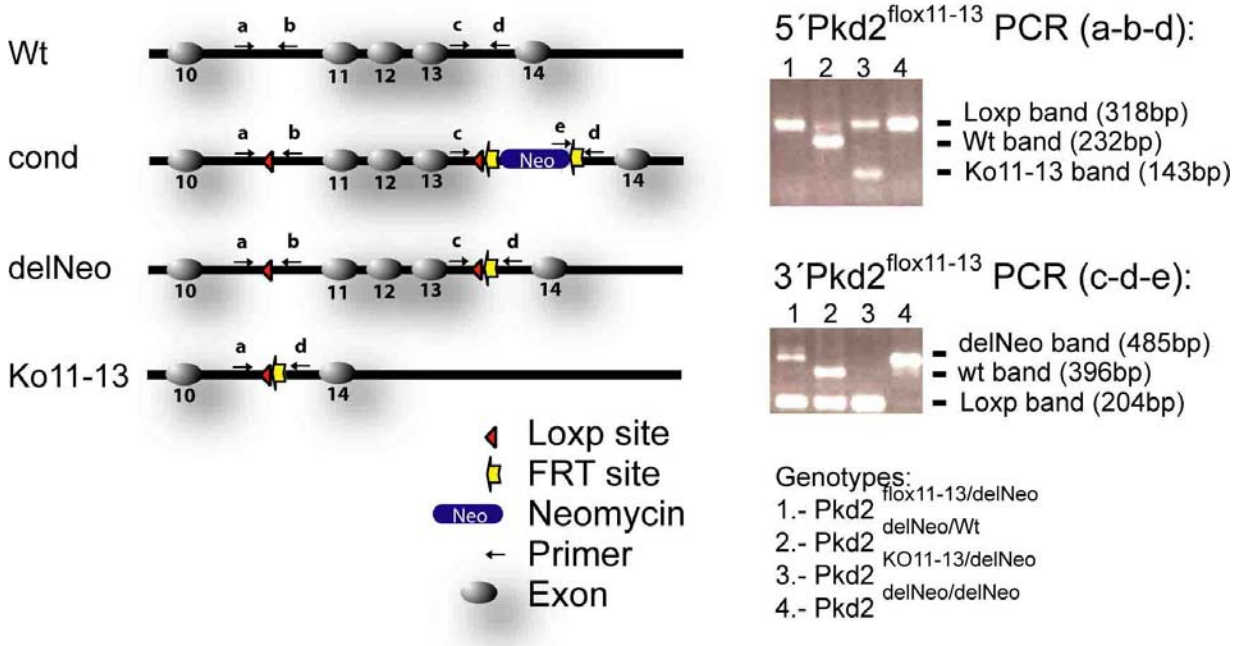

Figure 21. Pkd2 genotypes derived from the Pkd2^{Cond} allele (Pkd2$^{flox11-13}$). Schematic illustration of the *Pkd1*^{cond}(*PKD2*$^{flox11-13}$), *Pkd2*^{delNeo} and *Pkd2*$^{ko11-13}$ alleles and the positions of the primer pairs for the genotyping strategy. The predicted sizes for the various products are illustrated into the schematic gel drawing on the right. Different genotypes are shown as an example of PCR-based genotyping strategy.

4.2.4. Preparation for Histology.

Kidney, liver, and pancreas specimens from adult animals were collected and immediately fixed in 10% buffered formalin at 4°C overnight. Embryos at different ages were fixed with ice-cold 4% paraformaldehyde in PBS via cardiac perfusion of the mother and then kept in 4% paraformaldehyde overnight at 4°C. Following rehydration in water for 2h, all samples were dehydrated in a graded alcohol series and embedded in paraffin for histological analysis.

4.2.5. Immunofluorescent staining.

For immunolabeling, tissues were fixed, sectioned and stained as previously described (Esni et al., 2004). The following antibodies were used at the indicated dilutions for immunofluorescence analysis; rat monoclonal anti-E-cadherin (Zymed Laboratories, 1:200), rabbit polyclonal anti-Pdx1 (gift from Christopher Wright, 1:500), goat polyclonal anti-amylase (Santa Cruz Biotechnology, 1:500), and guinea pig polyclonal anti-insulin and anti-glucagon (Linco Research, 1:1000). The following reagents were purchased from Jackson ImmunoResearch Laboratories: Biotin-conjugated anti-rat (1:500), anti-guinea pig (1:500) and anti-goat IgG (1:500). Cy3- and Cy2-conjugated streptavidin (1:1000, 1:300), Cy3-conjugated anti-rabbit (1:300), and Cy5-conjugated anti-rat (1:300). For each antibody, specificity was confirmed using negative control slides omitting primary antibody. Fluorescence confocal microscopy was performed with a confocal laser scanning microscope (410LSM, Zeiss) using a 40x (NA 1.5) C-apochromat objective, and image analysis was performed using MetaMorph series 5.0 software (Universal Imaging).

4.2.6. Reverse Transcription–PCR.

Total RNA was extracted from fetal tissues using the Qiagen RNA extraction kit according to the manufacturer's protocol. First-strand cDNA was synthesized using Superscript II (Invitrogen) from 100 ng of total RNA and then used as template for PCR amplification of *Pkd1* transcripts (Platinum Taq; Invitrogen). Primers; (a) MGcPkd2-10F: CAGCAGAAAGCAGAAATGG; (b) MGcPkd2-14R:

CGTCCTAACACCTCTCGTCT; (c) MGcPkd2-15F: GGAAGTGGAAATGGAAGTGCTAAC; (d) MGcPkd2-15F: CTTATCATTGTCGTACTGGACAGCC; were used to amplify the different products of the entire mouse *Pkd2* cDNA (Figure 27C), with a common T^m of 55.5 ºC.

4.3. Results.

It is anticipated that the gene modifications described above will result in animals with four different *Pkd2* alleles (Figure 21), with which three of them would be use for its characterization. The first will have the correctly targeted allele with both lox P sites and the FRT-flanked neo gene (*PKD2$^{flox11-13}$,* Figure 21). It is very possible that the neomycin gene, which is within 400 base pairs of exon 13, will impair the transcriptional efficiency of *Pkd2*, thereby yielding a loss-of-function type allele with variable penetrance. The second allele will be created by FLP-mediated deletion of the neomycin gene (*Pkd2^{delNeo},* Figure 21). It is expected that this allele will function completely normally. The third allele will be a true mutant after Cre-mediated excision of exons 11-13 (*Pkd2$^{ko11-13}$*, Figure 21). The goal of the first two aims is to test each of these alleles.

4.3.1. Confirm that the floxed allele is functional

It has been generated a floxed allele with the possibility of generating three functional conditional alleles (Figure 22). First one, the Pkd2$^{flox11-13}$ with two loxP sites flanking exons 11, 12 and 13 and a neomycine selection marker flanked with two FRT sites in intron 13. It would be tested the possibility that this allele function as hypomorphic, due o the presence of three stop codons in three different frames causing transcription termination. A second *Pkd2$^{del11-13}$* allele has been generated by using the Cre/lox system into the Pkd2$^{flox11-13}$ to delete the exons 11-13 in presence of the neomycine cassette. The *Pkd2$^{del11-13}$*allele is predicted to be null, same as the *Pkd2$^{Ko11-13}$* allele. In order to generate a fully viable conditional allele (*Pkd2^{delNeo}* allele), the neomycin cassette has been deleted through recombination between the two FRT sites mediated by FLP recombinase expression

(FLP/FRT system). A forth allele, *Pkd2*$^{Ko11\text{-}13}$, can been generated through loxP site recombination by crossing the Pkd2^{delNeo} allele with a murine line expressing Cre recombinase (Cre/lox system using a Meox2-Cre expressing mice). This allele is predicted to delete an important region of the C-terminal portion of PC2, causing the disruption of this protein. Both the FRT sites, flanking the neomycin cassette, and the Lox-P sites have been proved to be functional in vivo through a PCR-based strategy (Figure 21). Figure 22 shows that the PCR from primer pairs 2/3 amplify bands of 2.4 kb or 385 bp in *Pkd2*$^{flox11\text{-}13}$ or wild type alleles, respectively. Therefore heterozygous mice (*Pkd2*$^{flox11\text{-}13/+}$; Figure 22, lane 1) have both bands. *Pkd2*$^{flox11\text{-}13/flox11\text{-}13}$ homozygotes (Lane 2) have only the 2.4 kb band while *Pkd2*$^{+/+}$ wild type mice (Figure 22, lane 5) have only the 385bp band. When the FRT sites are activated using FLPase, the Neomycin gene is deleted (*Pkd2*^{delNeo}) such that primers 2/3 amplify a PCR product of 473 base pairs. Therefore, *Pkd2*$^{delNeo/+}$ mice (Figure 22, lane 4) have both the 473 and 385 bp. bands. When a broadly expressed Cre activates the LoxP sites, primer 2 is deleted along with exons 11-13.

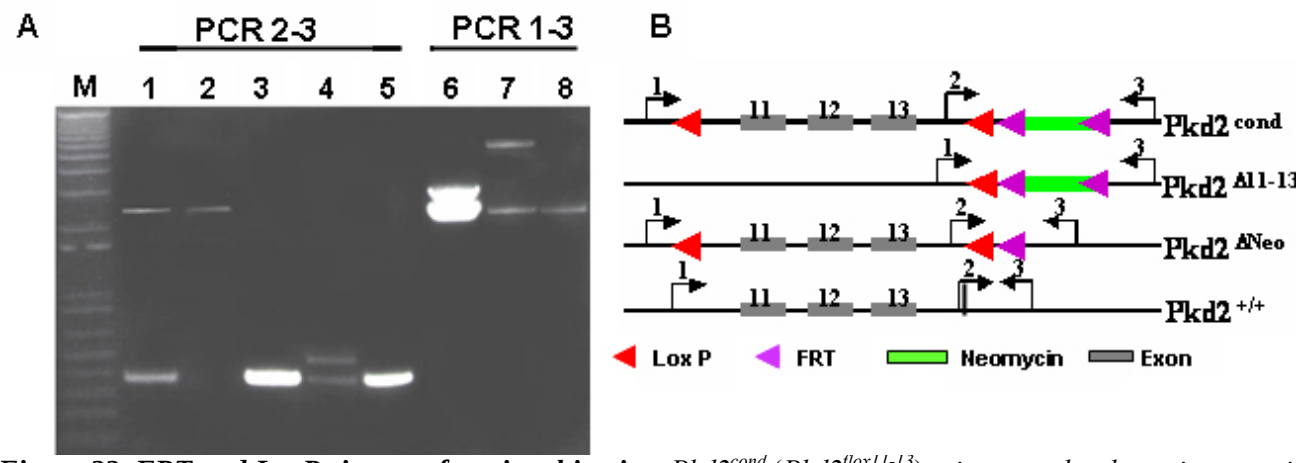

Figure 22. FRT and LoxP sites are functional in vivo. *Pkd2*^{cond} (*Pkd2*$^{flox11\text{-}13}$) *mice were bred to mice carrying broadly expressed FLPase or Cre enzymes. (A) PCR genotyping of the progeny using two primer pairs as demonstrated schematically (B). Lanes 1 &7: Pkd2*$^{flox11\text{-}13/+}$*, Lane 2: Pkd2*$^{flox11\text{-}13/flox11\text{-}13}$*, Lanes 3 & 6: Pkd2*$^{del11\text{-}13/+}$ *Primer #2 is deleted by deletion of exons11-13, Lane 4: PKD2*$^{delNeo/+}$*, Lane 5 &8: PKD2*$^{+/+}$ *(wild-type). M=1 Kb plus ladder, PKD2*$^{flox11\text{-}13}$ *is the targeted, floxed allele. PKD2*$^{del11\text{-}13}$ *results after activation of LoxP sites (deleting exons 11-13) while PKD2*^{delNeo} *is generated after activation of FRT sites, deleting the Neomycin gene. Primers 1,2,3 are designated by labeled arrows. LoxP sites: red arrows, FRT sites: purple arrows, Neomycin gene: Green box, Exons: Grey boxes.*

Therefore, *Pkd2*$^{del11\text{-}13/+}$ mice have only the wild type band (385 bp). Functionality of the LoxP sites is confirmed by PCR using primers 1/3. Primers 1/3 amplify a product of 4.1 kb or 2.2 kb in *Pkd2*^{cond} or wild type alleles, respectively (Figure 22, lane 7: *Pkd2*$^{flox11\text{-}13/+}$, lane 8: *Pkd2*$^{+/+}$ wild type mice). Activation of LoxP sites results in a band of 2.8 kb. As expected PCR 1/3 in *Pkd2*$^{\Delta 11\text{-}13/+}$ mice yields bands of 2.8 and 2.2 kb (Figure 24, lane 6).

Since the neomycin cassette may have an effect on *Pkd2* expression, we removed this element from a subset of mice at the outset. *Pkd2*^{cond} mice were crossed to mice expressing the Flp recombinase to generate mice with only loxP sites flanking exons 11-13 (*Pkd2*$^{delneo/+}$). Deletion of the neomycin gene was confirmed using PCR. Once the neomycin cassette is removed, this allele should behave in a wild-type fashion. In order to document this, males and females with the *Pkd2*$^{flox11\text{-}13/delneo}$ allele were crossed and homozygotes should be born in the expected Mendelian ratio. As expected, once the neomycin cassette was deleted, mice that were homozygous for *Pkd2*$^{delNeo/delNeo}$ were viable, fertile, and born in the expected Mendelian ratios.

4.3.2. Neomycin cassette results in a hypomorphic allele.

If the neomycin gene significantly impairs transcription of *Pkd2*, we would expect that homozygosity for *Pkd2*$^{flox11\text{-}13}$ would lead to a lethal phenotype as above. If there is some functional polycystin-2 made, however, then we may wind up with a hypomorphic allele represented by a milder phenotype. In order to establish a breeding colony for these experiments, it has been crossed *Pkd2*$^{flox11\text{-}13}$ mice with NIH Black Swiss mice. The highly chimeric male was also being crossed to 129SV/J (wild type) mice yielding offspring with germ line transmission of the *Pkd2*$^{flox11\text{-}13}$ allele in an inbred 129SV/J background. We first examined a small number of adult heterozygotes (N=5) for abnormalities associated with the heterozygous state. The literature suggests that adult *PKD2* null heterozygotes will have occasional kidney cysts and asymptomatic liver cysts.

The *Pkd2*$^{flox11\text{-}13}$ allele was bred to homozygosity. As expected, the *Pkd2*$^{flox11\text{-}13}$ allele has reduced viability due to the presence of the neomycin cassette, which is known to have a variable effect on splicing. From several *Pkd2*$^{flox11\text{-}13/+}$ matings, only 3/57 were homozygous for the *Pkd2*$^{flox11\text{-}13}$ allele (expected 1/4 or ~14), suggesting that around 80% of the *Pkd2*$^{flox11\text{-}13/flox11\text{-}13}$ offspring died in utero. It has been found three different manifestations these *Pkd2*$^{flox11\text{-}13/flox11\text{-}13}$ mice that survived to birth: a) those without any major observed phenotype, b) with a severe vascular phenotype and aneurisms, and c) those with a sonic hedgehog protein like-phenotype (Helms et at., 1997) with cleft palette and a central eye never associated previously to loss of *Pkd2* (Figure 23A). The *Pkd2*$^{flox11\text{-}13/flox11\text{-}13}$ embryos which died in utero have been associated with a very severe vascular phenotype, with a general dilatation of the vascular tree (Figure 21B). None of the *Pkd2*$^{flox11\text{-}13/flox11\text{-}13}$, the ones that survived to birth and the ones that died in utero, manifested the classic features associated with total loss of *Pkd2* (edema, cystic renal disease, cardiac abnormalities, and situs inversus) except the vascular phenotype.

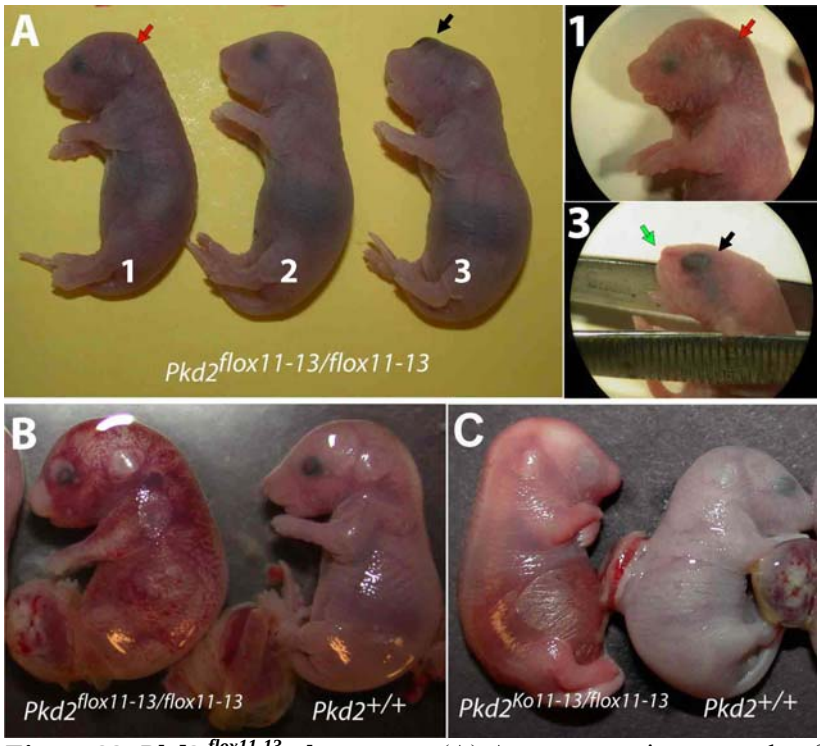

Figure 23. Pkd2 $^{flox11\text{-}13}$ ***phenotypes.*** (A) A representative example of *Pkd2*$^{flox11\text{-}13/flox11\text{-}13}$ mice at the first day of live that survived manifesting no obvious phenotype (pup #2), vascular phenotype and aneurisms (red arrow, pup #1), or a rare phenotype with an central eye (black arrow, pup #3) and cleft palette (green arrow, pup #3). (B) The *Pkd2*$^{flox11\text{-}13/flox11\text{-}13}$ embryos of developmental day E16.5 showed a severe dilatation of the vascular tree. (C) The *Pkd2*$^{Ko11\text{-}13/flox11\text{-}13}$ dead at E17.5 had the typical edema and hemorrhage similar to that previously reported for Pkd1 and Pkd2 null embryos, but without polycystic kidney and pancreas disease.

However, if pregnancies of *Pkd2*$^{flox11\text{-}13/+}$ vs. *Pkd2*$^{Ko11\text{-}13/+}$ were harvested at E17.5, the compound heterozygotes (*Pkd2*$^{Ko11\text{-}13/flox11\text{-}13}$) display a vascular phenotype similar to that described for

both *Pkd2* and *Pkd1* null alleles with gross edema and hemorrhage (Figure 23C). These studies suggest that the *Pkd2*$^{flox11\text{-}13}$ allele is hypomorphic targeting the *Pkd2* locus.

4.3.3. Inactivation of Pkd2 leads to PKD phenotypes.

In order to test whether deletion of exons 11-13 would result in a null phenotype, we bred *PKD2*^{delNeo} mice with Meox2-Cre transgenic mice. Since the Meox-2 Cre results in >95% deletion of floxed DNA segments in the germline of the carrier, we were able to generate mice that were heterozygous for *Pkd2*$^{KO11\text{-}13}$ (Tallquist et al., 2000). The embryos that were homozygous for this "knock out" allele exhibited the classic features of the "Pkd" null state with polyhydramnios, hemorrhage and edema (Figure 24).

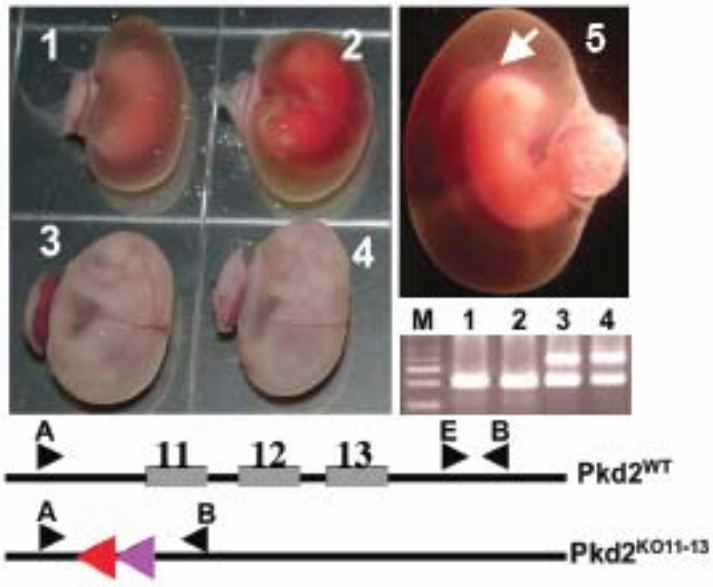

Figure 24. Pkd2$^{KO11\text{-}13}$ functions as a null allele. We used a Meox-2 Cre transgenic line to generate mice with a germ line *Pkd2*$^{KO11\text{-}13}$. We crossed heterozygotes and harvested the pregnancy at E15.5. A subset of the embryos (1-4) is shown with their corresponding PCR genotypes. Embryos 3 and 4 are *Pkd2*$^{KO11\text{-}13/+}$ and look normal, while 1 and 2 (close-up in panel 5) are homozygotes (*Pkd2*$^{KO11\text{-}13/KO11\text{-}13}$). Both homozygous embryos exhibit polyhydramnios and edema (arrow). Location of PCR primers for WT and *Pkd2*$^{KO11\text{-}13}$ alleles are mapped. All four primers are used in the genotyping reaction. The "E" primer is lost upon Cre mediated deletion so only a smaller band is amplified.

With the goal of determining whether *Pkd2*^{delNeo} could be inactivated *in vivo*, we used a breeding strategy to generate mice heterozygous for one *Pkd2*$^{KO11\text{-}13}$ allele in combination with *Pkd2*^{delNeo} and Meox-2 Cre. In this series of experiments, we used a Meox-2 Cre (B6.129S4-*Meox2tm1(Cre)Sor*, Jackson Laboratories) to test if the floxed allele (*Pkd2*^{delNeo}) functions as expected (i.e. results in deletion of *Pkd2* exons 11-13). In this line, the *Cre* recombinase has been "knocked in" to the Meox2 locus (mesenchyme homeobox 2 gene) and is thus expressed under control of the Meox-2 promoter. Since Meox-2 is broadly expressed in the early epiblast (not placenta), this

results in the Cre-mediated deletion of floxed DNA segments in greater than 90-95% of embryonic tissues including the germ line. The *Meox*-2 Cre has been bred to $Pkd2^{delNeo}$ homozygotes (generated above). Both PCR (primers flanking the deletion) and PCR analysis have been used to detect Cre mediated deletion of *Pkd2*. Only offspring inheriting the *Meox*-2 Cre should demonstrate the presence of the $Pkd2^{del11\text{-}13}$ allele. The $Pkd2^{+/delNeo}$-*Meox-2Cre*+ males have been "back-crossed" to $Pkd2^{flox11\text{-}13/delNeo}$ homozygous females. Since the *Meox*-2 Cre has greater than 95% activity in the male germ line, approximately half of the offspring carried a constitutive *Pkd2* deletion ($Pkd2^{KO11\text{-}13}$) and 50% had the $Pkd2^{delNeo}$ allele in combination with *Meox*-2 Cre. Therefore 1/4 (1/2X1/2) will be $PKD2^{\Delta neo/}$Ko11-13-*Meox-2Cre*+, a combination that should result in perinatal lethality.

In order to establish perinatal lethality, it has been allow pregnancies to come to term.

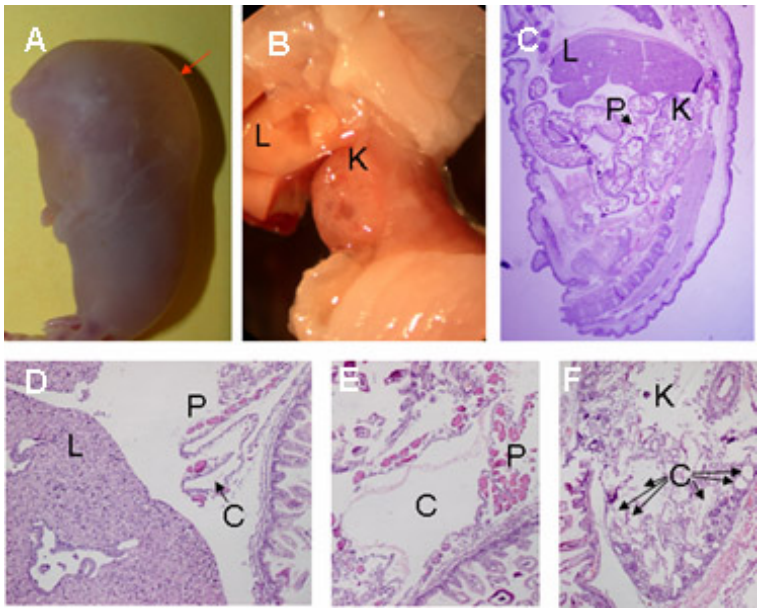

Figure 25. LoxP sites flanking PKD2 exons 11-13 recombine in vivo to yield a mutant phenotype. *A-D: Product of a* $PKD2d^{\Delta neo/\Delta neo}$, *and* $PKD2^{KO11\text{-}13}$ *Meox2Cre+ mating. This animal died shortly after birth with genotype* $PKD2^{KO11\text{-}13/PKD2delneo}$, *Meox2Cre+. The animal had profound edema (A, red arrow) and both renal cysts (B, C and F black arrows) and pancreatic cysts (D and E) on histopathology. L=liver, K=kidney, P=pancreas, C=cyst.*

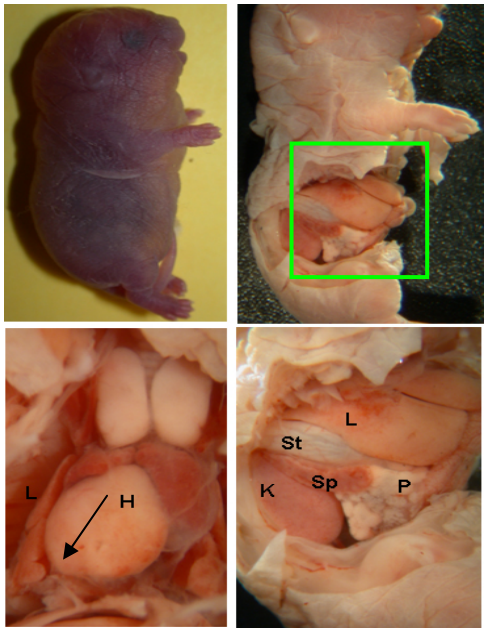

Figure 26. Situs inversus defined by rightside organs in $Pkd2^{Ko11\text{-}13/delNeo;}$***Meox2-Cre mouse.*** *Lower left image represents high magnification view of hearth (H) pointing to the left. The lower right shows cystic pancreas (P), spleen, stomach (St) and spleen (Sp). K (Kidney); L (Lungs).*

PKD2$^{delNeo/KO11\text{-}13}$*-Meox-2Cre+* animals died shortly after birth or with the typical *Pkd* loss of function phenotype including polyhydramnios, total body edema, hemorrhage, pancreatic and renal cysts.

The reason that the animals survive to birth is that the *Meox*-2 Cre is not active in placental tissues and data from our group suggests that embryonic lethality is due to a failure in placentation, same as shown for *Pkd1* conditional mouse (Piontek et al., 2004). All other genotypes should be phenotypically normal. The advantage of this breeding strategy is that there is no need to sacrifice pregnancies prior to birth, which limits the numbers animals needed. In addition to gross inspection, we performed a complete histopathologic survey, including 5 animals of each genotype. In Figure 25, we show a representative example of the phenotype, including severe edema, renal cystic disease, and pancreatic cysts. In addition, several of these animals exhibited *situs inversus*, which has been reported in two other *PKD2* targeted murine lines (Figure 26).

In summary, it has been generated a functional floxed allele that can be used to conditionally inactivate *PKD2* using Cre recombinases to control temporal and spatial gene inactivation. In addition, it has been created a new *PKD2* mutant allele (*PKD2*$^{KO11\text{-}13}$) that behaves as a functional null.

4.3.4. Pkd2$^{Ko11\text{-}13}$ is a null allele.

As predicted, the RT-PCR studies confirmed that the *Pkd2*$^{Ko11\text{-}13}$ allele is transcribed into a null pattern on the RNA level. Figure 27 shows 4 embryos from a pregnancy of embryonic development day e16.5. Two of the embryos were heterozigous (E2 and E3), one wild type (E1) and one homozygous for *Pkd2*$^{Ko11\text{-}13}$ allele. Embryo E4 showed a severe hemorrhage with severe edema, while the others did not show any phenotype (Figure 27A). As expected, E4 also manifested a severe polycystic pancreas and kidney disease, confirming the entire PKD phenotype spectrum associated with the complete loss of *Pkd2* (Figure 27B). In order to verify if the loss of exons 11, 12 and 13 could cause the disruption of the Pkd2 reading frame, a RT-PCR strategy has been design based on 3 different primer pair combination. The first includes amplification of a 572 bp fragment from exon 10

to 14 for the wild type allele and a small fragment of approximately 168 bp for the *Pkd2*$^{KO11-13}$ allele, indicating the loss of exons 11-12-13 and the disruption of the *Pkd2* reading frame. Based on this, the RT-PCR indicated that embryo E1 is wild type Embryo, embryos E2 and E3 RNA are heterozygous, and embryo E4 homozygous for the *Pkd2*$^{Ko11-13}$ allele. Same result was found when the RT-PCR primers were located in exons 10 and 15 (wild type band of 900 bp and a mutant band of approximately 496 bp). When a RT-PCR was developed with primers located into exon 15, similar ratio of amplification was found in *Pkd2*$^{+/+}$, *Pkd2*$^{ko11-13/+}$ and *Pkd2*$^{Ko11-13/Ko11-13}$.

Pkd2$^{Ko11-13}$ allele works as a complete null, where the removal of exons 11, 12 and 13 result in a truncated protein causing all the phenotypes associated with the loss of Pkd2.

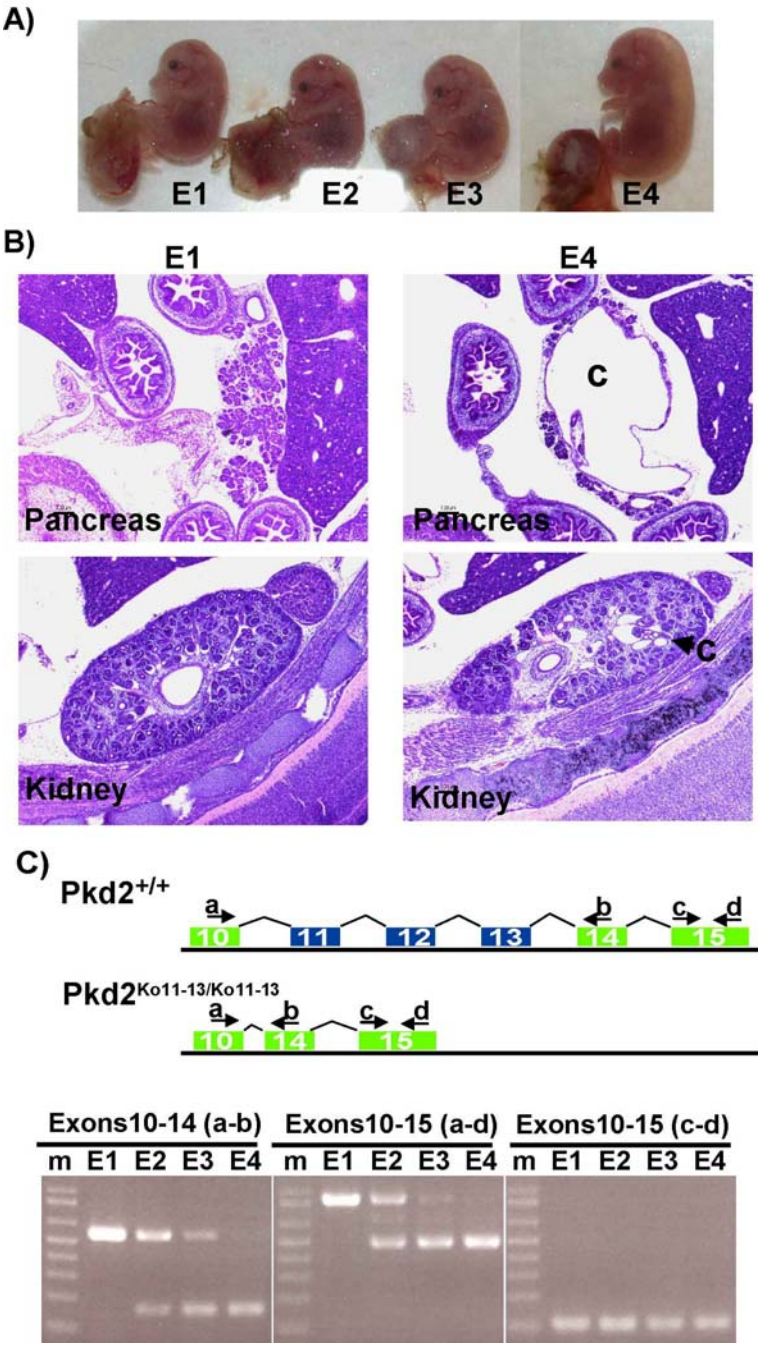

Figure 27. Pkd2Ko11-13 allele is a true null. *A) E16.5 pregnancy. E4 showed a severe edema and hemorrhage. B) E1 (E2 and E3 -data not shown-) did not any microscopic phenotype. E4 manifested a severe polycystic pancreas and kidney disease. C) Representation of the primer location for RT-PCR in the Ko11-13 and wild type alleles of Pkd2. RT-PCRs indicate that E2 and E3 were heterozygous for the Ko11-14 allele, E4 homozygous and E1 wild type. Primer combination a-b and a-d showed the total removal of exons 11, 12 and 13, causing a complete null allele.*

4.3.5. Explant culture of E10.5 mouse foreguts allows in vitro modeling of pancreatic cyst formation.

In collaboration with the Dr. Leach's group, it has been pursued the development of an in vitro model of cyst formation that can be used to clarify mechanisms of cyst initiation in PKD pancreas or kidney. Such a model would allow the observation of cyst formation in real time, and also provide a platform for pharmacologic and genetic manipulation of PKD pancreas and kidney. To achieve this model, we have taken advantage of cyst formation occurring in embryonic PKD pancreas, and capitalized on Dr. Leach´s group extensive experience with explant cultures of both intact E10.5 mouse foregut, as well as isolated E10.5 dorsal pancreatic buds. On E10.5, the dorsal and ventral pancreas are comprised of distinct buds of homogeneous, undifferentiated epithelium (Figure 28A, B). These can either be explanted in the context of an intact foregut (Figure 28B), or the dorsal bud and its surrounding mesenchyme can be explanted in isolation (Figure 28C). When associated mesenchymal elements were included in the explant, E10.5 pancreas undergoes to progressive growth and extensive branching morphogenesis, as

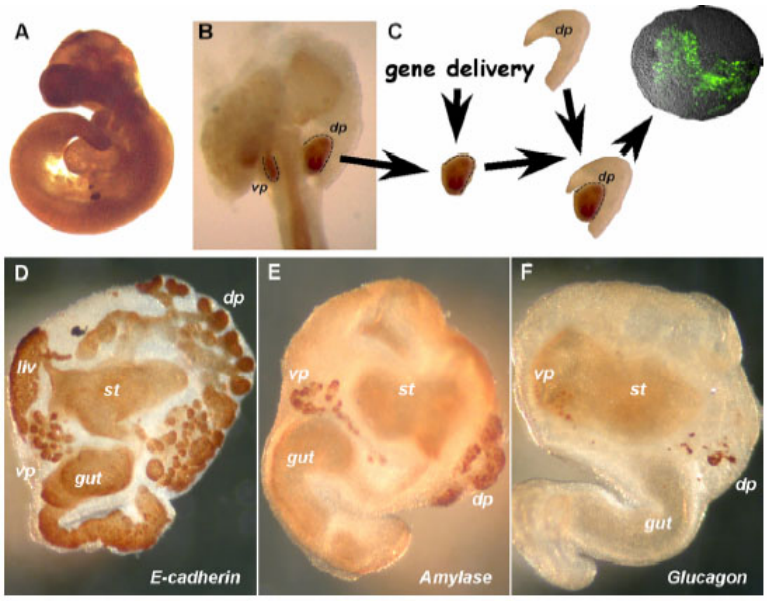

Figure 28. Explant cultures of E10.5 foregut structures. *A, E10.5 embryo with dorsal and ventral pancreatic epithelium marked by pdx1 expression (brown). B, isolated foregut comprised of stomach, proximal intestine, variable portions of liver, and dorsal and ventral pancreatic buds. Isolated foreguts can be cultured intact, or further isolation of dorsal bud epithelium can be performed. C, Lentiviral gene delivery to isolated dorsal bud epithelium, followed by recombination with isochoric mesenchyme and placement in explant culture. GFP fluorescence confirms efficient transgene delivery. D-F, isolated foreguts following seven day culture period. D, gastric, hepatic, intestinal and pancreatic epithelium marked by E-cadherin expression. Note extensive branching morphogenesis of pancreatic epithelium compared to E10.5 starting material in (B). E, amylase expression in dorsal and ventral pancreas. F, glucagons expression. St, stomach; liv, liver; vp, ventral pancreas; dp, ventral pancreas. Picture donated by Dr.Leach´s group.*

well as differentiation of both endocrine and exocrine lineages over a 7-day culture period (Figure 7D-F). In contrast, dorsal bud epithelium in isolation from mesenchymal elements fails to undergo growth or differentiation. As a further refinement of the explant system, Dr. Leach laboratory had developed unique methodology for transgene delivery to E10.5 dorsal bud epithelium. This technique involves enzymatic separation of the dorsal bud from its associated mesenchyme, and transduction with either adenoviral or lentiviral vectors.

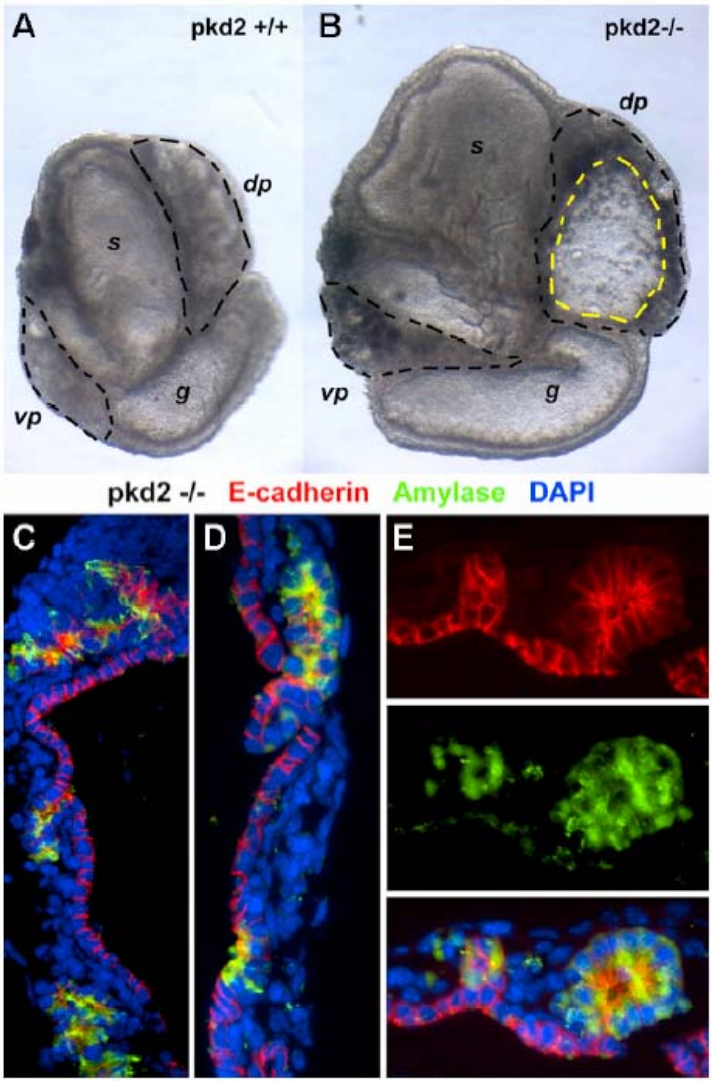

Figure 29. In vitro pancreatic cyst formation in explanted E10.5 Pkd2$^{-/-}$ isolated foregut. *A and B, bright field images of Pkd2+/+ and PKD2KO11-13/ KO11-13 foreguts following 7 days in culture. Note large translucent cyst in Pkd2-/- explant, outlined by yellow dashed line. C and D, Immunofluorescent staining of in vitro cyst epithelium for E-cadherin (red) and amylase (green) with DAPI nuclear counterstain. E, unmerged and merged images demonstrating amylase-positive acinar units immediately adjacent to E-cadherin-positive, amylasenegative cyst epithelium. Data done in collaboration with Dr. Leach´s group.*

Following 24 hours of exposure to viral particles, the isolated epithelium is recombined with isochronic mesenchyme and placed on Millipore transwell filters. As demonstrated by GFP fluorescence in Figure 28C, this methodology allows for relatively efficient gene delivery, allowing us to effectively express a variety of transgenes in dorsal bud epithelium.

Applying these techniques to PKD pancreas, it has been explanted intact E10.5 mouse foreguts harvested from litters established by crosses between *Pkd2*$^{KO11\text{-}13/+}$ heterozygotes (Figure 29). No gross

differences in foregut morphology were observed between $Pkd2^{+/+}$, $Pkd2^{KO11\text{-}13/+}$ and $Pkd2^{KO11\text{-}13/\ KO11\text{-}13}$ embryos at the time of tissue harvest. However, when explanted onto Millipore transwell filters, dramatic differences emerged. $Pkd2^{+/+}$ and $Pkd2^{KO11\text{-}13/+}$ explants underwent normal growth and branching morphogenesis, with typical expansion of dorsal and ventral pancreatic buds. In contrast, by the fifth day in culture, $Pkd2^{KO11\text{-}13/\ Ko11\text{-}13}$ pancreas demonstrated the dramatic formation of coalescing cystic structures. Of note, these cysts were much more prominent in the dorsal bud than in the ventral bud. As in the case of in vivo cysts, in vitro cyst epithelium was E-cadherin positive, but amylase negative, except for isolated amylasepositive cells participating in cyst formation (Figure 29).

4.4 Discussion.

Autosomal dominant polycystic kidney disease (ADPKD) is the most common form of (monogenic) inherited renal failure in the United States. The disorder is characterized by progressive renal cystic disease that results in end stage kidney disease in ~50% of the cases (Gabow, P.A., 1993). ADPKD is caused by mutations in either of two genes, *PKD1* or *PKD2* (protein products are called polycystins) (Calvet; 1998).

Since we still understand relatively little about PKD signaling pathways, much effort has been devoted to developing faithful animal models of ADPKD that could be used to better understand the biology of polycystin proteins. To this end, a number of laboratories have generated mice carrying targeted alleles of either *Pkd1* ($Pkd1^{-/-}$) or *Pkd2* ($Pkd2^{-/-}$) (Wu et al., 1998, Wu et al 2001, Boulter et al 2001, Lu et al 1997), but only for Pkd1 has been develop an conditional knockout that could allow the timing and spatial inactivation (Piontek et al., 2004). Since cysts are thought to form via a "two hit" mechanism, it is no surprise that heterozygotes are uniformly viable with only rare renal and hepatic cysts (Qian F et al., 1996). In contrast, the homozygous state results in mid-late embryonic lethality, depending on the model. At the time of demise, animals have diffuse renal cystic disease but most groups also describe a variety of other associated abnormalities including gross edema, spontaneous

hemorrhage and polyhydramnios (Wu G et al., 2000). Cardiac abnormalities have been associated with edema in some but not all of the targeted alleles (Boulter et al., 2000; Muto et al., 2002). Interestingly, *Pkd2* knock-out mice, although similar to *Pkd1* mutants, are not identical. *Pkd2*$^{-/-}$ mice display abnormalities in left/right axis determination (right pulmonary isomerism, randomization of embryonic turning, heart looping, and abdominal situs) which have not been described in *Pkd1*$^{-/-}$ mice (Pennekamp et al., 2002). This suggests that the function of the *Pkd1* and *Pkd2* may not overlap in every cell type. The early lethality of the homozygous state has limited the types of questions that can be answered with these models. Wu et al. generated an unstable allele of *Pkd2* with a local duplication that undergoes random somatic mutations (Wu et al., 1998). This is the only model that comes close to imitating human disease but it does not allow regulated gene loss. An important limitation of the currently available lines of mice with targeted mutations of *Pkd2* is that heterozygous animals rarely have cystic disease below six months of age.

Dr. Germino's group has developed a floxed *Pkd1* allele that can be used to control the timing and location of the *Pkd1* mutation (Piontek et al; 2004) but there is no such model for *PKD2*. Given that the role *PKD1* and *PKD2* may differ, we believe that both models are necessary to gain a full understanding of polycystin biology. In order to study the consequences of polycystin-2 loss in both a tissue and stage-specific fashion, we have generated mice with a floxed allele of *Pkd2* (*Pkd2*^{cond}).

The goal of this Thesis subproject was to generate and characterize this new murine allele. These studies will set the foundation for subsequent use of this model to test a range of *Pkd2* associated phenotypes. In this part, it has been described the first line of mice with a floxed allele of the *Pkd2* gene (*Pkd2*$^{flox11\text{-}13}$) that functions as a hypomorphic in the undeleted state and as a complete null after Cre-mediated deletion. After deletion of the Pgk-Neomycine cassette through the FLP/FRT system, it has been shown that mice homozygous for the *Pkd2*^{delNeo} allele are viable, fertile and born at expected Mendelian ratio. By breeding *PKD2*$^{delNeo/+}$ mice, to *PKD2*$^{\Delta 11\text{-}13/+}$ heterozygotes that also were

positive for a Cre-recombinase, it could be quickly evaluated the functional impact of Cre-mediated loss of *PKD2* exons 11-13. As expected, embryos with the *PKD2*$^{del11\text{-}13/del11\text{-}13}$ genotype were present in normal Mendelian ratios and recapitulated the range of phenotypes (polycystic kidney and pancreas disease, edema, polyhydramnios, hemorrhage and lateralization defect) with homozygous loss of *PKD2*. These results conclusively show that the floxed allele functions as a null allele after Cre-mediated deletion. Similar results were obtained using mice from different strains, excluding strain differences as a trivial explanation for our findings.

This is the first conditional knockout model described up the moment. This system has provided three new *Pkd2* alleles: a hypomorphic allele (*Pkd2*$^{flox11\text{-}13}$ allele) associated to a severe vascular phenotype, a new knock-out allele that is predicted to lack the *Pkd2* C-terminus (*Pkd2*$^{ko11\text{-}13}$ allele), and a conditional allele that can be used to selectively inactivate *Pkd2 in vivo* (*Pkd2*^{delNeo} allele). These models will provide a rich source of cells and organ culture for testing of *in vitro* inactivation and therapy consequences.

Pkd2*$^{flox11\text{-}13}$ *is a hypomorphic allele. It has been show that the presence of the neomycine cassette in intron 13 disrupts normal behavior of *Pkd2*, playing an important role in vascular phenotype development. *Pkd2*$^{flox11\text{-}13}$ allele could be established for a better understanding of the vascular phenotype in ADPKD patients. Several reports describe the vascular phenotype as a major cause of dead and disability in ADPKD (Rossetti et al., 2003). It has also been described that lower levels of Pkd1 is sufficient to cause PKD (Inma et al., 2004). This is not the case for *Pkd2* because as it has been shown, homozygous mice for the *Pkd2*$^{flox11\text{-}13}$ allele that dye in utero by a very severe vascular phenotype and as in those that survived to birth, never manifest PKD. Since *Pkd2*$^{flox11\text{-}13/flox11\text{-}13}$ developed a major vascular phenotype accompanied by intramural bleedings, it seems that reducing levels of Pkd2 result in structural weakness of arterial wall. Given that, *Pkd2*$^{flox11\text{-}13/flox11\text{-}13}$ can be proposed as an interesting model in the study of the vascular phenotype and the effects of therapy.

Cre-mediated deletion of Pkd2 in tissues. The floxed allele of *Pkd2* described in this report (*Pkd2*^{delNeo}) can be used to distinguish between different possibilities. It has been shown in this report that in utero expression of Cre recombinase (Meox2-Cre) in *Pkd2*$^{delNeo/Ko11\text{-}13}$ mice results in a null allele and cyst formation. As expected, embryos *Pkd2*$^{delNeo/ko11\text{-}13}$-Meox2-Cre^{+} recapitulated the range of phenotypes (edema, polyhydramnios, hemorrhage and lateralization defects) observed for *Pkd2*$^{ko11\text{-}13/ko11\text{-}13}$ embryos. This demonstrates the functional similarity of the Cre-mediated recombination to a true knock-out allele. Also, it can be used to examine the consequences of temporally and spatially regulated inactivation of *Pkd2*. For example, it can be examined what other factors affect the relative rate of cyst growth in the kidney and liver by fixing the time and location of gene inactivation. Equally, this model offers a uniquely powerful way of testing various interventions on the rate of cyst growth by removing the unpredictability of the timing of somatic mutation.

This new line of animals also is an invaluable tool in the study of different biological aspects of *PKD2*. It can be used for test if PKD2 is important for both formation and maintenance of tubules (controlling the *PKD1* inactivation timing), to determine the cause of fetal demise, assess the role of PC2 in the development of various other tissues that are altered in *PKD1* nulls (by selective inactivation of bypassing the embryonic lethality), to screen for post-developmental functions of *PKD2* that are not manifest in humans because of the two-hit nature of disease and not observed in mice because of the early lethality associated with its homozygous loss.

Pkd2$^{ko11\text{-}13}$, a new knock-out allele lacking the Pkd2 C-terminus. The present knock-out mouse derived from the conditional allele after Cre recombinase has, like other gene-targeted alleles for Pkd2, an embryonic lethal phenotype in the homozygous stage and recapitulates the range of phenotypes observed for *Pkd2*$^{ko11\text{-}13/ko11\text{-}13}$ embryos with polycystic kidney and pancreas disease, edema, polyhydramnios, hemorrhage and lateralization defects.

In vitro modeling of the pancreas cyst formation associated to the loss of Pkd2. Explant culture data demonstrate that *Pkd2*$^{KO11\text{-}13/\ KO11\text{-}13}$ embryonic pancreas undergoes rapid in vitro cyst formation, providing a novel platform for the study of PKD cyst pathogenesis. Specifically, the ability to culture multiple synchronous explants will allow precise temporal analysis of initiating events in cyst formation. This type of analysis will be critical in the accurate identification of cyst precursor lesions. In addition, the in vitro model opens the door to relatively high-throughput analysis of pharmacologic and/or genetic modifiers of the PKD phenotype, providing significant advantage over traditional in vivo work.

Together, these preliminary data define cyst formation in PKD mouse pancreas as a consistent and tractable event, and further suggest the likely participation of epithelial progenitors in cyst initiation. Whether progenitor cells are recruited to cyst formation by selective expansion or by acinar cell dedifferentiation remains to be determined. In this regard, it is notable that in vitro cyst formation is evident following only 5 days in explant culture, while acinar cell differentiation typically requires a full 6-7 days. The generation of new information regarding cyst formation in PKD pancreas, including the identification of pharmacologic and genetic modifiers of this event is very important. In addition to clarifying mechanisms of pancreatic cyst formation, these studies are also likely to generate new information regarding epithelial progenitor cells in adult and embryonic pancreas. Finally, by characterizing and manipulating pancreatic cyst formation in adult and embryonic pancreas, it can be anticipated that significant insights will also be generated regarding PKD associated cysts in other tissues, including liver and kidney.

This model concluded several important keys for understanding the biology of ADPKD. Polycystin-2 is essential for normal embryonic development, maintenance of the normal elongating nephron, pancreatic ductal structure and vascular tree. The develop of useful tool that help for a better

understanding of the cellular and molecular underpinnings of these findings will provide the discovery of possible targets for therapeutic intervention in ADPKD.

5. Generation of a conditional murine model of PKHD1 gene (SUBPROJECT III).

5.1 Abstract.

Mutations of human *PKHD1* result in ARPKD. A number of groups have tried to model the disease in mice by disrupting murine *PKHD1* by gene targeting but none have produced mice with PKD. Based on the gene's pattern of expression and its pattern of mutations in humans, we suspected that homozygous inactivation of mouse *Pkhd1* could be lethal. We thus developed a novel floxed allele of *Pkhd1* (*Pkhd1*$^{flox3-4}$) that has an FRT-flanked neomycin cassette inserted into intron 4 and loxP sites flanking exons 3-4. The floxed allele is fully functional and homozygotes are viable and healthy. We have shown that Cre-mediated recombination induces deletion of the exon 3-4 fragment as intended to produce a novel mutant allele (*Pkhd1*$^{del3-4}$). Matings of *Pkhd1*$^{del3-4/+}$ yielded only ~20% of the expected number of liveborn *Pkhd1*$^{ko3-4/del3-4}$(18/252; 63 expected) with a substantial fraction subsequently succumbing to respiratory failure. One *Pkhd1*$^{del3-4/del3-4}$ neonate died with an intracerebral hemorrhage. Among the survivors, all had a variety of hepatobiliary abnormalities including congenital hepatic fibrosis, choledochal cysts and ascending cholangitis. Most also had severe pancreatic cystic disease manifest by four weeks of age. Many were growth retarded and a subset had severe hindlimb abnormalities. Interestingly, mice that lacked gross pancreatic abnormalities had polycystic kidney disease that histopathologically resembles that of humans. Long-range RT-PCR of kidney and liver specimens from normal and *Pkhd1* mutant mice confirmed that the mutant allele is transcribed but it encodes a different pattern of transcripts. This new line of mice, which allows inactivation of *Pkhd1* in a spatio-temporally controlled manner, presents a complete spectrum of ARPKD phenotypes and will be a powerful tool in the study of *PKHD1* biology and the pathogenesis of human ARPKD.

5.2. Material and methods.

5.2.1. Generation of a conditionally activated Pkhd1 $^{flox3-4}$ targeting construct.

A floxed allele was generated to allow regulated removal of exons 3 and 4 (Figure 30A). It has been avoided exons 1 and 2 since it can be concerned, based on our human studies, that the gene might use alternative upstream exons. After examination of human data, it has been noted that exon 3 was an apparent hotspot for mutations in humans and that its removal with exon 4 should delete essential exons, remove an alternative translation start site42 and disrupt the reading frame.

~400 clones had been screened, identifying only one that was properly targeted and retained

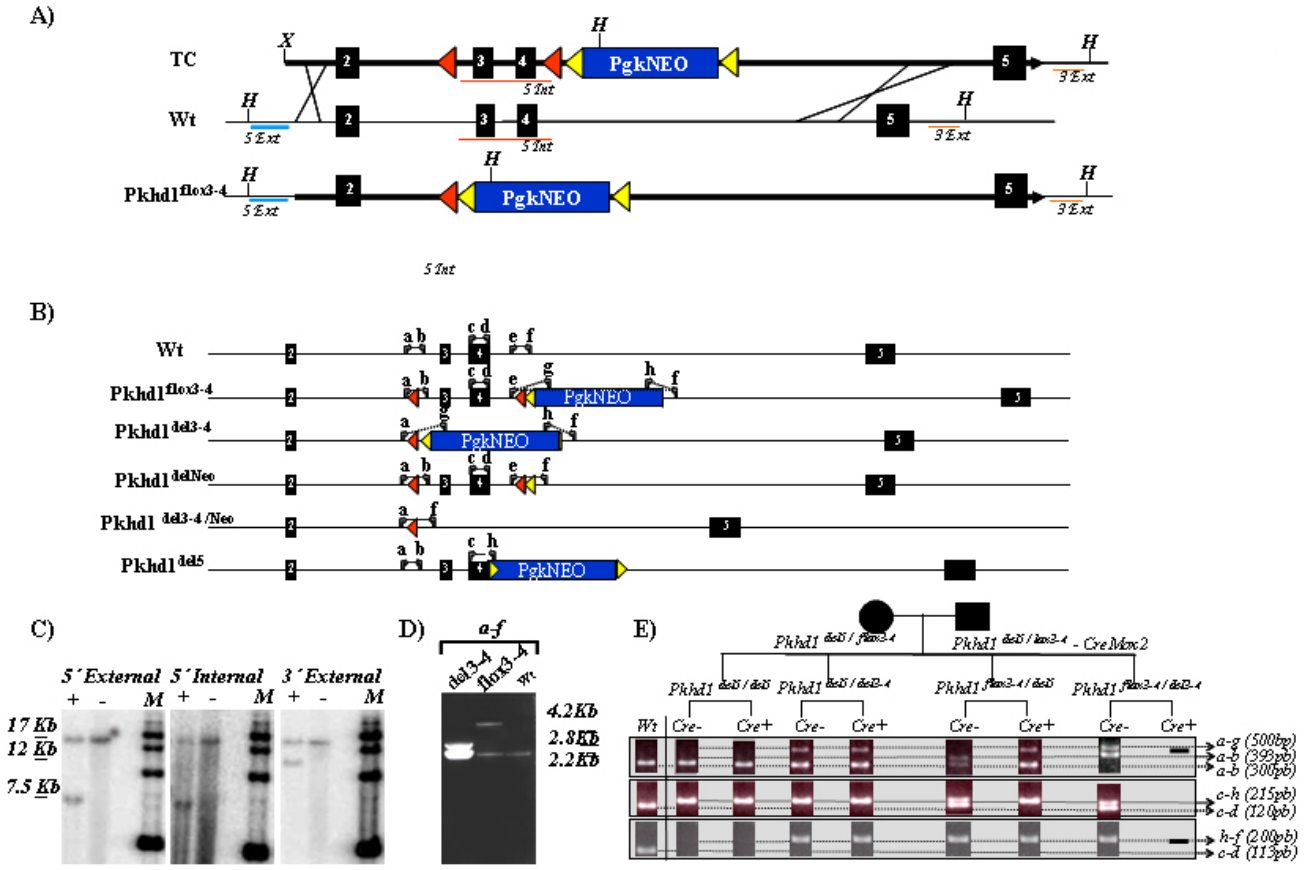

Figure 30: Gene-targeting of Pkhd1 to produce a floxed allele. A) Schematic of targeting construct (TC), wild type allele (WT) and Pkhd1$^{flox3-4}$ (Flox3-4). "Int" and "Ext" identify position of probes used in C. B) Same as in A except includes map of all possible alleles derived from Pkhd1flox3-4: Cre-mediated deletion (Pkhd1^{Del3-4}), FLP-mediated deletion (Pkhd1^{delNeo}) and both (Pkhd1$^{del3-4Neo}$. Pkhd1del5 allele was gently donated by Dr. Somlo. "a-h" identifies position of primers used to identify genotypes in D. C) Southern blot of ES cells, marker sizes in red identify properly targeted band sizes. D) PCR results showing that the allele deletes properly (Del3-4). E) Offspring Genotyping from a Pkhd1$^{del5/flox3-4}$ vs Pkhd1$^{del5/ lox3-4}$ mating.

both lox P sites as verified by multiple hybridizations and PCRs (Figure 30C and 30D). The clone was expanded and used to generate highly chimeric animals that transmitted the targeted allele (*Pkhd1*$^{flox3-4}$) with high frequency.

It has been verified that the allele can be transmitted through the germline, that *PKHD1*$^{flox3-4/flox3-4}$ are viable and thus far appear healthy, and we have also shown that Cre recombinase induces deletion of the exon 3-4 fragment as intended (Figure 30D).

5.2.2. Genotyping.

Genomic DNA from mouse-tails was obtained as follows. In short, ~5mm long piece of the tails were digested in Proteinase K buffer (50 mM Tris pH 8.5, 1 mM EDTA, .5% Tween 20) at 60°C for about 2h with shaking. After inactivation of the enzyme at 99°C for 15min, 1µl of the solution was used for PCR genotyping with primer locations shown in Figure 30B, and whose sequences are as follows: (a) M/loxP-F: GGG AAG CAG AAA TTC AGG; (b) C2R: AGA TGA AGC ACG GAT CAG TGG G; (c) Ko*PKHD1*-F: CTT TAC CCC AAC AAT GGC; (d) ko*PKHD1*-R: GTG TAC CTC GTC TGG CAT GTC; (f) M/Pgk-R: AAA GCT AAA AGT GGG AGA GAC G; (g) PgkNEO-R1: GCT CAT TCC TCC CAC TCA T; (h) PGKR2: GCCAGAGGCCACTTGTGTAG; For detection of Cre + animals we used: CRE-F (200bp): ATT GCT GTC ACT TGG TCG TGG C; CRE-R (200bp): GGA AAA TGC TTC TGT CCG TTT GC.

5.2.3. Preparation for Histology.

Kidney, liver, and pancreas specimens from adult animals were collected and immediately fixed in 10% buffered formalin at 4°C overnight. Embryos at different ages were fixed with ice-cold 4% paraformaldehyde in PBS via cardiac perfusion of the mother and then kept in 4% paraformaldehyde overnight at 4°C. Following rehydration in water for 2h, all samples were dehydrated in a graded alcohol series and embedded in paraffin for histological analysis.

5.2.4. Immunofluorescent staining.

For immunolabeling, tissues were fixed, sectioned and stained as previously described (Esni et al., 2004). The following antibodies were used at the indicated dilutions for immunofluorescence analysis; rat monoclonal anti-E-cadherin (Zymed Laboratories, 1:200), rabbit polyclonal anti-Pdx1 (gift from Christopher Wright, 1:500), goat polyclonal anti-amylase (Santa Cruz Biotechnology, 1:500), and guinea pig polyclonal anti-insulin and anti-glucagon (Linco Research, 1:1000). The following reagents were purchased from Jackson ImmunoResearch Laboratories: Biotin-conjugated anti-rat (1:500), anti-guinea pig (1:500) and anti-goat IgG (1:500). Cy3- and Cy2-conjugated streptavidin (1:1000, 1:300), Cy3-conjugated anti-rabbit (1:300), and Cy5-conjugated anti-rat (1:300). For each antibody, specificity was confirmed using negative control slides omitting primary antibody. Fluorescence confocal microscopy was performed with a confocal laser scanning microscope (410LSM, Zeiss) using a 40x (NA 1.5) C-apochromat objective, and image analysis was performed using MetaMorph series 5.0 software (Universal Imaging).

5.2.5. Reverse Transcription–PCR.

Total RNA was extracted from fetal tissues using the Qiagen RNA extraction kit according to the manufacturer's protocol. First-strand cDNA was synthesized using Superscript II (Invitrogen) from 100 ng of total RNA and then used as template for PCR amplification of *Pkhd1* transcripts (Platinum Taq; Invitrogen). Primers; (a) MFL-F1: GTGAGTTCCAGTCCAACAGG; (b) MFL-R1: GAGCAGTTACAGTGGGATTCA; (c) MFL-R2: GGGTGAAGATGCTGCTGTAATC; (d) MFL-R3: CCAGGGACAATCTGACTGAAG; (e) MFL-R4: TCTATTCCCACTTCTCCATCAG; (f) MFL-RF2: GAATGTGGTGGAGTCAGTATCG; (g) MFL-F3: GCAGGCTTGTCTAACAGTGAAC; (h) MFL-F4: ATCAAGAGACCTACTCGCTGC were used to amplify the different products of the entire mouse *PKHD1* cDNA (figure 44), with a common T^m of 55.5 ºC.

5.3. Results

5.3.1. Test the hypothesis that inactivation of Pkhd1 can mimic the human disease.

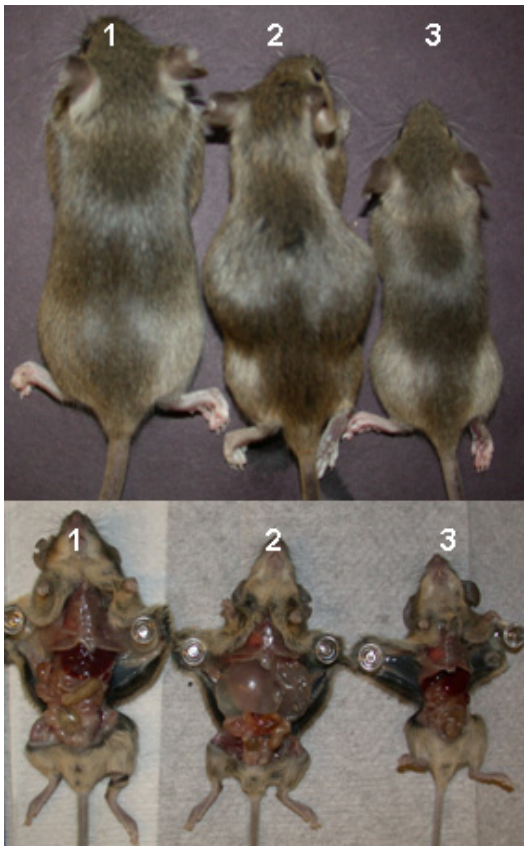

Figure 31. Characterization of 12 weeks old Pkhd1$^{del5/del5}$. Homozygous Pkhd1^{del5} can show polycystic pancreas (2), eventually growth retardation (3), or do not show any phenotype at all (1).

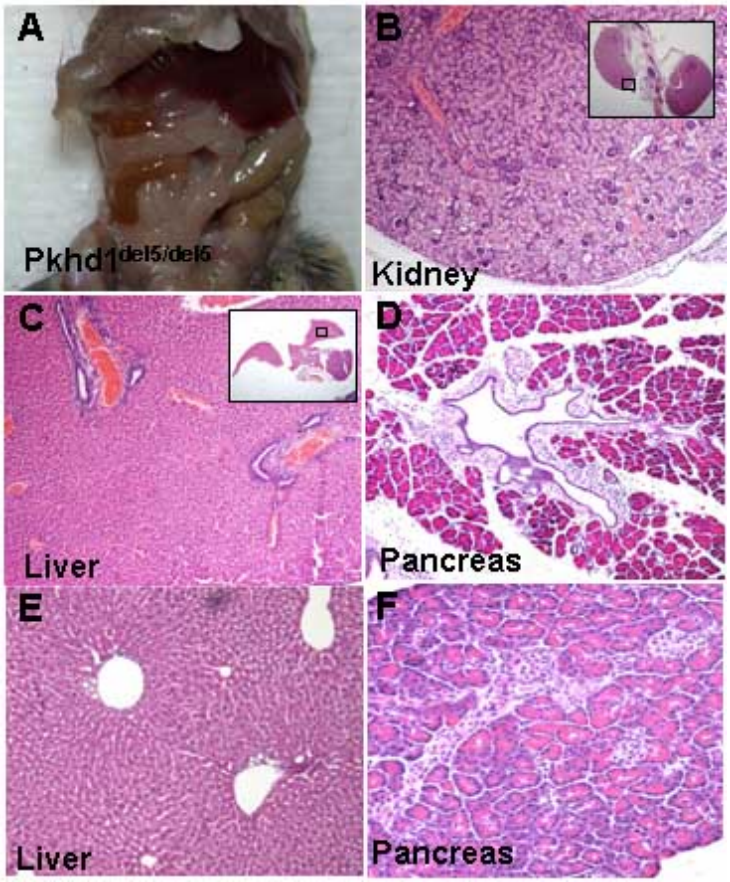

Figure 32. H & E staining of kidney (b), liver (c and e) and pancreas (d and f) from 16 week old animals. Pkhd1$^{del5/del5}$ (a-d); wild type (e-f).

The characterization of *Pkhd1* models created by other collaborators has been developed previously to the *Pkhd1$^{flox3-4}$* allele.

Dr. Somlo's laboratory has developed a Pkhd1 allele with the insertion of a Neomycine cassette in the end of exon 4, generating a splice donor skipping the exon 5 into the RNA level (*Pkhd1^{del5}*, ASN 2004). *Pkhd1^{del5}* homozygotes mice are born at expected Mendelian rates and are fertile. By 12 weeks, large pancreatic cyst formation with adjacent acinar destruction and chronic pancreatitis was noted in 10% of the homozygous mice (Figure 31-2). A mild abnormal growth was

seen in more than 1 % of the animals compared to their own littermates (Figure 31-3). Histologic examination of kidneys revealed normal glomerular and tubular development, with no cysts apparent at 16 weeks of age (Figure 32B). Intrahepatic bile duct proliferation, with features reminiscent of von Meyenburg complexes/ductal plate malformation, was noted as early as two weeks. By 16 weeks, microscopic liver cysts were present (Figure 32C). Pancreatic ductal ectasia was found in all null animals (Figure 32D).

Our results for the *PKHD1*$^{del5/del5}$ mice are similar to what has been described by other groups, for example, Ward et al. (ASN, 2004) targeted exon 2 of mouse *Pkhd1* showing a similar liver and pancreatic disease manifestation. Interestingly, other two Pkhd1 mouse model with truncated exons from the 5´of the gene where associated with only the liver phenotype. When Moser et al. (2005) targeted exon 42, the homozygous mice only developed the liver phenotype similar to the *Pkhd1*^{del5} mouse model, but no evidence of polycystic kidney disease, polycystic pancreas disease, perinatal demise or other ARPKD associated phenotypes. The same happen with the *Pkdhd1*^{cl} mouse, where a cystic liver (*cl*) associated mutation arose spontaneously in a congenic strain generated by introgressing a segment of distal chromosome 4 from C57BL/6J (B6) onto the DBA/2J strain (Jackson Laboratories). Dr. Guay-Woodford's group mapped the *cl* locus to the *PKHD1* interval and identified a frameshift mutation, c.7589delGGinsT, in *Pkhd1* exon 49. *Pkdhd1*^{cl} mutants develop massive cystic liver disease by four months of age and histopathological analysis demonstrated a biliary dysgenesis lesion that resembles human ARPKD (Figure 33).Curiously, none of the mouse models thus far described has a renal phenotype. This thesis follows up on these

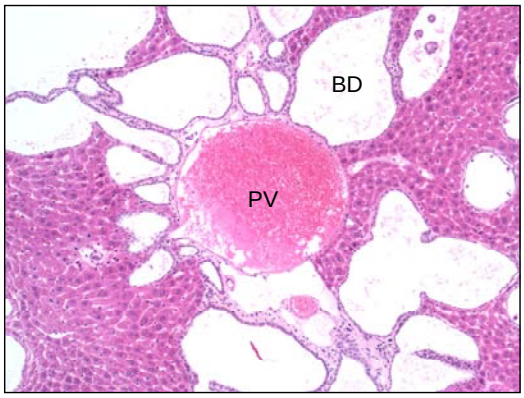

Figure 33: Biliary lesion in cl mutant. 4 months *Pkhd1* $^{cl/cl}$ liver with irregularly shaped & dilated bile ducts (BD). PV portal vein, 100X.

observations and seeks to test the hypothesis that the lack of a renal phenotype is due to the complicated pattern of splicing.

As explained previously, a new conditional *Pkhd1* allele (*Pkhd1*$^{flox3-4}$) has been generated though the insertion of a Pgk-Neomycin cassette in intron 4 with exons 3 and 4 flanked by loxP sites. Using the Cre/loxP system, exons 3 and 4 can be deleted through recombination between the two loxP sites when Cre-recombinase is expressed. Offspring from mice where deletion of these exons was induced in the epiblast using a Cre-recombinase driven by the Meox2 promoter, will carry out a germline allele (*Pkhd1*$^{del3-4}$) predicted to delete the exons 3, 4 and 5 at the RNA level. Crosses of *Pkhd1*$^{del3-4}$ with the *PKHD1*^{del5} allele have shown that *PKHD1*$^{del5/del3-4}$ has a more severe manifestation that *PKHD1*$^{del5/del5}$. Compound *PKHD1*$^{del5/del3-4}$ mice were born at expected Mendelian rates. It has been found animals with severe polycystic pancreas disease and liver fibrosis. By 5-6 weeks, large pancreatic cyst formation with adjacent acinar destruction and chronic pancreatitis was noted in 23% of the homozygous mice (Figure 34D). A mild abnormal growth was seen in 4% of the animals. Histologic examination of kidneys revealed normal glomerular and tubular development

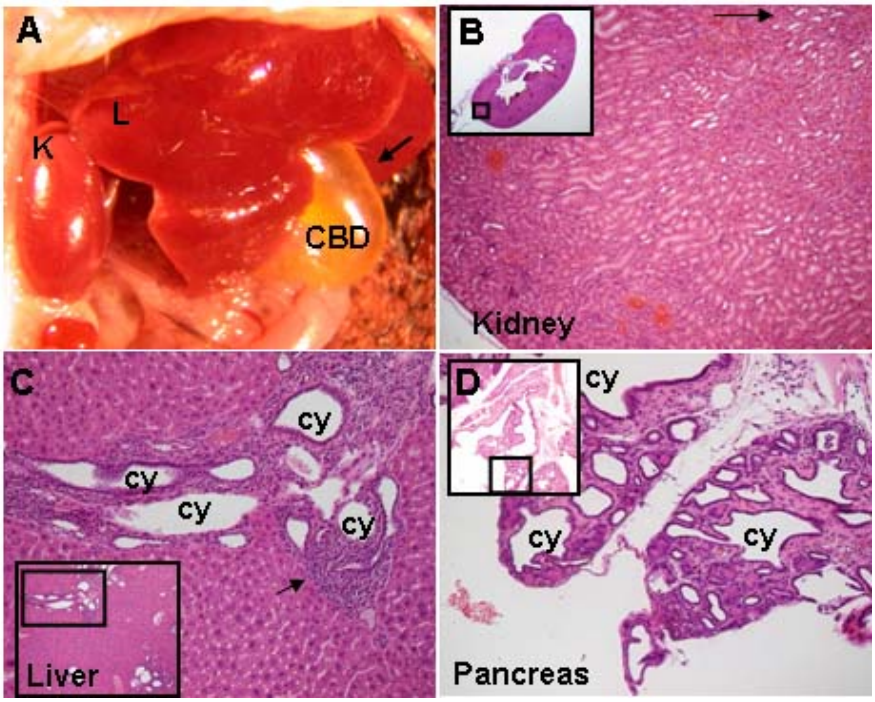

Figure 34. Phenotypes of Pkhd1$^{del3-4/del5}$**.** Panel A: Gross external appearance of 5-6 wk old mice with a dilated gallbladder. Panel B-D: Gross internal appearance and histopathology of same mice in A. Inset shows low power image and position from where specimen was selected. K: Kidney, L: Liver, CBD, common bile duct, Cy: cyst. Arrow shows mild dilatation into the collecting ducts.

(we can observe a mild dilatation in the collecting ducts), with no cysts apparent at this age. Intrahepatic bile duct proliferation, with features reminiscent of von Meyenburg complexes/ductal plate malformation, was noted as early as two weeks. Microscopic liver cysts were present (Figure 34C).

5.3.2. Pkhd1$^{del3-4/del3-4}$ model mimics the human disease.

Breeding studies were developed to test whether *Pkhd1*$^{del3-4}$ homozygotes have more severe disease than *Pkhd1*$^{del5/del5}$, *Pkhd1*$^{del5/del3-4}$compound heterozygous, *Pkhd1*$^{cl/cl}$ allele or any other publicly described *Pkhd1* mutant alleles.

Pkhd1$^{del3-4/+}$ x *Pkhd1*$^{del3-4/+}$ crosses have produced 84 offspring, of which only six of 21 expected have the *Pkhd1*$^{flox3-4/flox3-4}$ genotype. The viable homozygote mutants have a range of phenotypes: three are smaller than their littermates (~P28) and two have obvious bony abnormalities (Figure 35A). Two have been harvested at five to six weeks of live to test for *PKHD1* expression and were found to have small kidney, liver and pancreatic cysts.

Also, it has been produced a number of other crosses, founding the following:

a) *PKHD1*$^{del3-4/flox3-4}$*;Meox2*$^{cre/+}$. These mice have a germline mutation in one allele and the deletion of the other allele in 95% of the cells after Cre-mediated deletion in the epiblast through the Meox2-Cre. 16 mice of 18 expected with this combination presented a range of phenotypes that includes some mice that appear grossly normal (N=7, two of them developed pancreatic cyst and liver fibrosis at five to six weeks), multiple newborns that died by respiratory failure in the perinatal period (N=7, gastrointestinal tract filled with air, Figure 35B), and a set that was significantly smaller than its littermates (N=2, Figure 35C);

b) *PKHD1*$^{flox3-4/del5}$*;Meox2*$^{cre/}$. It has been characterized a total number of 18 mice with this genotype (of 19 expected) with a range of phenotypes including one that died of respiratory failure,

one that apparently died of intracerebral hemorrhage shortly after birth (Figure 35D), 11 that were growth retarded, and 5 that appeared grossly normal;

c) *PKHD1*$^{del3\text{-}4/del5}$. These mice carry two different germline mutations. Six mice were born while 12 were expected based on the genotypes of the parents; three of six have had massive pancreatic disease by four weeks of age with hepatic fibrosis (Figure 35E). This is in contrast to only 8/173 *PKHD1*$^{del5/del5}$ that develops this feature between 6-16 wks.

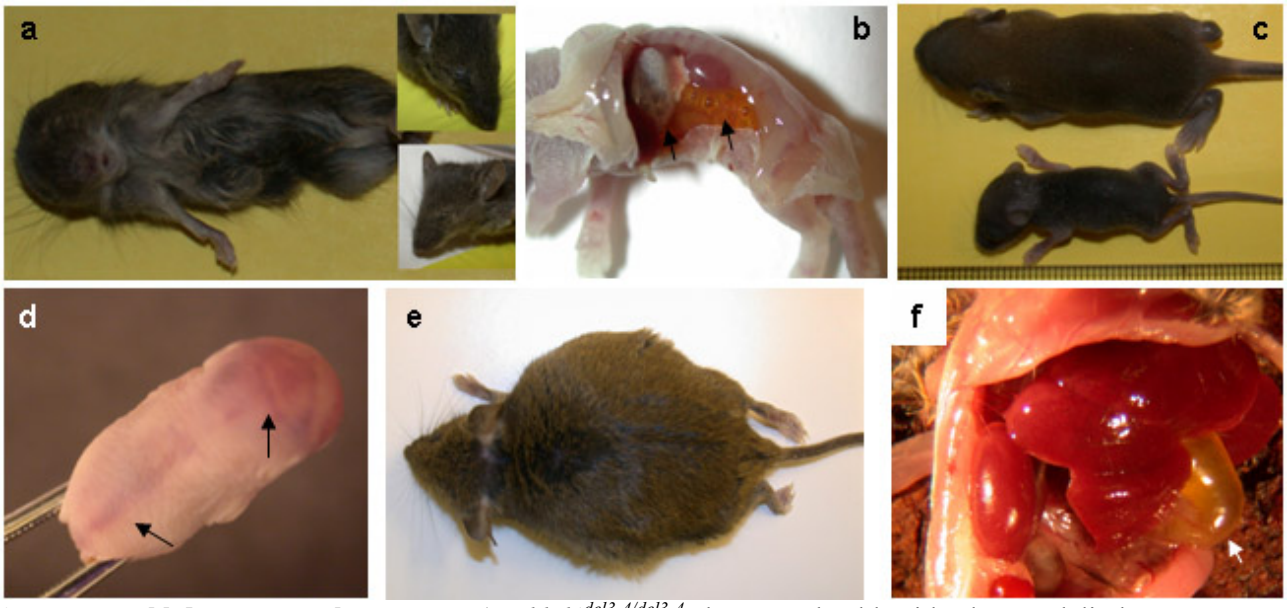

Figure 35: Pkhd1 mutant phenotypes. a) *Pkhd1*$^{del3\text{-}4/del3\text{-}4}$ three week old with abnormal limb structure and function and eye abnormalities; b) *Pkhd1*$^{del3\text{-}4/flox3\text{-}4}$;*Meox2*$^{cre/+}$ that died shortly after birth due to respiratory failure. The stomach and intestines are filled with air (arrows); c) *Pkhd1*$^{flox3\text{-}4/del5}$; *Meox2*$^{cre/+}$ three week old (bottom) and its normal (*Pkhd1*$^{del5/+}$) littermate (top). d) *Pkhd1*$^{flox3\text{-}4/del5}$;*Meox2*$^{cre/+}$:Newborn that died shortly after birth with multiple hemorrhages/vascular abnormalities (arrows); e)*Pkhd1*$^{del3\text{-}4/del5}$:a four week old with massive abdominal distension due to pancreatic cysts; f) *Pkhd1*$^{del3\text{-}4/del5}$:a three week old with very large cysts of the bile duct (arrow).

Because human ARPKD patients suffer from cystic biliary dysgenesis and polycystic kidneys, detailed histological analyses of all internal organs with special emphasis on liver and kidneys were performed.

<u>- *Pkhd1*$^{del3\text{-}4/del3\text{-}4}$ renal phenotype.</u>

Comparison of kidneys from *Pkhd1* $^{del5/del5}$, *Pkhd1*$^{del3\text{-}4/del5}$, and *Pkhd1*$^{del3\text{-}4/del3\text{-}4}$ at five to six weeks of age showed a severe cystic disease in the *Pkhd1*$^{del3\text{-}4/del3\text{-}4}$ mice and a very mild kidney

disease with focal areas of dilated ducts in the *Pkhd1*$^{del3\text{-}4/del5}$ (Figure 36). ~ 10% of *Pkhd1*$^{del3\text{-}4/del3\text{-}4}$ showed a very severe polycystic kidney disease at 3 months of live, increasing up to 80% at 6 months of age. No obvious changes have been found in kidneys for the *Pkhd1*$^{del5/del5}$ mice at any stage.

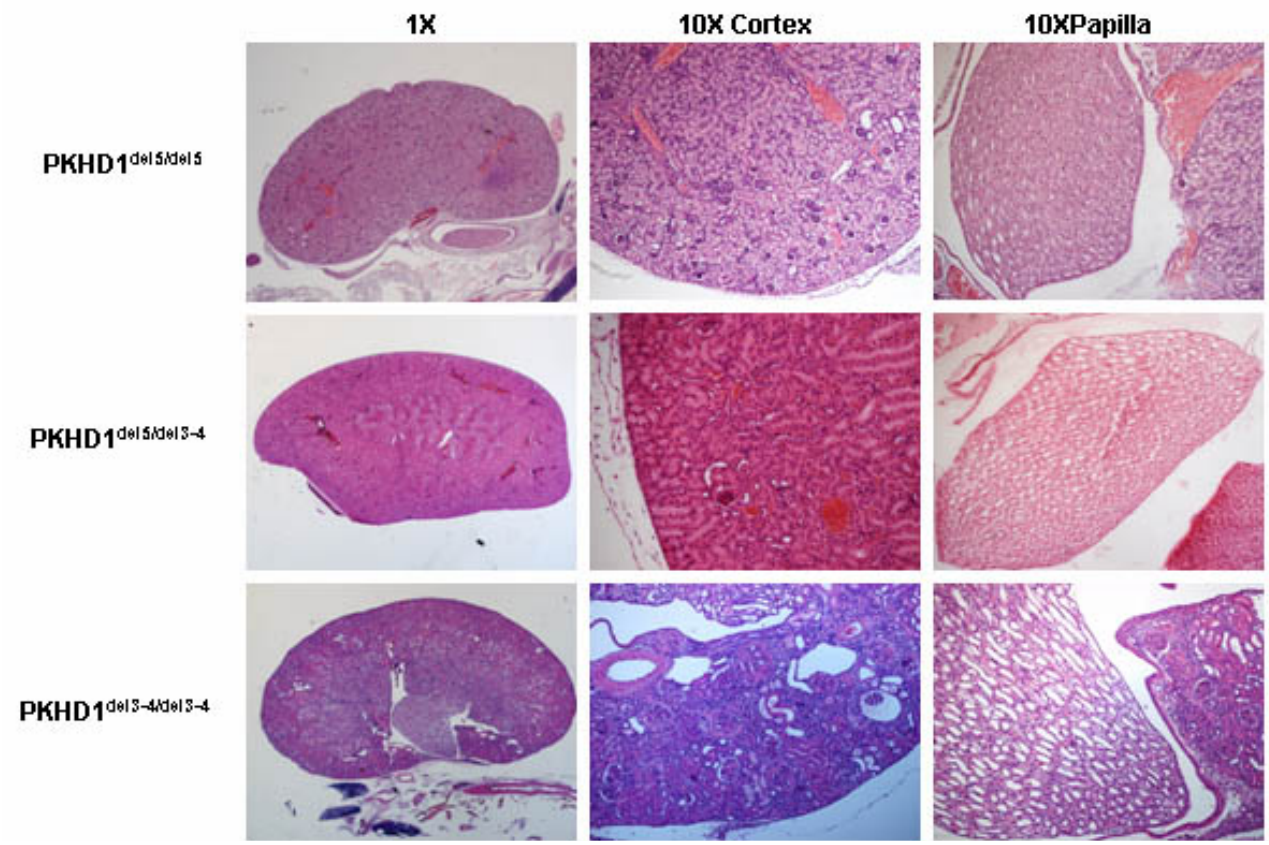

Figure 36. Pkhd1*$^{del3\text{-}4/del3\text{-}4}$ *shows a severe kidney phenotype. Focal duct dilatation was found in Pkhd1$^{del3\text{-}4/del5}$ kidneys. Massive Polycystic disease has been found in kidneys from Pkhd1$^{del3\text{-}4/del3\text{-}4}$. No alterations were found in Pkhd1$^{del5/del5}$.kidneys.

Figure 37 shows *Pkhd1*$^{del3\text{-}4/del3\text{-}4}$ kidneys at five to six weeks, three months, and six months of age. Not only the disease progression is enhanced, also the penetrance with an increase from ~ 10% at three months of age to almost all at six months.

In order to ensure that the kidney phenotype originates from the collecting ducts, it has been used a specific marker for collecting duct epithelial cells (Aquaporin-2, Figure 38). As in humans, the majority of the cysts have a collecting duct origin, being the *Pkhd1*$^{del3\text{-}4}$ model the only one that completely mimics human ARPKD.

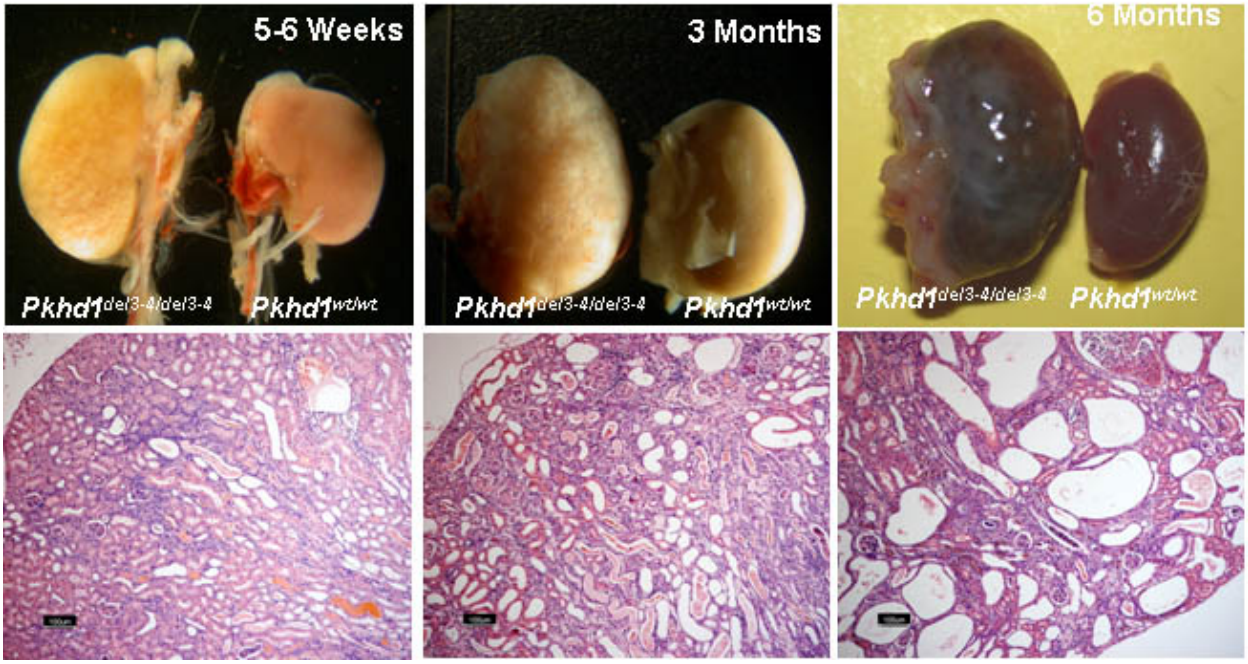

Figure 37. Polycystic Kidney disease progression in Pkhd1$^{del3-4/del3-4}$ mouse.

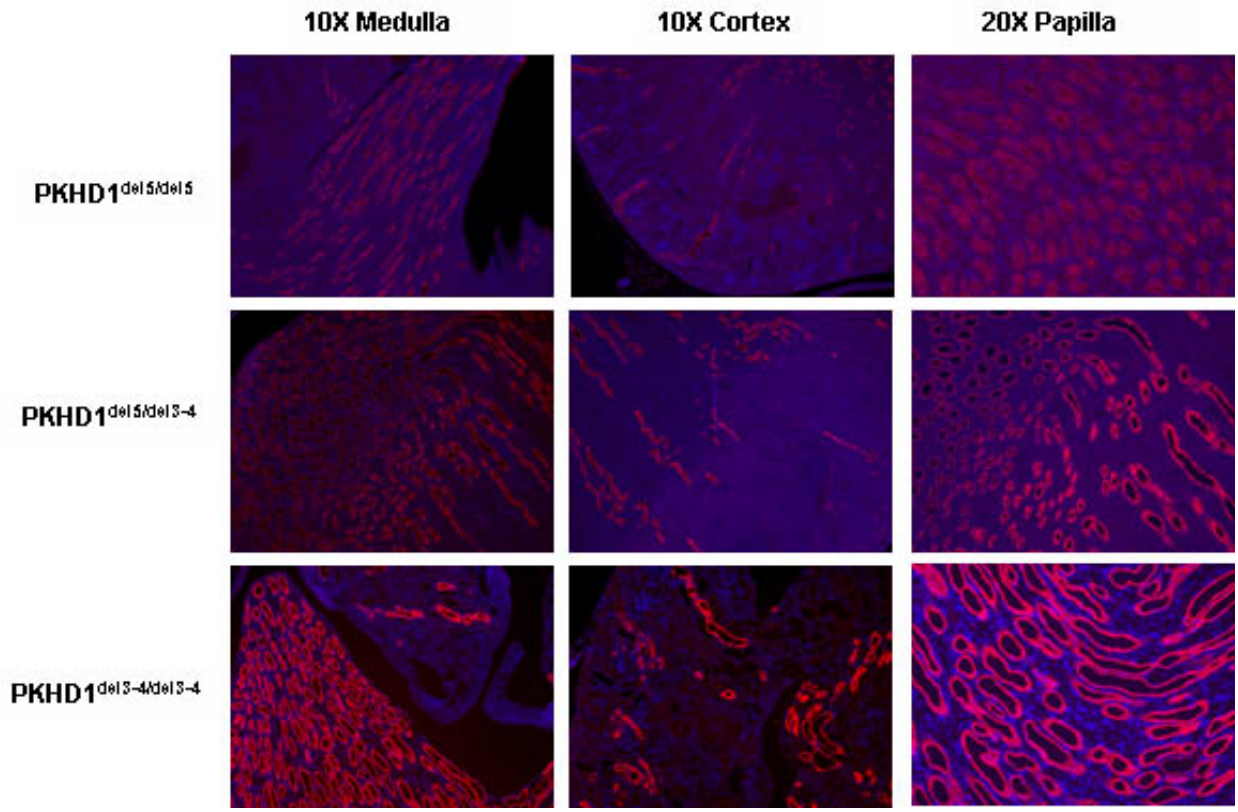

Figure 38. Cysts from ARPKD model (Pkhd1$^{del3-4/del3-4}$) have a dilated collecting duct origin. Aquaporin-2 staining (red) of the dilated collecting ducts in adult mouse kidneys (5-6 weeks). DAPI-stained nuclei appear in blue.

- *PKHD1*$^{del3\text{-}4/del3\text{-}4}$ hepatic phenotype.

Severe congenital hepatic fibrosis is been found in homozygous *PKHD1*$^{del3\text{-}4/del3\text{-}4}$ mice. The size of cystic liver degeneration was slightly variable, differing from multiple small cysts to huge liver cysts (Figure 39). Liver histology of *PKHD1*$^{del3\text{-}4/del3\text{-}4}$ mice at five to six weeks of age showed maximal polycystic liver transformation. The liver changes were confined to abnormal bile duct architecture, fibrosis in the portal tracts and the lobular hepatic parenchyma.

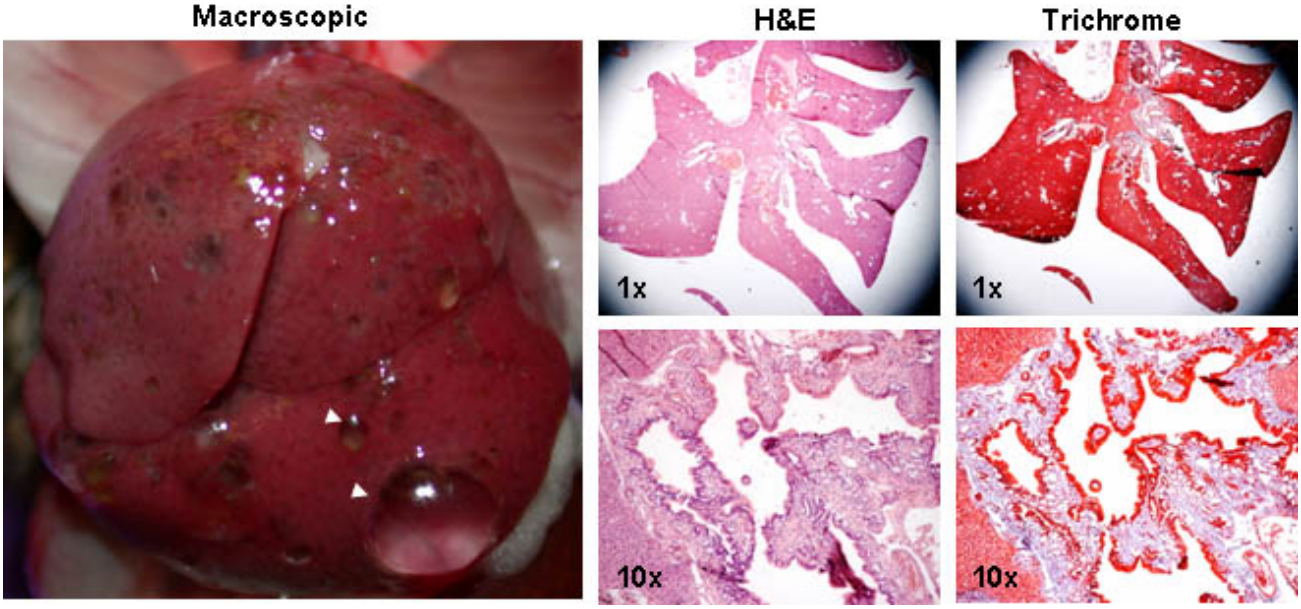

Figure 39. Macroscopic and histological liver sections of a 6 weeks old Pkhd1$^{del3\text{-}4/del3\text{-}4}$ mouse. Degenerated hepatic lobules between cystic bile ducts (H&E) surrounded by fibrosis (Blue staining of the Tricome).

As in humans, defects in *PKHD1*/Polyductin lead to abnormal and/or arrested development of the biliary and portal systems. The classical pathological findings in ARPKD is the ductal plate malformation, in which there is an increased numbers of dilated and irregular or tortuous bile ducts present in an interrupted ring around the periphery of a portal tract which frequently lacks a centrally located bile duct. These biliary findings recapitulate the ductal plate, a stage of normal bile duct development, and persistence of this stage is evidence for developmental arrest as part of the physiopathology of ARPKD. The portal tracts are expanded by mature collagenous tissue, which eventually forms interportal bridges that initially do not disrupt the acinar architecture (a pattern that

has been termed congenital hepatic fibrosis -CHF-).

- *PKHD1*$^{del3\text{-}4/del3\text{-}4}$ Pancreatic Phenotype.

Since the pancreatic phenotype is not one of the most common manifestations of human ARPKD and has a very high penetrance in all of the described models, we decided to define an in depth characterization of this phenomenon.

As in the liver, we found massive pancreatic cyst formation as early as P0 in *PKHD1*$^{del3\text{-}4/del3\text{-}4}$ mice that initiate in a centroacinar position, implying that pancreatic cysts may arise from an undifferentiated pancreatic progenitor cell (Figure 40C and 40D). *PKHD1*$^{del3\text{-}4/del3\text{-}4}$ shows cystic dilatation of the central duct, with peripheral displacement of the acini. The expansion of the parenquima was associated to the large progression of the ductal cysts, with periductal fibrosis, chronic inflammation and progression of cystic acini associated to the destruction of the normal acini (Figure

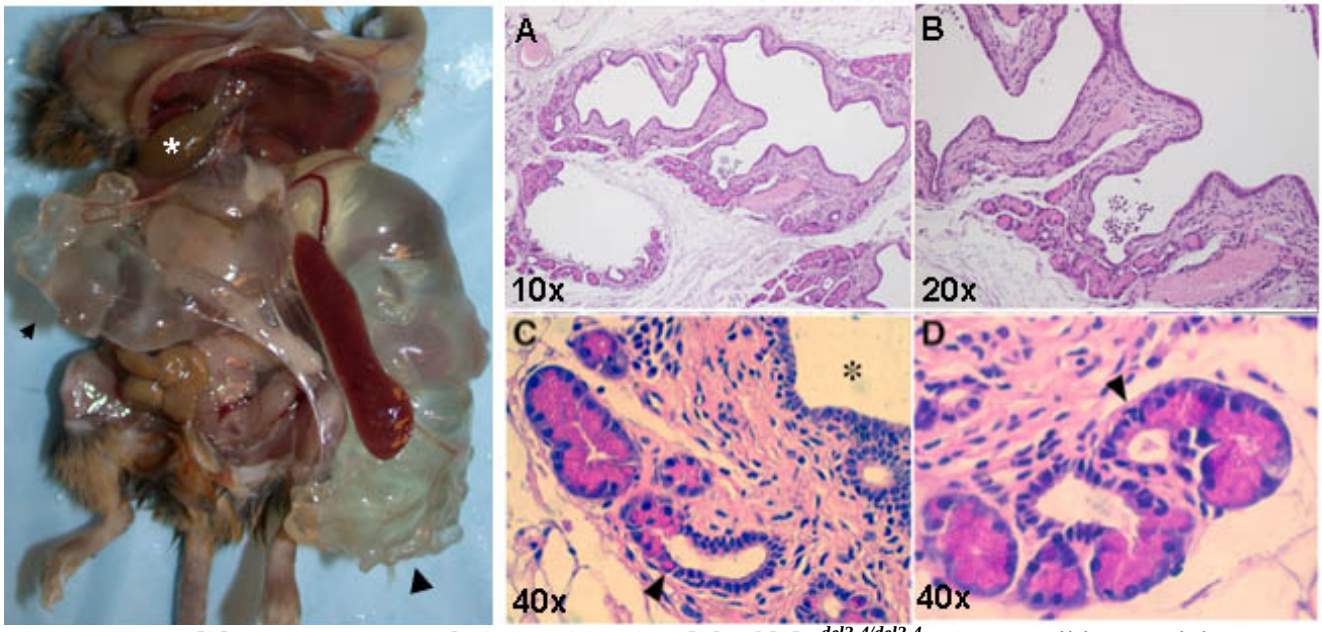

Figure 40. Candidate cyst precursor lesions arising in adult Pkhd1 $^{del3\text{-}4/del3\text{-}4}$ ***mice. A,*** wild-type adult pancreas demonstrating lack of dilated epithelium immediately adjacent to acinar units; arrowhead indicates centroacinar zone comprised of the most terminal branches of the ductal epithelial tree. B-D, candidate cyst precursor lesions. Arrowheads in B-D indicate zones of apparent acinar cell participation in early cyst formation. Note occasional gradual transition between columnar, highly eosinophilic acinar cells and cuboidal cystic epithelium, as indicated by arrowhead in (D). Asterisk in (B) indicates lumen of non-dilated inter-lobular duct. Asterisk in C indicates lumen of adjacent large cystic structure.

40A and 40B). In adult mice, sometimes the weight of the cystic pancreas was similar to the total body weight of the mouse (Figure 40). All this suggests the need for further evaluation at various embryonic time points, as well as the role of Polyductin in normal pancreatic development.

As an initial step towards clarifying mechanisms of pancreatic cyst formation in ARPKD, we have examined H&E-stained sections of tissues harvested from P0 as well as adult *PKHD1*$^{del3\text{-}4/del3\text{-}4}$ mice. While large pancreatic cysts are apparent in each of these conditions, we have further identified candidate cyst precursor lesions delineated by an initially subtle expansion of the "centroacinar" zone, defined by the most terminal elements of the ductal epithelial tree immediately adjacent to the acinar units.

In order to rigorously resolve the question of "selective expansion" vs. "dedifferentiation", Cre/lox-based lineage tracing was developed. Pancreatic cyst epithelium shares common features with undifferentiated embryonic epithelium. To further characterize pancreatic cell types participating in cyst formation, it has been compared epithelial gene expression patterns between wild-type and *PKHD1*$^{del3\text{-}4/del3\text{-}4}$ adult mice through immunofluorescent staining of pancreatic epithelial markers (Figure 41), including E-cadherin as general epithelial marker, as well as amylase, insulin, and pdx1. It is well known that, while pdx1 is ubiquitously expressed in embryonic pancreatic epithelium and restricted to mature β-cells in the adult mice. In the wild-type pancreas (Figure 41, left column), β-cells that are clustered in the endocrine islet are pdx1-positive, while the ductal epithelium is negative for pdx1 (indicated by arrowheads). In contrast, cyst epithelium arising in the setting of *PKHD1* deficiency (Figure 41, right column) shows strong ongoing pdx1 expression, suggesting a much closer analogy to embryonic pancreatic epithelium than to normal ductal epithelium. Assessment of amylase and insulin expression underscores this analogy, with insulin-positive endocrine cells arising and budding from cyst epithelium (Figure 42). Insulin positive cells are almost never seen in the normal

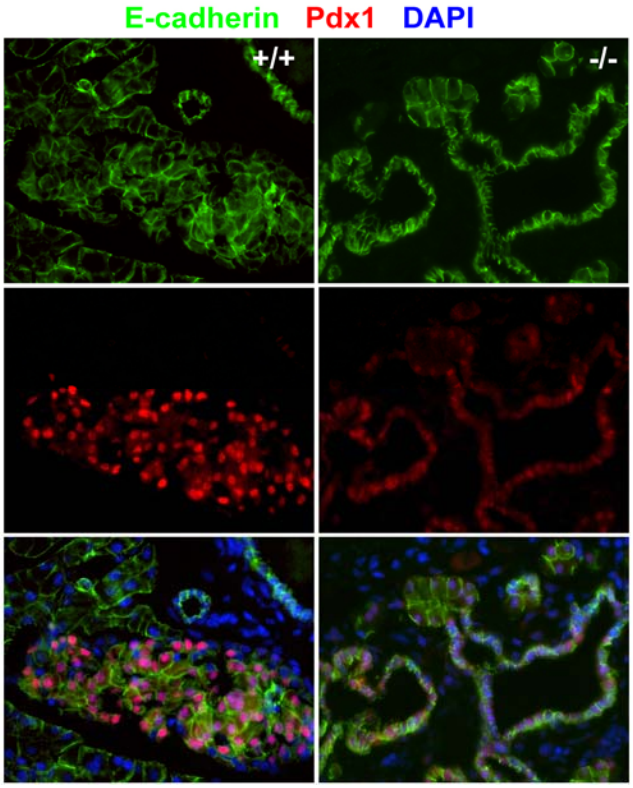

Figure 41. Epithelial gene expression in wild-type and Pkhd1del$^{3-4/del3-4}$ adult pancreas. Images show single-channel and merged images following immunostaining for E-cadherin (green) and pdx1 (red), with DAPI nuclear counterstain. In wild-type adult pancreas (left column), pdx1 expression is restricted to mature β-cells in islet cluster, and absent from ductal epithelium, marked by arrowheads. In contrast, Pkhd1$^{del3-4/del3-4}$ adult pancreas shows strong pdx1 expression in cyst epithelium, suggesting analogy to embryonic pancreas.

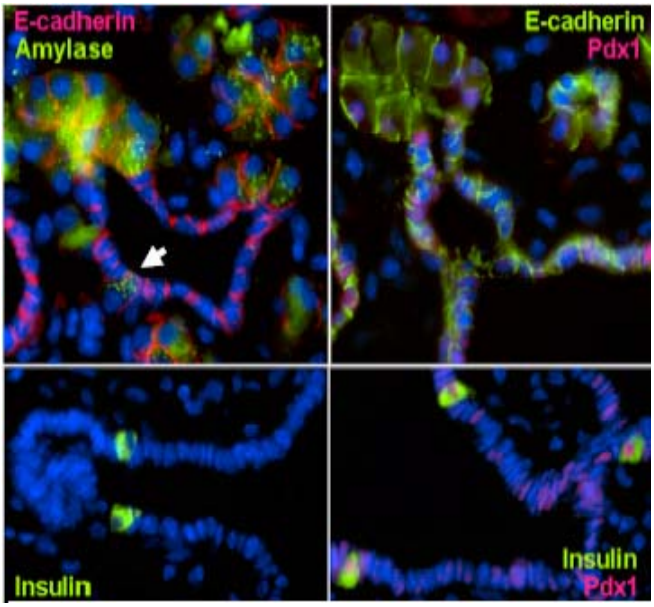

Figure 42. Amylase, insulin, and pdx1 expression in Pkhd1$^{del3-4/del3-4}$ adult pancreas. Images represent merged images following Immunostaining for E-cadherin, amylase and insulin. Note that acinar cells with apical amylase expression in punctate zymogen granules are located immediately adjacent to cuboidal cyst epithelium, with isolated amylasepositive cell also identified within cyst epithelium itself (arrow). Staining for insulin and pdx1 reveals that while the vast majority of pdx1-positive cyst epithelial cells remain undifferentiated, isolated cells undergo β-cells differentiation, marked by insulin expression. A similar appearance of isolated endocrine cells is observed in embryonic pancreas.

ductal epithelium of the adult pancreas, but instead recall the mechanism underlying normal generation of islet cells during embryonic development. These observations call into question the traditional characterization of PKD pancreatic cysts as "ductal cysts", and further support the hypothesis that these cysts represent an expansion of undifferentiated progenitor cells, similar to those present in embryonic pancreas.

5.3.3. Determine whether Pkhd1^{del3-4} is a null allele.

RT-PCR studies confirmed that the Pkhd1del3-4 allele is transcribed and not a complete null on an RNA level. Until now, it could not be possible to determine whether the observed phenotypic

variability results from variants at modifying loci that encode pathway components or splicing variants encoded by the mutant Pkhd1 alleles. RT-PCR amplification of two different wild type mice using primers located in exons 2 and 6 showed a unique band of 416pb including a small fragment of the exon 2 and 6 exon 3, exon 4, exon 5 and small fragment of the exon 6. RT-PCRs from three different Pkhd1$^{del3\text{-}4/del3\text{-}4}$ mice showed the absence of the 416bp band, indicating the deletion of exons 3 and 4, and the amplification of four fragments of ~650bp, ~600bp, 196bp and 87bp. These correspond to aberrant splicing as the result of the deletion of exons 3 and 4. Sequencing of the ~650bp and ~600bp fragments indicated splicing events from exon 2 into the Pgk-Neomycin cassette which contains three different frame stops codons, resulting in the loss of the full-length transcript. Splicing events from exon 2 to 5 generate a 196bp-fragment, lacking exons 3 and 4 and disrupting also the frame of the protein. A small fragment of 87 bp represents the splice event between exons 2 to 6, recovering the frame of the protein (Figure 43A).

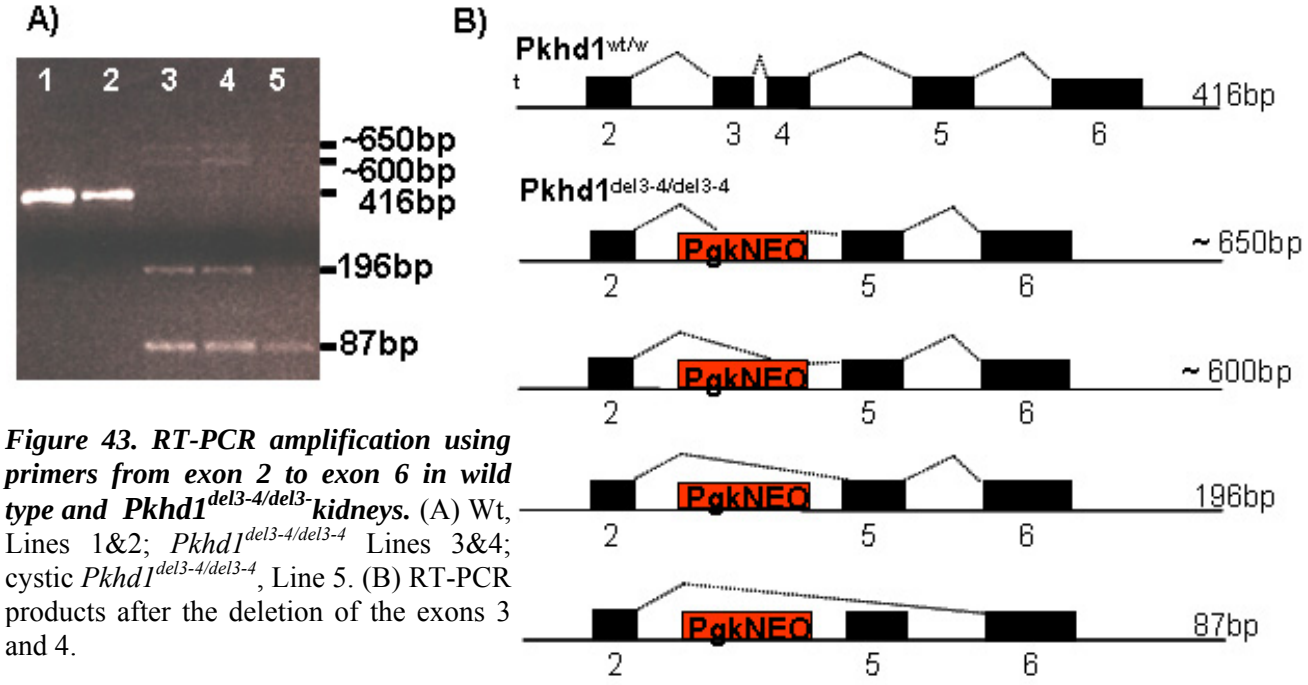

Figure 43. RT-PCR amplification using primers from exon 2 to exon 6 in wild type and Pkhd1$^{del3\text{-}4/del3\text{-}}$ kidneys. (A) Wt, Lines 1&2; *Pkhd1$^{del3\text{-}4/del3\text{-}4}$* Lines 3&4; cystic *Pkhd1$^{del3\text{-}4/del3\text{-}4}$*, Line 5. (B) RT-PCR products after the deletion of the exons 3 and 4.

When RT-PCR amplification was develop in cystic kidneys, it has been noticed a very low amplification of the different fragments, suggesting the possibility of an instable RNA due provably to

a non sense mediated decay mechanism (Figure 43A, line 5). Figure 44B resumes schematically all these splicing events derived from the deletion of exons 3 and 4 in the *Pkhd1*$^{del3-4}$ allele.

In a parallel experiment, liver tissue from wild type, *Pkhd1*$^{del5/del3-4}$, and two different *Pkhd1*$^{del3-4/del3-4}$ mice have been harvest to test splicing differences of the *Pkhd1* alleles associated to polycystic liver disease. Long range RT-PCRs have been performed using a primers pair located in exons 1 and 25 (Figure 44). The expected 2.8 Kb product, as well as other smaller products due to the splice variants, were observed in the *wt* mice. *PKHD1*$^{del5/del3-4}$ and *PKHD1*$^{del3-4/del3-4}$ mice have an altered splice pattern predicted to disrupt the full length product of Polyductin-1. In addition, several new large products were observed in the *Pkhd1*$^{del3-4/del3-4}$ resulting of the splice into the intronic sequence, and demonstrating that the splice pattern is completely altered.

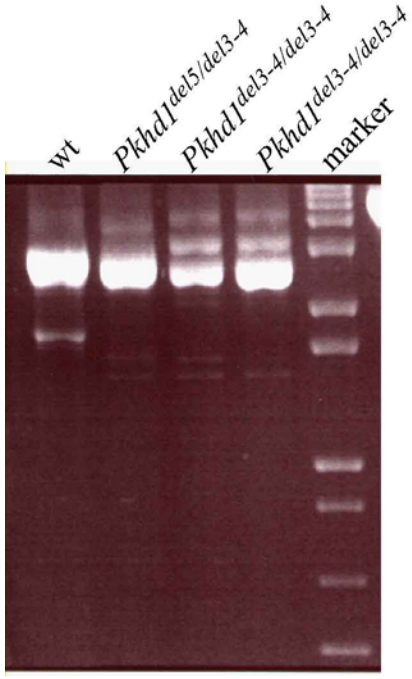

Figure 44. RT-PCR using Ex1F and Ex25R primer set and liver total RNA as source. Lane 1: wild type litter mate control. Lane 2: Pkhd1$^{del5/del3-4}$; Lanes 3 & 4: Pkhd1$^{del3-4/del3-4}$; M: 1 kb marker. The expected 2.8kb product is present in lane 1 (as well as a smaller 1.7kb product). The predominant product in the mutant samples is slightly smaller, consistent with splicing around the deleted segment. Several larger novel products are also present in the Pkhd1$^{del3-4/del3-4}$ specimens.

It has been interpreted positive RT-PCR products as evidence that our allele is not a complete null into the transcriptional level, but it can not be said that the "new" splice variants result in functional products. Comparing the relative level of expression between mutants and "controls" can not be definitive concluded the impact of a reduced expression, since we do not know how much mRNA/protein is required for normal function.

5.3.4. Characterization the complex transcriptional profile in Pkhd1.

We performed RT-PCR using primers spaced along the entire gene's length. Long-range RT-

PCR of kidney and liver specimens from normal and *PKHD1* mutant mice supports previous impression that the gene is subject to a complex pattern of splicing.

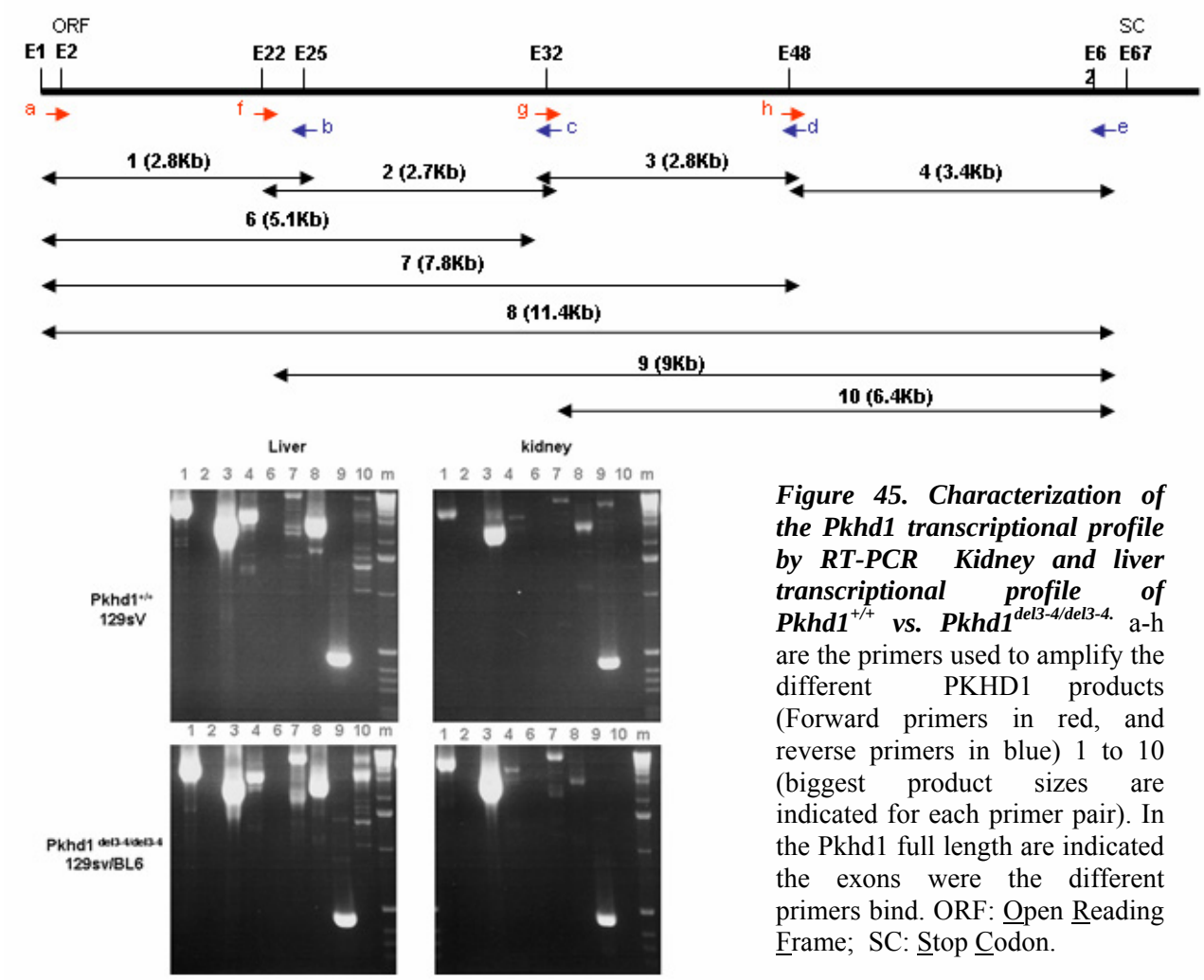

Figure 45. Characterization of the Pkhd1 transcriptional profile by RT-PCR Kidney and liver transcriptional profile of Pkhd1$^{+/+}$ vs. Pkhd1$^{del3-4/del3-4.}$ a-h are the primers used to amplify the different PKHD1 products (Forward primers in red, and reverse primers in blue) 1 to 10 (biggest product sizes are indicated for each primer pair). In the Pkhd1 full length are indicated the exons were the different primers bind. ORF: Open Reading Frame; SC: Stop Codon.

Figure 45 shows the pattern of RT-PCR products that are attained from normal kidney and liver in comparison with the kidney and liver *PKHD1*$^{del3-4/del3-4}$ using a panel of forward primers in combination with different reverse primers. By using these forward/reverse primer pair combinations, we found as even more complex pattern varying between the liver and the kidney (eg. a product of ~6.4kb amplified using an ex32 and ex62 primer pair that is present in liver and absent in kidney). The *PKHD1* mutant splicing pattern of laddering differs between tissues of normal. This figure is a

representative picture of the complicated splice pattern followed by the Pkhd1 gene. This could explain why none of the previous mouse models did not mimicked the entire spectrum of ARPKD.

5.4. Discussion.

Several lines of mice have thus far been described with mutations of *Pkhd1* involving exons 2, 4, 42, and 49 (Moser et al., 2005, Ward et al., ASN2004, Somlo et al., 2004 and Guay-Woodford, personal communication). Curiously, none of the homozygous mutants manifest any signs of kidney disease. Remarkably, all develop liver disease of variable severity and a subset also develops pancreatic cysts. This is a completely unanticipated result since the gene is most abundantly expressed in kidney and its mutation results in kidney disease in both humans and rats. It has been proposed by several groups that the lack of a renal phenotype in this mouse models suggests two possibilities: 1) *Pkhd1* is not essential for kidney development in this species, having different or partially redundant functions replaced by one or more other molecules. This possibility has precedence in the functional overlap between mouse *Inpp5b* and *Ocrl1*, which may explain why *Ocrl1* deficiency does not cause Lowe syndrome in mice (Suchy et al., 2002). 2) The mutations thus far have not disrupted transcripts essential for the kidney. In this Thesis, It has been proposed the latter explanation for the following reasons: a) the gene is predominantly expressed in mouse kidney, as it is in humans and rats; b) other rodents develop renal disease when *PKHD1* is mutated; c) the mutant *PKHD1* allele still encodes transcripts in each of the mutant mouse lines thus far described. The complicated splicing pattern of the gene, coupled with the possibility of multiple transcriptional start sites, accounts for the lack of a mutant renal phenotype in the mouse models produced to date. Human, rat and mouse have been predicted to require a *PKHD1*-encoded gene product for proper kidney formation/function but that each species may have different requirements as to what features the protein must have. The species may also differ in their pattern of splicing and thus each may have a different ability to respond to

mutations altering specific exons. Therefore, it can be possible that none of the *PKHD1* mutant alleles thus far described is a true null, and this likely explains the lack of a renal phenotype.

The goal of this subproject of the Thesis is test the hypothesis that appropriated exon targeting and complete inactivation of *PKHD1* in mice can mimic the human ARPKD, including renal disease and other manifestations. A second hypothesis, related to the first, is that inactivation of *Pkhd1* will result in abnormalities in organ systems besides those that have been described. Several lines of evidence support this hypothesis: 1) Germino's group found widespread expression of *PKHD1* in numerous tissues, with cell-type specific patterns of hybridization for some exons (Nagasawa et al., 2002), 2) there are reports of an association of aneurysms and AR*PKD1* (Neumann et al., 1999 and Lilova et al 2001) consistent with the gene's high level of expression in vascular tissue (Nagasawa et al., 2002). 3) *PKHD1* mutant mice can, depending on the exon targeted, develop pancreatic cysts. This observation suggests that the range of phenotypes that will result from mutation of *PKHD1* will depend on the nature of mutation that is introduced. The recent description of a human family with ARPKD and cystic pancreas disease suggests that findings in mice may equally apply to humans (Guay-Woodford, personal communication).

Pkhd1$^{flox3-4}$ is a functional allele . It has been generated the first *Pkhd1* conditional knockout flanking the exons 3 and 4 by loxP sites and introducing a cassette of Neomycin with three stop codons. Exons 3 and 4 are two of the exon with higher homology between mouse and humans, the deletion of this exons disrupt the reading frame of the protein, exon 3 has an alternative start site, exon 4 is been described as a hot spot for human mutation and the Neomycin cassette introduce alterations in the gene transcriptional pattern (for example, the *Pkd2$^{flox3-4}$* model described in this thesis). These were the major considerations taken in order to cause as much gene damage as possible, seeing the difficulty to generate a model that complete mimics the human ARPKD. As mentioned preciously for the conditional *Pkd2* mouse, this model offers a powerful tool to examine the consequences of

temporally and tissue specific regulated inactivation of *Pkhd1*. This system can be used to establish an unambiguous relationship between *PKHD1* inactivation and disease manifestations. It can be examined which factors are involved in the progression of the disease in each particular tissue.

After Cre-mediated recombination, it has been proven that the $Pkhd1^{flox3\text{-}4}$ is totally functional. Using a Meox2-Cre system, it has been generated a new allele ($Pkhd1^{flox3\text{-}4}$) which mimic a germline mutation deleting exons 3 and 4. In the Meox2-cre line, Cre recombinase has been "knocked-in" to the *Meox2* gene (mesenchyme homeobox-2 gene). Heterozygotes for Cre are phenotypically normal. The native promoter of *Meox2* restricts Cre expression to epiblast-derived tissues and thus induces deletion in 90-95% of somatic cells including germ cells but spares placental trophoblasts. The Meox-2 Cre+ mice transmitted the deleted allele to nearly 50% of offspring, and these were crossed to produce homozygotes for $Pkhd1^{flox3\text{-}4/del3\text{-}4}$.

Another important tool for the study of PKHD1 biology that can be derived from model is the establishment of immortalized cell lines from the $PKHD1^{flox3\text{-}4/flox3\text{-}4}$ after crossing to the Immortamouse116. It can be generated genetically null cell lines and their uninduced floxed controls as tools for exploring PD1 function and functional characteristics of PKHD1 splicing.

<u>$Pkhd1^{del3\text{-}4/del3\text{-}4}$ mouse model mimics the human ARPKD, including the renal phenotype .</u>

After performing series of $PKHD1^{del3\text{-}4/+}$ crosses it has been determined that homozygous mutants mimic all the phenotypes related to ARPKD. It has been proved that appropriated exon targeting of *PKHD1* in mice can reproduce ARPKD, including renal disease and other manifestations. The $Pkhd1^{del3\text{-}4/del3\text{-}4}$ is the only model described up to the moment manifesting perinatal demise, polycystic kidney, liver and pancreas disease, growth retardation and vascular phenotype.

Perinatal demise was a very common phenomenon in the offspring of inbred line 129SV. Mice dye with obvious symptoms of respiratory failure, but none of this mice ever have polycystic kidney disease. It has been describe that pressure given by the massive kidney from the abdominal cavity is

the direct responsible of the dead by respiratory insufficiency. This model would suggest that the respiratory insufficiency is a phenomenon independent of the size of the kidneys. It has been found several mice dead a couple hours after birth with partially inflated lungs and pulmonary hypertension in absence polycystic kidneys. This has very important implications in the understanding of the disease.

Another phenomenon independently of kidney manifestation in this model is the growth retardation. *Pkhd1*$^{del3\text{-}4/del3\text{-}4}$ and *Pkhd1*$^{del5/del5}$ have a very high penetrance of growth retardation. *Pkhd1*$^{del5/del5}$ is characterized by the absence of polycystic kidney disease. Also, it has been found growth retardation in absence of renal phenotype in the *Pkhd1*$^{del3\text{-}4/del3\text{-}4}$ model. It can be concluded that growth retardation and respiratory insufficiency are two manifestations independent of the kidney phenotype.

A very common phenotype found ether in *Pkhd1*$^{del3\text{-}4/del3\text{-}4}$ or *Pkhd1*$^{del5/del5}$, but not very common in human ARPKD is the severe polycystic pancreas disease (Neuhaus et al., 1996). It has been found impressive polycystic pancreas disease where the size of the pancreas was bigger than the total size of a mouse. This is the major responsible of spontaneous dead in these models. When the size of the polycystic pancreas became very prominent, mice start to have difficulties eating and drinking by limited movement. Striking, mice did not died by limited intake. Most of spontaneous dead has been associated with rupture of the polycystic pancreas. These mice are the unique ARPKD models with this phenotype, what makes them an invaluable tool in the study of this phenotype.

The vascular phenotype found in the *Pkhd1*$^{del3\text{-}4/del3\text{-}4}$ model was consider from the beginning based on the *in situ* hybridization results that Germino's group obtained using probes for exons 5 and 41 (Nagasawa et al., 2002). This result suggests that homozygous mutations of exon 5 would be expected to result in a vascular phenotype. It can be predicted that the ARPKD families with aneurysms or pancreatic disease likely are examples of situations where biallelic mutations affected

exons essential for the integrity of these other organs.

As in humans, *Pkhd1*$^{del3\text{-}4/del3\text{-}4}$ kidney phenotype manifestation is wild variable. It has been classified this phenotype in three major categories based on the severity presentation: milder, intermediate and severe renal phenotype. The mild phenotype is been found in mouse as early as three months of age, characterized by asymptomatic mild dilatation of the collecting ducts. The intermediate phenotype it has been found sporadically at three months, becoming more common in mouse of six months of age. This phenotype was characterized by the presence of sporadic cyst and dilated collecting ducts, considering a cyst when the lumen was 3 times bigger than normal and accompanied by change in the morphological change of the epithelia and glomerulosclerosis. It has been found severe kidney phenotype in a variable timing form 5 months up to a year, easy identifiable by the sickness of the mouse. Severe cyst formation with a lumen more than three times than normal, fibrotic areas associated to renal injury as well as glomerulosclerosis, has been found associated the alteration of renal morphology, compromising the mouse survival by renal dysfunction. As in humans, increased of the renal volume has been associated with progression of the cystic disease.

Liver phenotype is the only phenotype common for all the mouse models described until now, been found in variable severity and time manifestation for those models. *Pkhd1*$^{del3\text{-}4/del3\text{-}4}$ homozygous mice develop a more severe manifestation than previously describe for other mice knockouts. Enlargement and fibrosis of portal areas, aberrant proliferation of the bile ducts, hypoplasia of the portal vein leading to portal hypertension and splenomegalia, massive common bile dilatation sometimes associated with gallstones are very common findings in early time points. Ductal plate malformation starts in embryonic development, and fibrotic associated alterations have been found in the first day of live.

Pkhd1$^{del3\text{-}4/del3\text{-}4}$***is not a complete null, but disrupts the normal gene expression pattern.*** It has been concluded that the *PKHD1*$^{flox3\text{-}4}$ *i*s not true null on the RNA level but mimics the human

phenotype showing a severe presentation, by the disruption of the polyductin full length and important splice variants. The *PKHD1*$^{del3-4}$allele is not a true null into the transcriptional level (ie. defined as encoding transcripts containing 3' exons) but results in a severe phenotype with multiple organ dysfunction associated (principally with pancreas, liver and kidney abnormalities). This outcome indicates that the allele, despite producing transcripts with 3'exons, still functions as a complete null. These transcripts are functionally important because additional abnormalities have been found as the result from their complete loss. Mice with mutations of exons 42 or 49 only develop liver disease while those with mutations of exons 2 or 4 develop both liver and pancreatic disease. In addition to these phenotypes, it has been proven that deletion of exons 3, 4, and 5 can mimic the human disease, including kidney, pancreas disease, growth retardation and vascular phenotype.

Pkhd1 undergoes to a complicated splice pattern.. It has been shown that the gene is widely expressed, though its transcripts are most abundant in kidney, that it undergoes a complicated pattern of splicing and that not all exons are expressed in all tissues. It can be concluded that the reason other models failed to mimic the ARPKD was that alternative splicing produces transcripts "skipped" over *PKHD1* mutations and produced functional products that preserve renal, and possibly other organ, function. Different cell types have distinct requirements for specific classes of transcripts. Differences in patterns of splicing may modify disease expression.

The innovation of this model opens a spectrum of possible testing hypothesis in future directions. Using various Cre-recombinases, this system is going to be a powerful model to define the spectrum of abnormalities that result from the selective removal of exons 3 and 4 (and 5 into the RNA level). This information will ultimately be helpful in determining the types of transcripts that are essential for proper formation of each organ. It can be test the hypothesis that PKHD1 has essential functions in post-developmental tissues. Since PKHD1 is required for kidney development in mice, we predict that it is required for maintenance of tubular morphology and that its loss will either result in

cell death (with increased fibrosis) or renal cysts. This hypothesis can be tested producing a mice Pkhd1flox3-4/flox3-4 positive for either the taMeoxifen- or interferon-inducible Cre recombinase and determine the short and long-term effects of post-natal inactivation in target organs. The mice also could carry a reporter gene (Z/AP) that can be used to track Cre recombinase activity.

Three major conclusions can be done. Mutation of PKHD1 in mice can result in renal disease if a suitable segment of the gene is selected for targeting. PKHD1 is essential for maintenance of normal renal and biliary tubular morphology. Complete inactivation of the gene can result in a severe phenotype, involving additional organ systems (lung, vasculature and pancreas), fetal/perinatal demise and growth retardation.

6. Conclusiones.

1. En el primer capítulo de esta tesis ha sido desarrollada una estrategia de búsqueda de mutaciones mediante secuenciación directa de los exones y sus regiones colindantes de los genes PKD1 y PKD2, causantes de la enfermedad poliquística renal autosómica dominante (ADPKD).El establecimiento de una estrategia racional en el análisis de la totalidad de la región codificadora de ambos genes basada en secuenciación directa ha reducido el esfuerzo y los costes en el estudio de familias con ADPKD.

2. Para garantizar la eficacia de dicha estrategia, un grupo de 82 pacientes pertenecientes a familias con ADPKD fueron sometidos a estudio. De las 82 familias, 55 poseían mutaciones causantes de la enfermedad en el gen PKD1 y 13 en el gen PKD2. Esto indica un nivel de detección del 83%, el más alto descrito hasta el momento.

3. Se ha trabajado de una manera muy cercana con Athena Diagnostics para ayudar en el traslado de los métodos de investigación en una herramienta clínica útil. La estrategia ha demostrado ser la más eficiente descrita hasta el momento y ahora forma la base del único test de DNA de ADPKD utilizado en práctica clínica (PKDX).

4. El análisis completo de ambos genes es esencialmente importante puesto que no han sido identificados lugares calientes o "hot spots" en PKD1 o PKD2. Se ha observado un nivel extraordinariamente elevado de variabilidad en el gen *PKD1,* con una media de 13.2 variantes genéticas y un rango entre 0 a 60 variantes por paciente.

5. Hasta 17 SNPs han sido localizados en PKD1 y 2 en PKD2, hablando de la alta flexibilidad de PKD1 y proporcionando una "huella dactilar" para cada uno de los genes ADPKD.

6. La secuenciación directa es un método de detección sensitivo de variables del DNA en PKD1 y PKD2, pero es necesaria una interpretación estricta de los resultados esencialmente si han de ser utilizados en la toma de decisiones clínicas. Para ello se ha establecido un criterio estricto de calificación de las variantes basado en tres principios: conservación del cambio, su patogenicidad y la probabilidad de generar un splice site.

7. Se demuestra que los sistemas *in vitro* no solo pueden ser una herramienta muy útil para distinguir entre polimorfismos y mutaciones, sino que también pueden ser utilizados para demostrar los efectos de las distintas variantes encontradas en PKD1.

8. Se ha establecido un método de estudio del comportamiento génico, basado en la información de los cambios encontrados mediante las completa secuenciación de los genes. Así pues, se ha analizado sistemáticamente todas las variantes a lo largo de ambos genes, concluyéndose que el gen PKD1 es casi 6 veces más mutable que PKD2. Esto se debe principalmente a la presencia de un tracto de polipirimidina en el exón 21 del gen PKD1, a la conversión génica con sus homólogos y al alto GC. Éste método puede ser aplicado a otros genes para un mejor conocimiento de su comportamiento.

9. Los estudios *in sílico* e *in vitro* han sentado las bases del primer modelo condicional trialélico de ratón del gen *Pkd2*, un alelo condicionado hipomórfico (*Pkd2*^{cond}), un alelo condicionado de función normal *Pkd2*^{delneo} que puede ser inactivado *in vivo*, y un alelo de función nula o *knockout* (*Pkd2*$^{del11\text{-}13}$) cuya predicción presenta una disrupción del C-terminal de *Pkd2*.

10. Se ha demostrado que se puede inactivar *in vivo* el alelo *Pkd2*^{delneo}, a través de una deleción en un 95% de los segmentos de DNA *floxeados*, mediada por la recombinasa-Cre de una forma somática y regulada por el promotor Meox-2. Estos ratones mueren inmediatamente después del nacimiento con todas las manifestaciones de un fenotipo defectivo de Pkd2, incluyendo edema severo, quistes renales, quistes pancreáticos y alteración al azar eje axial derecha/izquierda.

11. Se exhiben las bases de un modelo in vitro de formación quística basado en el cultivo de cortes tangenciales embrionarios, que no solo proporciona el seguimiento en tiempo real de la formación quística, sino que también proporciona una plataforma de manipulación farmacológica y génica de la poliquistosis pancreática y renal.

12. En esta tesis se presenta el primer modelo de ratón de la PKD recesiva (ARPKD) que muestra todas las manifestaciones fenotípicas de la enfermedad. Se desarrolló un alelo funcional *floxeado* de *Pkhd1* (*Pkhd1*$^{flox3\text{-}4}$) que produce la deleción mediada por la recombinasa-Cre de los exones 3 y 4.

13. Los ratones *Pkhd1*$^{D3\text{-}4/D3\text{-}4}$ manifiestan los mismos fenotipos de la enfermedad en humanos con muerte en fase perinatal, los sobrevivientes desarrollan una variedad de malformaciones hepatobiliares con fibrosis hepática congénita, quistes codelocales y colangitis ascendente. También presenta una severa poliquistosis pancreática, manifestación variable de la poliquistosis renal y retraso en el crecimiento

14. Estas nuevas líneas de ratón permiten la inactivación espacio-temporal de Pkhd1 y Pkd2 de una manera controlada, presentan un espectro completo de fenotipos ARPKD y ADPKD, y serán una herramienta poderosa en el estudio de la biología y la patogénesis de PKHD1 y PKD2. A su vez, de estos modelos se derivará un novedoso sistema celular de inactivación in vitro de los genes Pkd2 y Pkhd1.

7. References

- Ariza, M.; Alvarez, V.; Marin, R.; Aguado, S.; Lopez-Larrea, C.; Alvarez, J.; Menendez, M. J.; Coto, E. : **A family with a milder form of adult dominant polycystic kidney disease not linked to the *PKD1* (16p) or *PKD2* (4q) genes.** *J. Med. Genet.* 34: 587-589, 1997.
- Arnould, T., Kim, E., Tsiokas, L., Jochimsen, F., Gruning, W., Chang, J.D., and Walz, G. **The polycystic kidney disease 1 gene product mediates protein kinase C-alphadependent and c-Jun N-terminal kinase-dependent activation of the transcription factor AP-1.** *J. Biol. Chem.* 273, 6013-6018, 1998.
- Bhunia, A. K.; Piontek, K.; Boletta, A.; Liu, L.; Qian, F.; Xu, P.-N.; Germino, F. J.; Germino, G. G. : ***PKD1* induces p21-waf1 and regulation of the cell cycle via direct activation of the JAK-STAT signaling pathway in a process requiring *PKD2*.** *Cell* 109: 157-168, 2002.
- Bogdanova, N.; Markoff, A.; Gerke, V.; McCluskey, M.; Horst, J.; Dworniczak, B. : **Homologues to the first gene for autosomal dominant polycystic kidney disease are pseudogenes.** *Genomics* 74: 333-341, 2001.
- Boletta, A.; Qian, F.; Onuchic, L. F.; Bhunia, A. K.; Phakdeekitcharoen, B.; Hanaoka, K.; Guggino, W.; Monaco, L.; Germino, G. G. : **Polycystin-1, the gene product of *PKD1*, induces resistance to apoptosis and spontaneous tubulogenesis in MDCK cells.** *Molec. Cell* 6: 1267-1273, 2000.
- Boulter C, Mulroy S, Webb S, Fleming S, Brindle K, Sandford R: **Cardiovascular, skeletal, and renal defects in mice with a targeted disruption of the *PKD1* gene.** *Proc Natl Acad Sci* USA 98(21):12174-9. 2001.
- Bukanov, N. O.; Husson, H.; Dackowski, W. R.; Lawrence, B. D.; Clow, P. A.; Roberts, B. L.; Klinger, K. W.; Ibraghimov-Beskrovnaya, O. : **Functional polycystin-1 expression is developmentally regulated during epithelial morphogenesis in vitro: downregulation and loss of membrane localization during cystogenesis.** *Hum. Molec. Genet.* 11: 923-936, 2002.
- Burn, T. C.; Connors, T. D.; Dackowski, W. R.; Petry L. R.; Van Raay, T. J.; Millholland, J. M.; Venet, M.; Miller, G.; Hakim, R. M.; Landes, G. M.; Klinger, K. W.; Qian, F.; Onuchic, L. F.; Watnick, T.; Germino, G. G.; Doggett, N. A. : **Analysis of the genomic sequence for the autosomal dominant polycystic kidney disease (*PKD1*) gene predicts the presence of a leucine-rich repeat.** *Hum. Molec. Genet.* 4: 575-582, 1995.
- Calvet JP: Molecular genetics of polycystic kidney disease. J Nephrol 11:24 -34, 1998.
- Calvet, J. P. : **Ciliary signaling goes down the tubes.** *Nature Genet.* 33: 113-114, 2003.
- Daoust, M. C.; Reynolds, D. M.; Bichet, D. G.; Somlo, S. : **Evidence for a third genetic locus for autosomal dominant polycystic kidney disease.** *Genomics* 25: 733-736, 1995
- de Almeida, S.; de Almeida, E.; Peters, D.; Pinto, J. R.; Tavora, I.; Lavinha, J.; Breuning, M.; Prata, M. M. : **Autosomal dominant polycystic kidney disease: evidence for the existence of a third locus in a Portuguese family.** *Hum. Genet.* 96: 83-88, 1995.
- de Boer JG, Ripley LS. **Demonstration of the production of frameshift and base-substitution mutations by quasipalindromic DNA sequences.** *PNAS.* 1984 Sep;81(17):5528-31.
- Esni, F., Stoffers, D. A., Takeuchi, T. and Leach, S. D. **Origin of exocrine pancreatic cells from nestin-positive precursors in developing mouse pancreas.** *Mech. Dev.* **121**, 15-25, 2004.
- European Polycystic Kidney Disease Consortium : **The polycystic kidney disease 1 gene encodes a 14 kb transcript and lies within a duplicated region on chromosome 16.** *Cell* 77: 881-894, 1994.

- Fonck, C., et al., ***Autosomal recessive polycystic kidney disease in adulthood.*** *Nephrol Dial Transplant.* 16(8): p. 1648-52, 2001.
- Gabow PA: **Autosomal dominant polycystic kidney disease: More than a renal disease**. *Am J Kidney Dis.* 16:403 -413, 1990.
- Gabow, P. A. : **Autosomal dominant polycystic kidney disease.** *New Eng. J. Med.* 329: 332-342, 1993.
- Gasslander, T., I. Ihse, and S. Smeds, **The importance of the centroacinar region in cerulein-induced mouse pancreatic growth. Scand J Gastroenterol.** 27(7): p. 564-70, 1992.
- Gattone, V.H., Wang, X., Harris, P.C., and Torres, V.E. **Inhibition of renal cystic disease development and progression by a vasopressin V2 receptor antagonist.** *Nat Med* 9,1323-1326, 2003.
- Geng, L., Segal, Y., Pavlova, A., Barros, E.J.G., Lohning, C., Lu, W., Nigam, S.K., Frischauf, A., Reeders, S.T. and Zhou, J. **Distribution and developmentally regulated expression of murine polycystin.** *Am. Physio. Soc.* F451-F459, 1997.
- Germino, G. G. : Personal Communication. Baltimore, Md., 7/30/1998.
- Germino, G. G.; Barton, N. J.; Lamb, J.; Higgs, D. R.; Harris, P.; Xiao, G. H.; Scherer, G.; Nakamura, Y.; Reeders, S. T. : **Identification of a locus which shows no genetic recombination with the autosomal dominant polycystic kidney disease gene on chromosome 16.** *Am. J. Hum. Genet.* 46: 925-933, 1990.
- Germino, G. G.; Weinstat-Saslow, D.; Himmelbauer, H.; Gillespie, G. A. J.; Somlo, S.; Wirth, B.; Barton, N.; Harris, K. L.; Frischauf, A.-M.; Reeders, S. T. : **The gene for autosomal dominant polycystic kidney disease lies in a 750-kb CpG-rich region.** *Genomics* 13: 144-151, 1992.
- Germino, G.G., and Chapman, A.B. **Autosomal Dominant Polycystic Kidney Disease. In "The Metabolic and Molecular Basis of Inherited Disease"**. Scriver, C.R., Beaudet, A.L., Sly, W.S. and Valle, D., editors. *McGraw-Hill*. New York, USA. 5467- 5489, 2001.
- Grantham, J. J.; Calvet, J. P. : **Polycystic kidney disease: in danger of being X-rated?** *Proc. Nat. Acad. Sci.* 98: 790-792, 2001.
- Grimm, D.H., Cai, Y., Chauvet, V., Rajendran, V., Zeltner, R., Geng, L., Avner, E.D., Sweeney, W., Somlo, S., and Caplan, M.J. **Polycystin-1 distribution is modulated by polycystin-2 expression in mammalian cells.** *J. Biol. Chem.* 278, 36786-36793, 2003.
- Guay-Woodford, L.M. **Murine models of polycystic kidney disease: molecular and therapeutic insights.** Am. J. Physiol. Renal. Physiol., 285, F1034-1049, 2003.
- Guay-Woodford, L.M. **Murine models of polycystic kidney disease: molecular and therapeutic insights.** *Am. J. Physiol. Renal. Physiol.,* 285, F1034-1049, 2003.
- Hanaoka, K.; Qian, F.; Boletta, A.; Bhunia, A. K.; Piontek, K.; Tsiokas, L.; Sukhatme, V. P.; Guggino, W. B.; Germino, G. G. : **Co-assembly of polycystin-1 and -2 produces unique cation-permeable currents.** *Nature* 408: 990-994, 2000.
- Hateboer, N.; van Dijk, M. A.; Bogdanova, N.; Coto, E.; Saggar-Malik, A. K.; San Millan, J. L.; Torra, R.; Breuning, M.; Ravine, D. : **Comparison of phenotypes of polycystic kidney disease types 1 and 2.** *Lancet* 353: 103-107, 1999.
- Hayashi, K., et al., Regional differences in the cellular proliferation activity of the regenerating rat pancreas after partial pancreatectomy. Arch Histol Cytol, 1999. 62(4): p.337-46.
- Helms, J.A., Kim, C.H., Hu, D., Minkoff, R., Thaller, C. and Eichele, G: Sonic hedgehog participates in craniofacial morphogenesis and is downregulated by teratogenic doses of retinoic acid. *Dev. Biol.:* 187, 25-35, 1997.

- Huan, Y.; van Adelsberg, J. : **Polycystin-1, the *PKD1* gene product, is in a complex containing E-cadherin and the catenins.** *J. Clin. Invest.* 104: 1459-1468, 1999.
- Hughes, J.; Ward, C. J.; Peral, B.; Aspinwall, R.; Clark, K.; San Millan, J. L.; Gamble, V.; Harris, P. C. : **The polycystic kidney disease 1 (*PKD1*) gene encodes a novel protein with multiple cell recognition domains.** *Nature Genet.* 10: 151-160, 1995.
- International Polycystic Kidney Disease Consortium : **Polycystic kidney disease: the complete structure of the *PKD1* gene and its protein.** *Cell* 81: 289-298, 1995.
- Kim, E., Arnould, T., Sellin, L.K., Benzing, T. Comella, N., Kocher, O., Tsiokas, L., Sukhatme, V.P., and Walz, G. **Interaction between RGS7 and polycystin.** *Proc. Natl. Acad. Sci.* USA. 96, 6371-6376, 1999.
- Kim, K.; Drummond, I.; Ibraghimov-Beskrovnaya, O.; Klinger, K.; Arnaout, M. A. : **Polycystin 1 is required for the structural integrity of blood vessels.** *Proc. Nat. Acad. Sci.* 97: 1731-1736, 2000.
- Kimberling, W. J.; Kumar, S.; Gabow, P. A.; Kenyon, J. B.; Connolly, C. J.; Somlo, S. : **Autosomal dominant polycystic kidney disease: localization of the second gene to chromosome 4q13-q23.** *Genomics* 18: 467-472, 1993.
- Kottgen, M., Benzing, T., Simmen, T., Tauber, R., Buchholz, B., Feliciangeli, S., Huber, T.B., Schermer, B., Kramer-Zucker, A., Hopker, K., Simmen, K.C., Tschucke, C.C., Sandford, R., Kim, E., Thomas, G., and Walz, G. **Trafficking of TRPP2 by PACS proteins represents a novel mechanism of ion channel regulation.** *J. EMBO.* 24, 705-716, 2005.
- Koulen, P.; Cai, Y.; Geng, L.; Maeda, Y.; Nishimura, S.; Witzgall, R.; Ehrlich, B. E.; Somlo, S. : **Polycystin-2 is an intracellular calcium release channel.** *Nature Cell Biol.* 4: 191-197, 2002.
- Lu W, Shen X, Pavlova A, Lakkis M, Ward CJ, Pritchard L, Harris PC, Genest DR, Perez-Atayde AR, Zhou J: **Comparison of *PKD1*-targeted mutants reveals that loss of polycystin-1 causes cystogenesis and bone defects.** *Hum Mol Genet* 10(21): 2385-96, 2001.
- Lu, W.; Peissel, B.; Babakhanlou, H.; Pavlova, A.; Geng, L.; Fan, X.; Larson, C.; Brent, G.; Zhou, J. : **Perinatal lethality with kidney and pancreas defects in mice with a targeted *PKD1* mutation.** *Nature Genet.* 17: 179-181, 1997.
- Lilova MI, Petkov DL. **Intracranial aneurysms in a child with autosomal recessive polycystic kidney disease.** *Pediatr Nephrol.* Dec;16(12):1030-2, 2001.
- Masyuk, T.V., et al., *Defects in cholangiocyte fibrocystin expression and ciliary structure in the PCK rat.* Gastroenterology, 2003. **125**(5): p. 1303-10.
- McConnell, R. S.; Rubinsztein, D. C.; Fannin, T. F.; McKinstry, C. S.; Kelly, B.; Bailey, I. C.; Hughes, A. E. : **Autosomal dominant polycystic kidney disease unlinked to the *PKD1* and *PKD2* loci presenting as familial cerebral aneurysm.** (Letter) *J. Med. Genet.* 38: 238-239, 2001.
- Menezes, L.F., et al., **Polyductin, the *PKHD1* gene product, comprises isoforms expressed in plasma membrane, primary cilium, and cytoplasm.** *Kidney Int.* **66**(4): p. 1345-55, 2004.
- Miyamoto, Y., et al., **Notch mediates TGFalpha-induced changes in epithelial differentiation during pancreatic tumorigenesis.** *Cancer Cell.* 3(6): p. 565-76, 2003
- Mochizuki, T.; Wu, G.; Hayashi, T.; Xenophontos, S. L.; Veldhuisen, B.; Saris, J. J.; Reynolds, D. M.; Cai, Y.; Gabow, P. A.; Pierides, A.; Kimberling, W. J.; Breuning, M. H.; Constantinou Deltas, C.; Peters, D. J. M.; Somlo, S. : ***PKD2*, a gene for polycystic kidney disease that encodes an integral membrane protein.** *Science* 272: 1339-1342, 1996.
- Moy, G.W., Mendoza, L.M., Schulz, J.R., Swanson, W.J., Glabe, C.G., and Vacquier, V.D.. **The sea urchin spern receptor for egg jelly is a modular protein with extensive homology to the human polycystic kidney disease protein, *PKD1*.** *J. Cell Biol.* 133, 809-817, 1996.

- Murti, J. R.; Bumbulis, M.; Schimenti, J. C. : **Gene conversion between unlinked sequences in the germline of mice.** *Genetics* 137: 837-843, 1994.
- Muto S, Aiba A, Saito Y, Nakao K, Nakamura K, Tomita K, Kitamura T, Kurabayashi M, Nagai R, Higashihara E, Harris PC, Katsuki M, Horie S: **Pioglitazone improves the phenotype and molecular defects of a targeted *PKD1* mutant.** *Hum Mol Genet* 11(15):1731-42, 2002.
- Nagasawa, Y., et al., **Identification and characterization of *PKHD1*, the mouse orthologue of the human ARPKD gene.** *J Am Soc Nephrol*. **13**(9): p. 2246-58, 2002
- Nauli, S. M.; Alenghat, F. J; Luo, Y.; Williams, E.; Vassilev, P.; Li, X.; Elia, A. E. H.; Lu, W.; Brown, E. M.; Quinn, S. J.; Ingber, D. E.; Zhou, J. : **Polycystins 1 and 2 mediate mechanosensation in the primary cilium of kidney cells.** *Nature Genet.* 33: 129-137, 2003.
- Newby, L. J.; Streets, A. J.; Zhao, Y.; Harris, P. C.; Ward, C. J.; Ong, A. C. : **Identification, characterization, and localization of a novel kidney polycystin-1-polycystin-2 complex.** *J. Biol. Chem.* 277: 20763-20773, 2002.
- Neumann HP, Krumme B, van Velthoven V, Orszagh M, Zerres K. **Multiple intracranial aneurysms in a patient with autosomal recessive polycystic kidney disease.** *Nephrol Dial Transplant.* 1999 Apr;14(4):936-9.
- Nishio, S., Hatano, M., Nagata, M., Horie, S., Koike, T., Tokuhisa, T., and Mochizuki, T. ***PKD1*** **regulated immortalized proliferation of renal tubular epithelial cells through p53 induction and JNK activation.** J. Clin. Invest. 115, 910-918, 2005.
- Olsson, P. G.; Lohning, C.; Horsley, S.; Kearney, L.; Harris, P. C.; Frischauf, A.-M. : **The mouse homologue of the polycystic kidney disease gene (*PKD1*) is a single-copy gene.** *Genomics* 34: 233-235, 1996.
- Ong, A.C., Ward, C.J., Butler, R.J., Biddolph, S., Bowker, C., Torra, R., Pei, Y, and Harris, P.C. **Coordinate expression of the autosomal dominant polycystic kidney disease proteins, polycystin-2 and polycystin-1, in normal and cystic tissue.** *Am. J. Pathol.* 154, 1721-172, 1999.
- Onuchic, L.F., et al., ***PKHD1*****, the polycystic kidney and hepatic disease 1 gene, encodes a novel large protein containing multiple immunoglobulin-like plexin-transcription-factor domains and parallel beta-helix 1 repeats.** *Am J Hum Genet*. 70(5): p. 1305-17, 2002.
- Parnell, S.C., Magenheimer, B.S., Maser, R.L., Rankin, C.A., Smine, A., Okamoto, T., and Calvet, J.P. **The polycystic kidney disease-1 protein, polycystin-1, binds and activates heterotrimeric G-proteins *in vitro*.** *Biochem. Biophys. Res. Comm.* 251, 625- 631, 1998.
- Pei, Y.; Paterson, A. D.; Wang, K. R.; He, N.; Hefferton, D.; Watnick, T.; Germino, G. G.; Parfrey, P.; Somlo, S.; St. George-Hyslop, P. : **Bilineal disease and trans-heterozygotes in autosomal dominant polycystic kidney disease.** *Am. J. Hum. Genet.* 68: 355-363, 2001.
- Pennekamp P, Karcher C, Fischer A, Schweickert A, Skryabin B, Horst J, Blum M, Dworniczak B: **The ion channel polycystin-2 is required for left-right axis determination in mice.** *Curr Biol* 12(11):938-43, 2002.
- Peral, B.; Gamble, V.; Strong, C.; Ong, A. C. M.; Sloane-Stanley, J.; Zerres, K.; Winearls, C. G.; Harris, P. C. : **Identification of mutations in the duplicated region of the polycystic kidney disease 1 gene (*PKD1*) by a novel approach.** *Am. J. Hum. Genet.* 60: 1399-1410, 1997.
- Peral, B.; San Millan, J. L.; Ong, A. C. M.; Gamble, V.; Ward, C. J.; Strong, C.; Harris, P. C. : **Screening the 3-prime region of the polycystic kidney disease 1 (*PKD1*) gene reveals six novel mutations.** *Am. J. Hum. Genet.* 58: 86-96, 1996.
- Peters, D. J. M.; Spruit, L.; Saris, J. J.; Ravine, D.; Sandkuijl, L. A.; Fossdal, R.; Boersma, J.; van Eijk, R.; Norby, S.; Constantinou-Deltas, C. D.; Pierides, A.; Brissenden, J. E.; Frants, R. R.; van

Ommen, G.-J. B.; Breuning, M. H. : **Chromosome 4 localization of a second gene for autosomal dominant polycystic kidney disease.** *Nature Genet.* 5: 359-362, 1993

- Peters, D.J.M., van de Wal, A., Spruit, L., Saris, J.J., Breuning, M.H., Bruijn, J.A., and de Heer, E. **Cellular localization and tissue distribution of polycystin-1.** *J. Pathol.* 188, 439-446, 1999.
- Piontek, K.B., Huso, D.L., Grinberg, A., Liu, L., Bedja, D., Zhao, H., Gabrielson, K., Qian, F., Mei, C., Westphal, H., and Germino, G.G. **A functional floxed allele of *PKD1* that can be conditionally inactivated *in vivo*.** *J Am Soc Nephrol.* Dec;15(12):3035-43, 2004
- Puri, S., Magenheimer, B.S., Maser, R.L., Ryan, E.M., Zien, C.A., Walker, D.D., Wallace, D.P., Hempson, S.J. and Calvet, J.P. **Polycystin-1 activates Calcineurin/NFAT (Nuclear Factor of Activated T-cells) Signaling Pathway.** *J. Biol. Chem.* 279, 55455-55464, 2004.
- Qian, F.; Boletta, A.; Bhunia, A. K.; Xu, H.; Liu, L.; Ahrabi, A. K.; Watnick, T. J.; Zhou, F.; Germino, G. G. : **Cleavage of polycystin-1 requires the receptor for egg jelly domain and is disrupted by human autosomal-dominant polycystic kidney disease 1-associated mutations.** *Proc. Nat. Acad. Sci.* 99: 16981-16986, 2002.
- Qian, F.; Germino, F. J.; Cai, Y.; Zhang, X.; Somlo, S.; Germino, G. G. : ***PKD1* interacts with *PKD2* through a probable coiled-coil domain.** *Nature Genet.* 16: 179-183, 1997.
- Qian, F.; Watnick, T. J.; Onuchic, L. F.; Germino, G. G. : **The molecular basis of focal cyst formation in human autosomal dominant polycystic kidney disease type I.** *Cell* 87: 979-987, 1996.
- Neuhaus TJ, Sennhauser F, Briner J, Van Damme B, Leumann EP. **Renal-hepatic-pancreatic dysplasia: an autosomal recessive disorder with renal and hepatic failure.** *Eur J Pediatr.* 1996 Sep;155(9):791-5.
- Ravine, D.; Walker, R. G.; Gibson, R. N.; Sheffield, L. J.; Kincaid-Smith, P.; Danks, D. M. : **Treatable complications in undiagnosed cases of autosomal dominant polycystic kidney**
- Rossetti, S.; Strmecki, L.; Gamble, V.; Burton, S.; Sneddon, V.; Peral, B.; Roy, S.; Bakkaloglu, A.; Komel, R.; Winearls, C. G.; Harris, P. C. : **Mutation analysis of the entire *PKD1* gene: genetic and diagnostic implications.** *Am. J. Hum. Genet.* 68: 46-63, 2001.
- Scheffers, M. S.; Le, H.; van der Bent, P.; Leonhard, W.; Prins, F.; Spruit, L.; Breuning, M. H.; de Heer, E.; Peters, D. J. M. : **Distinct subcellular expression of endogenous polycystin-2 in the plasma membrane and Golgi apparatus of MDCK cells.** *Hum. Molec. Genet.* 11: 59-67, 2002.
- Scheffers, M. S.; van der Bent, P.; Prins, F.; Spruit, L.; Breuning, M. H.; Litvinov, S. V.; de Heer, E.; Peters, D. J. M. : **Polycystin-1, the product of the polycystic kidney disease 1 gene, co-localizes with desmosomes in MDCK cells.** *Hum. Molec. Genet.* 9: 2743-2750, 2000.
- Somlo, S.; Rutecki, G.; Giuffra, L. A.; Reeders, S. T.; Cugino, A.; Whittier, F. C. : **A kindred exhibiting cosegregation of an overlap connective tissue disorder and the chromosome 16 linked form of autosomal dominant polycystic kidney disease.** *J. Am. Soc. Nephrol.* 4: 1371-1378, 1993.
- Suchy SF, Nussbaum RL. **The deficiency of PIP2 5-phosphatase in Lowe syndrome affects actin polymerization.** *Am J Hum Genet.* 2002 Dec;71(6):1420-7. Epub 2002 Nov 11.
- Tallquist MD, Soriano P: **Epiblast-restricted Cre expression in MORE mice: a tool to distinguish embryonic vs. extra-embryonic gene function.** *Genesis* 26 :113-5, 2000.
- Thomas, R.; McConnell, R.; Whittacker, J.; Kirkpatrick, P.; Bradley, J.; Sandford, R. : **Identification of mutations in the repeated part of the autosomal dominant polycystic kidney disease type 1 gene, *PKD1*, by long-range PCR.** *Am. J. Hum. Genet.* 65: 39-49, 1999.

- Torra, R.; Badenas, C.; San Millan, J. L.; Perez-Oller, L.; Estivill, X.; Darnell, A. : **A loss-of-function model for cystogenesis in human autosomal dominant polycystic kidney disease type 2.** *Am. J. Hum. Genet.* 65: 345-352, 1999.
- Veldhuisen, B.; Saris, J. J.; de Haij, S.; Hayashi, T.; Reynolds, D. M.; Mochizuki, T.; Elles, R.; Fossdal, R.; Bogdanova, N.; van Dijk, M. A.; Coto, E.; Ravine, D.; Norby, S.; Verellen-Dumoulin, C.; Breuning, M. H.; Somlo, S.; Peters, D. J. M. : **A spectrum of mutations in the second gene for autosomal dominant polycystic kidney disease (*PKD2*).** *Am. J. Hum. Genet.* 61: 547-555, 1997.
- Ward, C. J.; Turley, H.; Ong, A. C. M.; Comley, M.; Biddolph, S.; Chetty, R.; Ratcliffe, P. J.; Gatter, K.; Harris, P. C. : **Polycystin, the polycystic kidney disease 1 protein, is expressed by epithelial cells in fetal, adult, and polycystic kidney.** *Proc. Nat. Acad. Sci.* 93: 1524-1528, 1996.
- Ward, C.J., et al., *Cellular and subcellular localization of the ARPKD protein; fibrocystin is expressed on primary cilia.* Hum Mol Genet, 2003. **12**(20): p. 2703-10.
- Watnick, T. J.; Piontek, K. B.; Cordal, T. M.; Weber, H.; Gandolph, M. A.; Qian, F.; Lens, X. M.; Neumann, H. P. H.; Germino, G. G. : **An unusual pattern of mutation in the duplicated portion of *PKD1* is revealed by use of a novel strategy for mutation detection.** *Hum. Molec. Genet.* 6: 1473-1481, 1997.
- Watnick, T. J.; Torres, V. E.; Gandolph, M. A.; Qian, F.; Onuchic, L. F.; Klinger, K. W.; Landes, G.; Germino, G. G. : **Somatic mutation in individual liver cysts supports a two-hit model of cystogenesis in autosomal dominant polycystic kidney disease.** *Molec. Cell* 2: 247-251, 1998.
- Watnick, T.; Phakdeekitcharoen, B.; Johnson, A.; Gandolph, M.; Wang, M.; Briefel, G.; Klinger, K. W.; Kimberling, W.; Gabow, P.; Germino, G. G. : **Mutation detection of *PKD1* identifies a novel mutation common to three families with aneurysms and/or very-early-onset disease.** *Am. J. Hum. Genet.* 65: 1561-1571, 1999.
- Watnick TJ, Gandolph MA, Weber H, Neumann HP, Germino GG. **Gene conversion is a likely cause of mutation in PKD1.** *Hum Mol Genet.* 1998 Aug;7(8):1239-43.
- Wu, G.; D'Agati, V.; Cai, Y.; Markowitz, G.; Park, J. H.; Reynolds, D. M.; Maeda, Y.; Le, T. C.; Hou, H., Jr.; Kucherlapati, R.; Edelmann, W.; Somlo, S. : **Somatic inactivation of *PKD2* results in polycystic kidney disease.** *Cell* 98: 177-188, 1998.
- Wu, G.; Markowitz, G. S.; Li, L.; D'Agati, V. D.; Factor, S. M.; Geng, L.; Tibara, S.; Tuchman, J.; Cai, Y.; Park, J. H.; van Adelsberg, J.; Hou, H., Jr.; Kucherlapati, R.; Edelmann, W.; Somlo, S. : **Cardiac defects and renal failure in mice with targeted mutations in *PKD2*.** *Nature Genet.* 24: 75-78, 2000.
- Wu, G.; Mochizuki, T.; Le, T. C.; Cai, Y.; Hayashi, T.; Reynolds, D. M.; Somlo, S. : **Molecular cloning, cDNA sequence analysis, and chromosomal localization of mouse *PKD2*.** *Genomics* 45: 220-223, 1997.
- Xu, G. M.; Sikaneta, T.; Sullivan, B. M.; Zhang, Q.; Andreucci, M.; Stehle, T.; Drummond, I.; Arnaout, M. A. : **Polycystin-1 interacts with intermediate filaments.** *J. Biol. Chem.* 276: 46544-46552, 2001.
- Yoder, B.K., Hou, X., and Guay-Woodford, L.M. **The polycystic kidney disease proteins, polycystin-1, polycystin-2, polaris, and cystin, are co-localized in the renal cilia.** *J. Am. Soc. Nephrol.* 13, 2508-2516, 2002.
- Zerres, K., et al., *Prenatal diagnosis of autosomal recessive polycystic kidney disease (ARPKD): molecular genetics, clinical experience, and fetal morphology.* Am J Med Genet, 1998. **76**(2): p. 137-44.

- Zerres, K.; Mucher, G.; Rudnik-Schoneborn, S. : **Autosomal recessive polycystic kidney disease does not map to the second gene locus for autosomal dominant polycystic kidney disease on chromosome 4.** *Hum. Genet.* 93: 697-698, 1994.
- Zhang, Q., et al., **Loss of the Tg737 protein results in skeletal patterning defects.** *Dev Dyn.* 227(1): p. 78-90, 2003.

CURRICULUM VITAE

Miguel Garcia-Gonzalez

DEMOGRAPHIC INFORMATION

Current: Miguel Garcia-Gonzalez Visiting Graduate Student (Physiology program, Faculty of Medicine, Universidad Santiago de Compostela, Spain) and Member of Lab, 07/12/02-present.

Personal Data: The Johns Hopkins University
School of Medicine
Department of Medicine
Nephrology / 958 Ross Research Building
720 Rutland Avenue
Baltimore, Maryland 21205-2196
Telephone: 410-614-1650
Fax: 410-614-5129
e-mail: mgarci15@jhmi.edu

Education and Training:

- Biological Science. Universidad de Navarra, Spain. B.S.(1999).
- Graduate Program. Department of Physiology. School of Medicine. Universidad de Santiago de Compostela, Galicia, Spain (2000-2002).
- Physiology and Nutrition. Department of Physiology. School of Medicine. Universidad de Santiago de Compostela, Galicia, Spain. M.S.(2002).
- Medicine Training. Department of Medicine, Division of Nephrology, Johns Hopkins University School of Medicine, Baltimore, Maryland (2002-2004).

Professional Experience:

- Teaching. Department of Physiology and Nutrition. Universidad de Navarra, Spain (1996-1997)
- Member of Lema and Bandín Diagnostic Laboratory, Vigo, Galicia, Spain (1997).
- Graduate student of the Xose Manuel Lens Neo Lab. Hospital Clínico de Santiago de Compostela, A Coruña, Galicia, Spain (1999-2002)
- Member of Gregory G. Germino Lab. Department of Medicine, Division of Nephrology, Johns Hopkins University School of Medicine, Baltimore, Maryland (2002-present).

RESEARCH ACTIVITIES:

Publications.

1. Wânia Rezende-Lima, Kleber S. Parreira, Miguel Garcia-Gonzalez, Eva Riveira, Julio F. Banet, Xosé M. Lens. Homozygosity for Uromodulin disorders: FJHN and MCKD type 2. Kidney Inter., 2004, 66:1-6.
2. Garcia-Gonzalez M, Abdulkader I, Boquete AV, Lens Neo XM, Forteza J, Cameselle-Teijeiro J. Cyclooxygenase-2 expression in neoplastic and non-neoplastic follicular cells of the thyroid gland. Virchows Arch. 2005 Jun 10.
3. Allen, E., Piontek, K., Garrett-Mayer, E., Garcia-Gonzalez, M., Gorelick, K.L., Germino, G. Loss of polycystin-1 or polycystin-2 results in dysregulated apolipoprotein expression in murine tissues. Hum. Mol. Genet. 2006 Jan 1;15(1):11-21.
4. Garcia-Gonzalez, M., Allen, E., Lan, Z., Jones, J., Germino, GG., Watnick, T. Mutational screening and analysis of the entire PKD1 and PKD2 genes in 82 unrelated ADPKD Families. [In Preparation].
5. Garcia-Gonzalez, M.,, Zhou, Q., Germino, GG., Watnick, T. Conditional Inactivation of Murine Pkd2 using a tri-allelic system. [In Preparation].
6. Garcia-Gonzalez, M., Menezes, L., Kaimori, J Y., D Huso, Piontek, K ., Somlo, S ., Onuchic, L F., Guay-Woodford, L M., Germino, GG. A floxed allele of murine Pkhd1 that results in a range of phenotypes including polycystic kidney disease and neonatal respiratory failure when inactivated. [In Preparation].
7. Garcia-Gonzalez, M., Garrett-Mayer, E., Germino, GG., Watnick, T. Intragenic and extragenic analysis of the genes responsible of autosomal dominant polycystic kidney disease. [In Preparation].
8. Tan, PL., Inglis, N., Barr, T., Mitsuma, N., Coforio, S., Huang, S., Garcia-Gonzalez M., Watnick, T., Germino, GG., Beales, PL., Caterina., M., Leroux, ML., Rice FL., Katsanis N. Ciliary and basal body proteins have an evolutionarily conserve role in the nociceptive response of primary sensory neurons. [In Preparation].
9. Kirkwood, SC., Germino, G., Price, RA., Garcia-Gonzalez, M, Piontek, K., Menezes, L., Ballinger, D., Downing, A., Bromley, E., Mukhopadhyay, N., Cox, D., Breier, A., Hockett. Implication of the Cilia Gene, PKHD1, in weight Control. [In Preparation].
10. Jun-Ya Kaimori, Yasuyuki Nagasawa, Miguel A. Garcia-Gonzalez, Luis F. Menezes, Luis F. Onuchic, Lisa M. Guay-Woodford, Gregory G. Germino. The PKHD1 Product, Polyductin/Fibrocystin, (PD1) Undergoes Notch-Like Post-Translational Processing. [In Preparation].

Other publications:

1. Garcia-Gonzalez, M., "Polycystic Kidney Disease. From the clinical/genetic test, through in vivo and in vitro analysis and back to humans". PhD. Thesis.
2. Garcia-Gonzalez, M., "Ciclooxigenasa-2 (Cox-2) en las enfermedades poliquísticas renales: ADPKD, ARPKD, y ADMCKD". M.Sc. Thesis.

Meetings and Abstracts:

Invited lectures.

- A floxed allele of murine Pkhd1 that results in a range of phenotypes including polycystic kidney disease and neonatal respiratory failure when inactivated". American Society of Nephrology (ASN). 38th Annual Renal Week Meeting. Philadelphiia, PA. 2005.

Poster Presentation.

1. DAVILA S, GARCÍA VIDAL M, GARCÍA-GONZÁLEZ M.A, CORDAL T, BARROS F, QUINTEIRO C, LENS X.M. Genética Molecular de las enfermedades renales de cadenas alfa 3, 4 y 5 del colágeno 4. XXX Congreso Nacional de la SEN. 2000.Oviedo, Spain
2. GARCÍA-GONZÁLEZ M.A , DAVILA S, GARCÍA VIDAL M, FRAGA M, PINTOS E, FORTEZA J, GÓMEZ-REINO J, LENS X.M. Ciclooxigenasas 1 y 2 en la Poliquistosis Renal Autosómica Dominante. XXX Congreso Nacional de la Sociedad Española de Nefrología. 2000.Oviedo, Spain
3. GARCÍA-GONZÁLEZ M.A, DAVILA S, GARCÍA VIDAL M, BARROS F, QUINTEIRO C, ALONSO M, ALONSO R, LENS X.M. Enfermedad Quística Medular Autosómica Dominante: Heterogeneidad y Refinamiento Genético en 16p12. XXX Congreso Nacional de la SEN. 2000.Oviedo, Spain
4. DAVILA S, CORDAL T, GARCÍA VIDAL M, GARCÍA-GONZÁLEZ M.A, ALONSO R, LENS X.M. Mutaciones en la región 5' del gen de la Poliquistosis Renal del Adulto, PKD1. XXX Congreso Nacional de la SEN. 2000.Oviedo, Spain
5. GARCÍA-GONZÁLEZ M.A , DAVILA S, GARCÍA VIDAL M, BARROS F, QUINTEIRO C, ALONSO M, ALONSO R, LENS X.M. "Autosomal Dominant Medullary Cystic Kidney Disease; Genetic Heterogeneity and refinement on locus 16p12". The ASN 33th Annual Meeting. 2000.Toronto, Canada
6. GARCÍA-GONZÁLEZ M.A., GARCÍA VIDAL M., DAVILA S., CALO-MATA P., VÁZQUEZ-BOQUETE A., FRAGA M., CAMESELLE-TEIJEIRO J., GARCÍA-CABALLERO T., PINTOS E., FORTEZA J., GÓMEZ-REINO JJ., LENS X.M. "Sobreexpresion y Localizacion de Ciclooxigenasa-2 en las Enfermedades Quisticas Renales Hereditarias". XXXI Congreso Nacional SEN. 2001. Zaragoza, Spain.
7. CALO-MATA P., GARCÍA-GONZÁLEZ M.A., CORDAL T., GARCÍA VIDAL M., DAVILA S., QUINTEIRO C., WATNICK T., BARROS F., GERMINO G., LENS X.M. "Plasticidad Proteica de la Policistina 1".. XXXI Congreso Nacional de la SEN. 2001. Zaragoza, Spain.
8. CASAL J.A., DAVILA S., PÉREZ L., GARCÍA-GONZÁLEZ M. A., CALO P., TUTOR J.C., LENS X.M. "Predictores de Severidad en Fase Preclinica de la Poliquistosis". XXXI Congreso Nacional de la SEN. 2001. Zaragoza, Spain.
9. M.A. GARCÍA-GONZÁLEZ, S. DAVILA, P. CALO-MATA, J. FORTEZA, JJ. GÓMEZ- REINO, LENS XM. "Over-expression of cyclooxigenase-2 in hereditary cystic kidney diseases: differences in ARPKD". ASN. San Francisco. 2001.
10. J.A. CASAL, S. DAVILA, L. PÉREZ, M. A. GARCÍA-GONZÁLEZ, P. CALO, J.C. TUTOR, LENS XM. "Tubular and glomerular markers of severity in the autosomal dominant polycystic kidney disease". ASN. San Francisco. 2001.
11. P. CALO, S. DAVILA, M.A. GARCÍA-GONZÁLEZ, T.CORDAL, M.A.,C. QUINTEIRO, T. WATNICK, F. BARROS, G. GERMINO, LENS XM. "Protein plasticity in polycystin 1". ASN. San Francisco. 2001.
12. P. CALO-MATA, M.A. GARCÍA-GONZÁLEZ, E. RIBEIRA, W. REZENDE, C. QUINTEIRO , F. BARROS, X.M. LENS. Dominios PKD y dominio REJ: plasticidad y conformación 3D. XXXII Congreso Nacional de la SEN. Bilbao, 12 al 16 de Octubre de 2002.

13. A. PERSU, M.A. GARCÍA-GONZÁLEZ, P. CALO-MATA, W. REZENDE, E.RIVEIRA, T. MESSIAEN, Y. PIRSON, D. CHAUVEAU, O. DEVUYST, X.M LENS. Variabilidad intra-familisr en la progresión de la insuficiencia renal en la Poliquistosis. XXXII Congreso Nacional de la SEN. Bilbao, 12 al 16 de Octubre de 2002.
14. W. REZENDE, M.A GARCÍA-GONZÁLEZ, P. CALO-MATA, E. RIBEIRA, X.M. LENS. Refinamiento del Locus ADMCKD-2 y genes candidatos para la enfermedad Quística Medular Auosómica Dominante. XXXII Congreso Nacional de la SEN. Bilbao, 12 al 16 de Octubre de 2002.
15. J.A. CASAL, L. PÉREZ, M.A. GARCÍA-GONZÁLEZ, P. CALO-MATA, E. RIVEIRA, W. REZENDE, J. C. TUTOR, X.M. LENS. Tubular markers as indicators of progression in the Autosomal Dominant, Polycystic Kidney Disease. ASN. Filadelfia Noviembre 2002.
16. P. CALO-MATA, M.A. GARCÍA-GONZÁLEZ, E. RIBEIRA, W. REZENDE, C. QUINTEIRO , F. BARROS, X.M. LENS. PKD domains and REJ domain: plasticity and 3D conformation. ASN. Filadelfia Noviembre 2002.
17. Miguel A. Garcia-Gonzalez, Gregory G. Germino, Terry Watnick. Mutational screening of the entire PKD1 and PKD2 genes in 88 unrelated ADPKD Families. Annual research retreat, DOM. Johns Hopkins School of Medicine. April 14, 2004.
18. Garcia-Gonzalez, Miguel A; Piontek, Klaus; Lijuan, Liu; Lens, Xose M. and Germino, Gregory. Over-expression of Cyclooxygenase-2 in the polycystic kidney disease knockout mouse associated with tubularization of the Bowman's capsule. ASN 37th Annual Meeting & Scientific Exposition. St. Louis, Missouri. Octubre 2004
19. Jun-ya Kaimori, Yasuyuki Nagasawa, Miguel A Garcia-Gonzalez, Moses Adetubi, Luis F Onuchic, Stefan Somlo, Lisa M. Guay-woodford, Gregory G Germino. Development of in vitro expression system of autosomal recessive polycystic kidney disease responsible gene product, Polyductin. ASN 37th Annual Meeting & Scientific Exposition. St. Louis, Missouri. Octubre 2004
20. Jun-ya Kaimori, Miguel A Garcia-Gonzalez, Luis F Onuchic, Stefan Somlo, Lisa M. Guay-woodford, Gregory G Germino. Development of in vitro expression system of autosomal recessive polycystic kidney disease responsible gene product, Polyductin. Annual research retreat, DOM. Johns Hopkins School of Medicine. April 14, 2004.
21. Parreira KS, Outeda P, Riveira E, Rezende-Lima W, Banet JF, García-González MA, Urisarri A, Lens XM. "Espectro de mutaciones de la Poliquistina 1: correlación genotipo-fenotipo, plasticidad y evolución". XXXIV Congreso Nacional de la S.E.N., Canarias, Spain. 2-5 Octubre 2004.
22. Parreira KS, Outeda P, Riveira E, Rezende-Lima W, Banet JF, García-González MA, Urisarri A, Lens XM. Mutations in the PKD, REJ and GPS domains of polycystin-1: genotype-phenotype correlation, plasticity and evolution. ASN 37th Annual Meeting & Scientific Exposition. St. Louis, Missouri. Octubre 2004
23. Parreira KS, Rezende-Lima W, Outeda P, Banet JF, García-González M, Riveira E, Urisarri A, García-Vidal M, Lens XM. spectro de mutaciones de la Poliquistina 1: correlación genotipo-fenotipo, plasticidad y evolución. Poster. XXXIV Congreso de la Sociedad Española de Nefrología.
24. M A Garcia-Gonzalez, J Y Kaimori, D Huso, K Piontek, S Somlo, L F Onuchic, L M Guay-Woodford and G G Germino. A floxed allele of murine Pkhd1 that results in a range of phenotypes including polycystic kidney disease and neonatal respiratory failure when inactivated. ASN 38th Annual Renal Week Meeting. Philadelphiia, PA. 2005.
25. M A Garcia-Gonzalez, Qin Zhou, Gregory G Germino, and Terry Watnick. Conditional Inactivation of Murine Pkd2 using a tri-allelic system. ASN 38th Annual Renal Week Meeting. Philadelphiia, PA. 2005.
26. B. Tao, M. Garcia-Gonzalez, L. F. Onuchic, E. M. Eicher, G. G. Germino, L. M. Guay-Woodford. Evidence That Pkhd1 Has a Complex Transcriptional Profile in a New Spontaneous Mouse Model of ARPKD. ASN 38th Annual Renal Week Meeting. Philadelphiia, PA. 2005.

27. J.Y. Kaimori, Y. Nagasawa, M.A. Garcia-Gonzalez, A.K. Bhunia, L.F. Onuchic, L.M. Guay-Woodford, G.G. Germino. The PKHD1 Product, Polyductin (PD1), Induces a Cell Density-Dependent, Phenotypic Switch in MDCK Cells. ASN 38th Annual Renal Week Meeting. Philadelphiia, PA. 2005.
28. Jun-Ya Kaimori, Yasuyuki Nagasawa, Miguel A. Garcia-Gonzalez, Luis F. Menezes, Luis F. Onuchic, Lisa M. Guay-Woodford, Gregory G. Germino. The PKHD1 Product, Polyductin/Fibrocystin, (PD1) Undergoes Notch-Like Post-Translational Processing. ASN 38th Annual Renal Week Meeting. Philadelphiia, PA. 2005.
29. M A Garcia-Gonzalez, J Y Kaimori, D Huso, K Piontek, S Somlo, L F Onuchic, L M Guay-Woodford and G G Germino. A floxed allele of murine Pkhd1 that results in a range of phenotypes including polycystic kidney disease and neonatal respiratory failure when inactivated. FASEB. Vermont. 2005.

Extramural Sponsorship:

- "Poliquistosis Renal de Adulto: Distribución de haplotipos y mutaciones en el gen PKD1", Science and Technology Ministry of Spain (FPI-Grant link to the Project PM98-0028 from Dr. Lens Neo), 6/01/00-1/1/03, (100%).

EDUCATIONAL ACTIVITIES:

Teaching:

Classroom Instruction:

- Teaching. Department of Physiology and Nutrition. Universidad de Navarra, Spain (1996-1997).

RECOGNITION:

Awards and Honors:

Awards:

- July 2001 - July 2004: study grant "Becas de Formación de Personal Investigador (FPI)".
- 1st Prize (HOSPAL) of the Spanish Society of Nephrology 2001." "Sobreexpresion y Localizacion de Ciclooxigenasa-2 en las Enfermedades Quisticas Renales Hereditarias". XXXI Congreso Nacional SEN. 2001. Zaragoza, Spain.
- Ayudas para Estancias Breves en el Extranjero (Ministerio de Ciencia y Tecnología) in the Johns Hopkins.